Charles University

Faculty of Science

Study programme: Physical Geography and Geoecology

Anna Jandová

Dating of moraines by cosmogenic isotopes

Datování morénových akumulací kosmogenními izotopy

Diploma thesis

Supervisor: Mgr. Martin Margold, Ph.D.

Prague, 2025

Prohlášení:

Prohlašuji, že jsem předloženou diplomovou práci zpracovala samostatně a že jsem uvedla všechnu použitou literaturu a informační zdroje. Tato práce ani její podstatná část nebyla předložena k získání jiného nebo stejného akademického titulu.

Declaration:

I declare that I wrote this diploma thesis independently and that I properly cited all the information sources and literature I used. Neither the thesis nor any of its substantial parts have been submitted to obtain the same or other academic degree.

29 April 2025, Prague

...…….

Anna Jandová

Acknowledgements

I would like to express my sincere gratitude to my supervisor, Martin Margold. I am especially thankful for his invaluable guidance, patience and support throughout my research as well as insightful ideas. He was always available for any help or feedback I needed.

I am also deeply thankful to Ben Stoker who provided valuable feedback, inspiring suggestions and was always willing to help me or discuss anything I needed. Special thanks go to Lukáš Brůha and Josef Laštovička. Without their assistance with Google Earth Engine, I would likely still be unsuccessfully trying to run my scripts.

Finally, I am deeply thankful to my family and partner Mikoláš, who always gave me unconditional support, encouraged me and tried to cheer me up, even when I was annoying and it was not easy to be around me.

Abstract:

Moraines are often used to reconstruct the extent and chronology of past glaciations. A common method to estimate the timing of their formation is cosmogenic nuclide exposure dating. However, the accuracy of the method is often affected by post-depositional processes and signal inheritance from prior exposure.

This thesis aims to evaluate the controls on moraine denudation and preservation and derive implications for the reliability of exposure dating. A global dataset of 10083 samples dated with ^{10}Be was compiled and grouped into 3243 moraine ridge groups (1620 suitable for the analysis with ≥ 3 samples). Clustering of moraine ages, used an indicator of dating quality, was compared to climate, topography, ice mass type, or sample size.

Only 23 % of analysed moraines showed well-clustered exposure ages, increasing to 46 % after removing outliers. The highest proportion of well-clustered ages was observed for moraines between 10 to 15 ka and significantly decreased for older and younger moraines. The well-clustered moraines were also more frequent in milder climates with higher temperatures and precipitation and lower annual temperature ranges. Nevertheless, the findings highlight the importance of considering also glacial dynamics. Poorly clustered regions (the Antarctic Ice Sheet, mountain glaciers, icefields and icecaps in Greenland, northeastern Asia, and High Asia) are likely affected by the extreme climate conditions and their complex glacial histories.

A key implication for sampling strategies is the effect of sample size. While 36 % of the examined moraines comprised only three samples per moraine, sampling at least four boulders significantly increases the likelihood of obtaining a well-clustered age by approximately 20 %.

Keywords: moraines, cosmogenic isotope ^{10}Be, denudation, Pleistocene

Abstrakt

Morénové akumulace představují významný archiv historie zalednění. Jednou z nejčastěji využívaných metod datování morén je datování kosmogenními nuklidy, jehož spolehlivost je však do značné míry ovlivněna post-depozičními procesy nebo přítomností zděděných nuklidů vlivem předchozí expozice kosmickému záření.

Cílem této práce je zhodnotit procesy denudace morénových akumulací a faktory, které mohou ovlivnit spolehlivost jejich datování kosmogenními nuklidy. Byl analyzován globální dataset obsahující 10083 vzorků z 3243 morén datovaných pomocí izotopu ^{10}Be, vhodných pro analýzu bylo 1620, neboť obsahovaly alespoň tři vzorky. Jako ukazatelem kvality datování byla použita míra klastrování (shody) stáří vzorků jednotlivých morén, která pak byla porovnána klimatickými podmínkami, topografií, typem zalednění či počtem datovaných vzorků.

Kvalitní datování vykazovalo pouze 23 % morén, resp. 43 % po odstranění odlehlých hodnot. Nejvyšší podíl dobře klastrovaných morén byl pozorován pro 10-15 tis. let staré morény, a s rostoucím i klesajícím stářím se významně snižoval. Kvalita datování se také zlepšovala pro mírnější klima s relativně vyššími teplotami, srážkami a nižší roční teplotní amplitudou. Výsledky zároveň ukazují, že nelze opomíjet význam historie a dynamiky zalednění. Oblasti s nejhoršími kvalitou dat se vyznačují nejen extremitou klimatu, ale i složitou historií zalednění (Antarktický ledovcový štít, horské zalednění, ledovcová pole a čapky v Grónsku, vysoká a severovýchodní Asie).

Výrazný vliv na spolehlivost datování má také počet datovaných vzorků. Zatímco nejčastěji (ve 36 %) jsou odebírány tři vzorky, datování nejméně čtyř výrazně zvyšuje pravděpodobnost spolehlivého výsledku, a to až o 20 %.

Klíčová slova: ledovcové morény, kosmogenní izotop ^{10}Be, denudace, pleistocén

Table of Contents

1. Introduction

Glaciers are sensitive indicators of climate conditions (Mackintosh et al., 2017), and a better understanding of glacier-climate interactions and accurate records of past glaciation are therefore crucial for improving projections of future glacier behaviour. Moraines and other glacial landforms record former ice advance and retreat, but accurate reconstructions based on these landforms require a robust understanding of their formation and age.

One of the most frequently used dating methods in paleoglaciology, well-suited to dating moraines, is cosmogenic nuclides exposure dating, allowing precise and direct dating of glacial deposits on timescales spanning hundreds (Abbühl et al., 2009; J. T. H. Anderson et al., 2017; Bakke et al., 2021; Balco et al., 2016; Barnard et al., 2004b; Braumann et al., 2020; Murari et al., 2014) to millions of years (Balter-Kennedy et al., 2020; Hodgson et al., 2012; Smith et al., 2005a; Valletta et al., 2017). Cosmic rays split atoms in exposed surface rocks at predictable rates, producing rare isotopes (^{10}Be, ^{26}Al, ^{36}Cl, ^{14}C, ^{3}He, ^{21}Ne). Their subsequent concentrations provide exposure ages or rates of surface processes (Gosse & Phillips, 2001). Glacial erosion transports fresh rocks to the surface, where they remain shielded by overlying ice until the glacier retreats, enabling direct dating of glacier fluctuations (Balco, 2020). Thanks to the abundance of target minerals in which cosmogenic nuclides are produced, this method is applicable on a global scale in a wide range of environments (Balco, 2011; Expage, 2023; ICE-D, 2024).

In theory, the concentrations of cosmogenic nuclides directly correspond to the exposure ages and, therefore, precisely record the depositional age of landform and glacier retreat. However, moraines are subject to post-depositional disturbances, which, together with nuclide inheritance, alter the nuclide concentration and can significantly affect the accuracy of the age estimate; therefore, the landform degradation cannot be ignored (Balco, 2011; Putkonen & O'Neal, 2006). Incomplete exposure due to erosion of surface material or post-glacial exhumation reduces cosmogenic nuclide concentrations, resulting in age underestimates. Conversely, inheritance from previous episodes of exposure results in overestimated ages (Balco, 2011; Heyman et al., 2011b).

Several studies have addressed the question of quantification of the effects of these geological processes on exposure ages (moraine age scatter) using numerical models of moraine degradation/moraine topographic evolution/boulder exhumation (Hallet & Putkonen, 1994; Putkonen & O'Neal, 2006; Putkonen & Swanson, 2003). These studies combined numerical modelling of moraine degradation with field observations of moraine topography (cross-profile – slope, crest height).

This work examines the reliability of cosmogenic nuclide exposure dating of moraines. All papers listed in the global database of published ^{10}Be and ^{26}Al data from glacial samples (Expage database; Heyman, 2023) were reviewed to compile a global dataset of all published exposure ages on moraine boulders, comprising more than 10,000 samples. Information from the original papers was then combined with climate and terrain data to assess the controls on

moraine preservation or denudation and derive implications for the reliability of exposure dating.

Unlike previous studies, which were either limited by the amount of data available at the time or focused on specific regions (Hallet & Putkonen, 1994; Putkonen & O'Neal, 2006; Putkonen & Swanson, 2003) this study benefits from the use of all currently available global data. Heyman (2016) examined moraines on a global scale but primarily focused on a specific characteristic – boulder height. Also, while some earlier studies examined detailed moraine topographic data (cross-profiles, moraine slope angle, moraine height) (Putkonen & Swanson, 2003; Putkonen & O'Neal, 2006), such an approach would be very time-consuming at the global scale. This work uses data from global datasets extracted for moraine locations and focuses on environmental controls rather than site-specific moraine morphology.

2. Cosmogenic nuclides production

The Earth is constantly bombarded with high-energy cosmic radiation, produced mainly by supernova explosions (Gosse & Phillips, 2001; Von Blanckenburg & Willenbring, 2014). This primary cosmic ray flux is composed of solar, and most importantly (for cosmogenic nuclides production), galactic cosmic rays. Approximately 87 % of galactic cosmic ray particles consist of protons, 12 % of alpha-particles (helium nuclei) and 1 % of heavier nuclei (Masarik & Beer, 1999). The sources of solar radiation are solar flares and coronal mass ejections, and it is composed in 98 % of protons, with the remaining 2 % accounting for heavier nuclei particles. Due to substantially lower energy of particles, solar radiation can cause nuclear reactions (and produce CN) only at the top of the atmosphere at higher latitudes, especially during higher solar activity (Masarik & Beer, 1999).

The trajectories of the charged particles of the primary cosmic radiation are affected by the Earth's magnetic field and need kinetic energy high enough to exceed cut-off rigidity R_c (momentum of a particle per unit charge) and penetrate the atmosphere (Dunai & Lifton, 2014). The rigidity changes with the angle of incidence or magnetic field "strength"; therefore, the highest cut-off rigidity values are at the equator (approx. 17 GV), decreasing towards the poles (almost 0) (Darvill, 2013; Dunai & Lifton, 2014; Masarik & Beer, 1999) (see Fig. 1). However, the increase in cosmic ray flux at high latitudes (due to low cut-off rigidity) does not cause an appropriate increase in cosmogenic nuclides production because the energy of particles is too low to induce nuclear reactions (Dunai & Lifton, 2014).

The interaction/collision of primary cosmic rays with atoms in the high atmosphere results in spallation, triggering a cascade of secondary cosmic rays composed of nucleons and mesons. For cosmogenic nuclide production, the most significant are neutrons and muons (Darvill, 2013; Dunai & Lifton, 2014). Spallation is a process in which high-energy nucleons collide with atmospheric nuclei, ejecting protons and neutrons and producing lighter nuclei. Spallation in the atmosphere produces meteoric cosmogenic nuclides such as ^{7}Be, ^{10}Be, ^{14}C, and

^{36}Cl; they attach to aerosols and are deposited on the Earth's surface via dry or wet deposition (Dunai & Lifton, 2014; Von Blanckenburg & Willenbring, 2014).

Figure 1 The effect of Earth's geomagnetic field on incoming primary cosmic rays (Darvill, 2013).

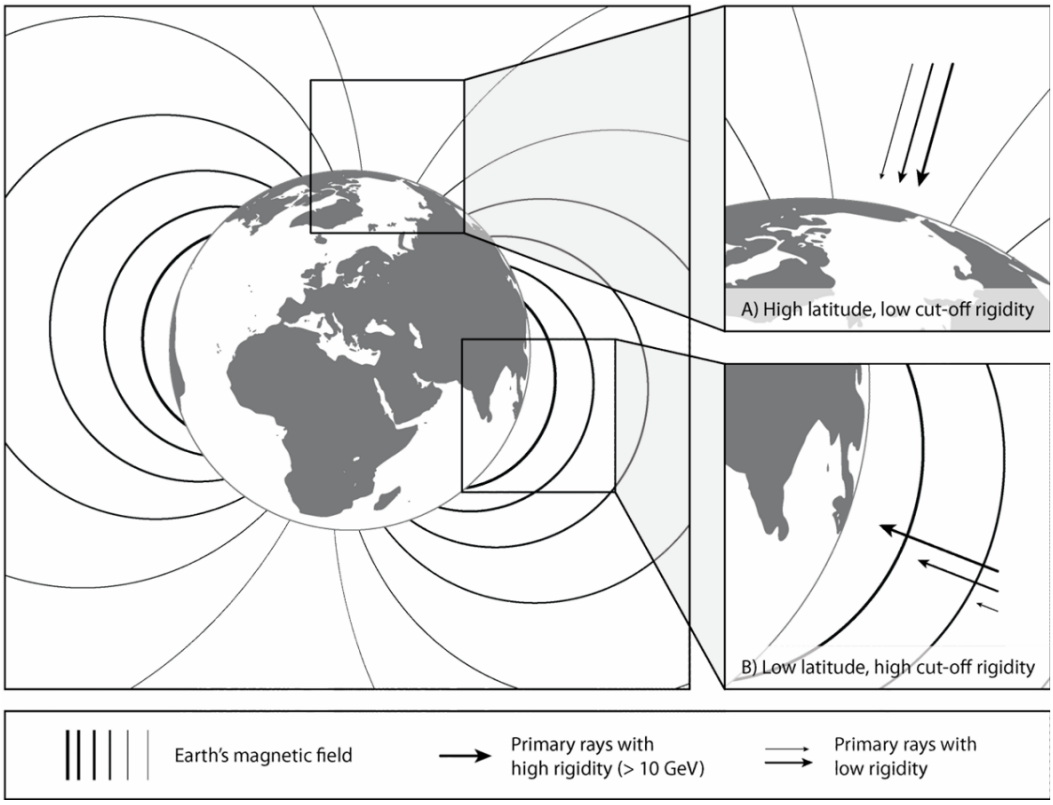

The secondary cosmic rays have maximum intensity at an atmospheric depth of 80-90 g/cm2 (collision length) and decrease exponentially with atmospheric depth due to the interactions/collisions with particles (Dunai & Lifton, 2014; Gosse & Phillips, 2001). This "attenuation" is described by attenuation length (a thickness of a material/mass that attenuates the intensity of cosmic radiation by e^{-1} ~ to 37 %) and varies with the energy of secondary

radiation being approx. 150g/cm2 in lower and 130 g/cm2 in higher latitudes and the material density (air vs. rock) (Dunai, 2000; Gosse & Phillips, 2001).

Part of the secondary ray particles that reach the Earth's surface interact with minerals in rocks/solids and produce in-situ cosmogenic nuclides in their surface layer (due to the attenuation). The radioactive cosmogenic nuclides (^{10}Be, ^{14}C, ^{26}Al, ^{36}Cl, ^{53}Mn) decay with time, while stable (noble gases – ^{3}He, ^{21}Ne) remain in minerals until they diffuse (Von Blanckenburg & Willenbring, 2014). Their production rate is substantially lower than that of meteoric cosmogenic nuclides (Von Blanckenburg & Willenbring, 2014).

3. Analysis of in-situ cosmogenic nuclides

First, the rock samples are physically (crushing, grounding, pulverization, sieving and magnetic separation, heavy liquid separation) and chemically processed (repeated acid etches) to isolate and purify the target minerals (see Tab. 1), isolate the nuclides and separate them from meteoric

cosmogenic nuclides (Corbett et al., 2016; Gosse & Phillips, 2001; Mifsud et al., 2023). The nuclide concentration is then measured as the ratio of the radioactive nuclide and its stable isotope using accelerator mass spectrometry (AMS) or gas mass spectrometry (for noble gases). This ratio is converted into isotope concentration to calculate age (Gosse & Phillips, 2001).

Table 1 The most common in-situ cosmogenic nuclides, production rate at SLHL. (Darvill (2013); Von Blanckenburg & Willenbring (2014).

Isotope	Half-life	Production rate [atoms $g^{-1}y^{-1}$]	Mineral
^{3}He	stable	75-120	olivine, pyroxene
^{21}Ne	stable	18-21	quartz, pyroxene, olivine
^{10}Be	1.4 Ma	4-5	quartz
^{26}Al	0.7 Ma	35	quartz
^{36}Cl	0.3 Ma	70 (Ca) 200 (K)	calcite, K-feldspar
^{14}C	5.7 Ka	18-20	quartz

3.1. Production rate and scaling

The second requirement for successful exposure age estimate is (besides the accurate nuclide concentration measurement) an estimate of the production rate of the nuclides at the sampling site, which is based on physical principles and empirical approaches, including measurements of contemporary cosmic-ray flux and long-term production rates derived from nuclide concentrations in independently dated features using alternative dating techniques (Balco, 2011; Davies, 2022). The production rate varies with latitude (position in the geomagnetic field), elevation, the thickness and density of the sample (Dunai, 2000; Lal, 1991; Stone, 2000), and with time because of the temporary changes in the geomagnetic field (Fig. 2) (Balco, 2020).

Published production rates are usually normalised to sea-level and high latitude (SLHL), so they must be scaled for a specific locality according to its latitude and elevation to get a site-specific production rate estimate. The scaling models consider latitude, elevation, atmospheric pressure, geomagnetic field variability and changes in solar activity (Darvill, 2013). The different scaling models have very similar results for higher latitudes (>30°) and lower elevations below 3000 m, but there are significant differences at lower latitudes and higher elevations (Balco et al., 2008; Dunai & Lifton, 2014). When comparing various results, they should be recalculated with the same scaling scheme, and hence, it is necessary that publications provide all the original input data (Balco et al., 2008).

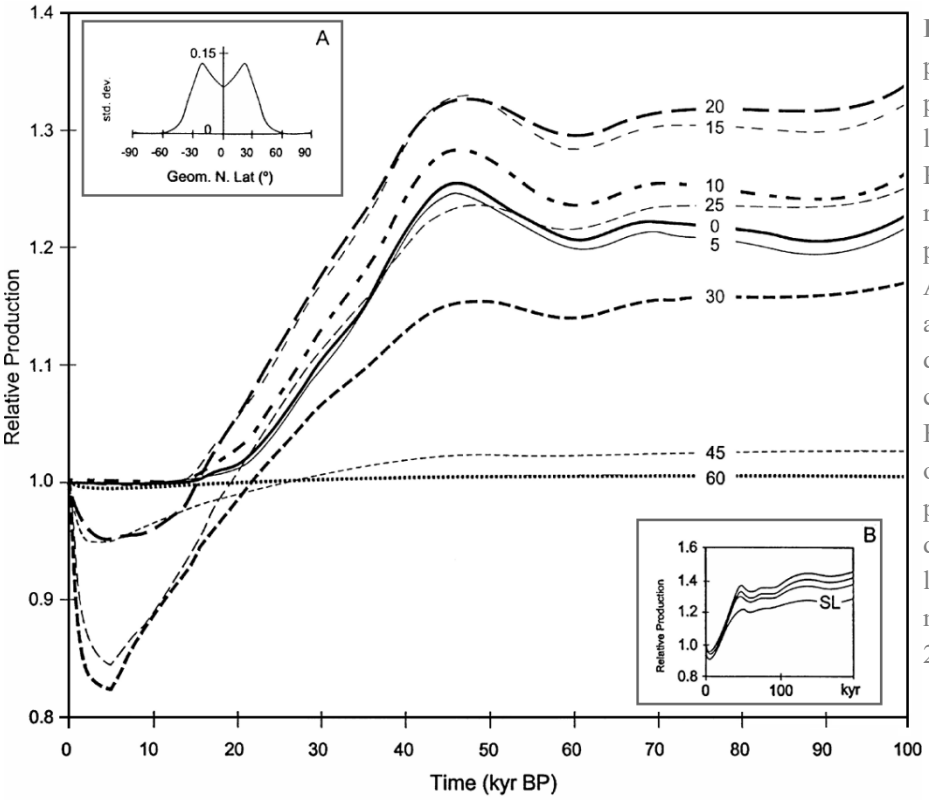

Figure 2 The effect of paleointensity on production rate in different latitudes (in 2000 masl). Relative production – the ratio of past and present production rate.
A: standard deviation of the average production rate during past 200 ky compared to latitude.
B: effect of paleointensity on cosmogenic nuclide production in time at different elevation (SL: sea level, 1000, 2000, 3000 masl). (Gosse & Phillips, 2001).

4. Exposure dating with cosmogenic nuclides

Cosmogenic nuclide exposure dating of glacial sediments allows a direct reconstruction of glacier retreat. Glaciers transport fresh rock previously shielded from cosmic radiation, resulting in negligible nuclide concentrations. This can occur through quarrying at the glacier bed, where ice removes fresh rock from the underlying surface, or by incorporating rockfall debris from surrounding mountain slopes (Balco, 2011; Ivy-Ochs & Briner, 2014). Once deposited on moraines, these boulders remain in place as the glacier retreats, becoming exposed to cosmic rays and accumulating cosmogenic nuclides. If they remain undisturbed for the duration of the exposure, their nuclide concentrations provide a reliable estimate of the exposure age (Balco, 2011; Ivy-Ochs & Briner, 2014). The timescale over which an isotope can be used for dating is limited by saturation, when the production rate of that particular cosmogenic nuclide reaches equilibrium with the erosion rate and decay (Darvill, 2013).

The relationship between the measured concentration of ^{10}Be nuclides (N_{10}, atoms g^{-1}) and the surface exposure age (t, years) assuming zero surface erosion is:

$$N_{10} = \frac{P_{10}}{\lambda_{10}}[1 - \exp(-\lambda_{10} t)]$$

where λ_{10} is the ^{10}Be decay constant ($4.99\times10^{-7}y^{-1}$), P_{10} is the production rate of ^{10}Be (atoms $g^{-1}y^{-1}$) (Balco, 2020). This equation describes the ^{10}Be concentration growth over time due to exposure to cosmic rays, and it reaches equilibrium once production equals decay.

When calculating the exposure age, two types of uncertainties are reported to reflect different sources of error: internal and external uncertainty. Internal uncertainty considers only

uncertainty in nuclide concentration measurement and should be applied to compare samples from a single site (e.g., single moraine). External uncertainty includes the measurement error and uncertainty corresponding to the production rate and scaling scheme. When comparing results to those from different sites (with different production rates) or to different dating methods, external uncertainty should be used (Balco et al., 2008).

4.1. Assumptions for exposure dating

The accuracy of exposure dating relies on several key assumptions: 1) The sample does not contain inherited nuclides from previous episodes of exposure (it has not been exposed to cosmic rays prior to the event studied, or subglacial processes sufficiently eroded its surface before deposition). 2) The sample has remained in a stable position and has not suffered from significant erosion since its deposition. 3) After the glacier retreat, the sample has not been shielded from cosmic rays by topographic obstacles, vegetation, snow, or sediment cover (Gosse & Phillips, 2001; Balco, 2011). These assumptions must be considered when selecting sampling sites and individual boulders to minimise the effect of inappropriate sampling. However, since these conditions are rarely met, it is crucial to account for these variables in data analysis.

4.1.1. Shielding of cosmic radiation

Shielding of cosmic rays by topography, slopes, or surrounding landforms reduces the production rate. Topographic shielding is quantified during sample collection and must be considered for exposure age estimate (Balco et al., 2008; Darvill, 2013). Similarly, other factors such as snow cover, vegetation, soil, or sediments can also shield cosmic rays, but this effect is difficult to quantify, so rock samples should be collected in locations least affected by this shielding (Darvill, 2013).

4.1.2. Incomplete exposure

After glacier retreat, several processes can cause incomplete exposure of boulders, resulting in lower nuclide concentrations and an underestimation of exposure age. These include slope processes and boulder movement (e.g., the overturning of boulders), which expose previously shielded rock surfaces with lower nuclides concentration or moraine denudation, resulting in the exhumation of previously buried boulders with an exposure time not corresponding to the age of moraine deposition (Balco, 2011; Darvill, 2013). The intensity of such processes varies by environment. For example, moraines formed by ice sheets further from rugged, high-mountain areas are typically larger and flatter with broader ridges (Balco, 2011; Barr & Lovell, 2014) with boulders in more stable positions, making the moraines less prone to processes like slope movements compared to moraines in mountain regions (Balco, 2011; Barr & Lovell, 2014). Other post-depositional processes affecting the reliability of exposure dating are

weathering and erosion, which remove the surface layers with high nuclide concentrations (Balco, 2011; Darvill, 2013).

4.1.3. Inherited cosmogenic nuclides

Accuracy of exposure dating is affected when boulders contain inherited cosmogenic nuclides accumulated during exposure prior to their transport and deposition by a glacier. This results in overestimating deposition age (Balco, 2011; Darvill, 2013). Nuclide inheritance can occur due to insufficient surface erosion during subglacial transport, particularly in cases of glacier readvances or the incorporation of material from non-glaciated surrounding areas transported to the glacier through rockfall or other mass movements (Balco, 2011). When multiple boulders are sampled, outliers with significantly higher nuclide concentrations typically indicate inherited nuclides (Balco, 2011; Putkonen & Swanson, 2003).

Understanding the depositional environment and related processes affecting a moraine is crucial for improving dating accuracy. Mountain glacier moraines are generally more susceptible to post-depositional disturbances and nuclide inheritance. Their sharper ridges and steeper slopes make them more prone to surface lowering caused by erosion or slope processes. Additionally, the rugged terrain increases the likelihood of slope processes (e.g., rockfalls) from surrounding unglaciated slopes and peaks. Moreover, the "re-deposition" of previously exposed boulders during subsequent glacier readvances can complicate age estimates (Balco, 2011; Barr & Lovell, 2014). Moraines deposited by ice sheets are generally supposed to be larger, broad-crested, flat, and deposited away from mountain centres (Barr and Lowell, 2014; Balco, 2011). The boulders are in more stable positions, and moraines are less likely to be exposed to, e.g. slope processes than in mountain environments (Barr and Lowell, 2014; Balco, 2011).

A specific challenge arises in polar and high-elevation regions with cold-based glaciers, which are frozen to their bed and cause minimal erosion. This leaves landforms and erratics deposited during previous glacial advances undisturbed, resulting in a mosaic of glacial deposits and landforms of mixed-age populations, leading to potential misinterpretation of exposure ages (Balco, 2011; Bentley et al., 2017). It is, therefore, essential to identify these areas and collect multiple samples to distinguish between different generations of moraines (Balco, 2011).

Climate conditions and related geomorphic processes significantly influence moraine degradation due to effects on weathering, slope, and stability. A range of weathering processes that might cause moraine degradation, operate in the periglacial environments. These include various types of chemical weathering like solution or oxidation (Auqué et al., 2019; Dixon & Thorn, 2005), biological or biochemical weathering, which involves the growth of biota (e.g. lichens, fungi) that colonise the rock surfaces and may directly lead to rock disintegration or contribute to chemical processes (Etienne, 2002; Ganyushkin et al., 2021), and mechanical weathering.

Mechanical weathering processes include, in particular, thermal stress fatigue (Hall, 1999), salt weathering (Matsuoka, 1995), and frost weathering (Hales & Roering, 2007; Kellerer-Pirklbauer, 2017). Thermally induced stress of rock surface caused by rapid temperature fluctuations (≥2°C/min) is important in cold, arid regions, as it can contribute to weathering even in the absence of moisture (Hall, 1999). Another key process in cold, arid regions is salt crystallisation within rock fractures due to evaporation or sublimation, which leads to the disintegration of rock (Matsuoka, 1995).

Frost weathering includes two main processes: freeze-thaw weathering and ice segregation, both of which have been extensively studied. First, the number of freeze-thaw cycles has been identified as a key parameter for frost weathering, even though it is most effective in shallow rock depths (Kellerer-Pirklbauer, 2017). Some authors have rather used effective freeze-thaw cycles (where temperature crosses ±2 °C thresholds) (Matsuoka, 1990) or have discussed the importance of the duration of a freezing event (Matsuoka, 1990) and freezing intensity (McGreevy & Whalley, 1982). The second process, ice segregation, is most effective within the temperature range of -3 to -8 °C in the presence of available moisture (R. S. Anderson, 1998; Hales & Roering, 2007; Hallet & Putkonen, 1994).

4.2. Moraine ages scatter and identification of processes from data analysis

To identify the processes affecting moraine boulders and improve age estimates, multiple samples should be collected from a single moraine. Although generally a higher number of samples is preferable, the cost constraints of the method often dictate the sampling strategies. The minimum recommended number of samples per moraine is at least three (Darvill, 2013; Gosse & Phillips, 2001), though even this is often not met. According to Putkonen & Swanson (2003), for the same level of accuracy, the minimum number of samples is one to four for smaller, younger moraines and six to seven samples for older, larger moraines.

In theory, without prior or incomplete exposure, all boulders from a single moraine would yield a well-clustered age, but due to the processes mentioned in section 2.1, that is not always true. Analysing more samples per moraine helps better to estimate the moraine age and gives evidence of the processes affecting the moraine. The scatter of exposure ages, their distribution, and identification of outliers or data skewness indicate signatures of inheritance or moraine degradation (Applegate et al., 2010, 2012; Balco, 2011; Hallet & Putkonen, 1994; Putkonen & Swanson, 2003).

The processes affecting moraine stability and degradation are crucial in estimating moraine deposition age. When exposure ages are well-clustered, the mean age of dated boulders reasonably approximates moraine formation (Balco, 2011). The mean age (after removing clear outliers) might be considered a robust approach, particularly for comparing moraines across different environments. However, some studies use the mean only when ages follow a normal distribution or are well-clustered (Amidon et al., 2013; Owen et al., 2012; Winsor et al., 2014).

Significant scatter in ages (indicating post-depositional processes or inheritance) complicates interpretation, and different studies propose alternative approaches. Some authors argue that moraine degradation plays a more significant role than prior exposure as inheritance produces rare and easily identifiable outliers and suggest preferring older ages when other evidence is absent (Heyman et al., 2011b; Putkonen & Swanson, 2003). The oldest age would then represent the most accurate estimate of moraine formation age (Chevalier et al., 2011; Hallet & Putkonen, 1994; Röhringer et al., 2012; Stübner et al., 2017; Zech J. et al., 2009).

Applegate et al. (2012) attempted to differentiate between the processes by analysing data skewness and suggested using the youngest, oldest, or mean age when skewness indicates inheritance, degradation, or neither. While statistical methods help distinguish these effects, they are most reliable with larger sample sizes. In smaller datasets, field observations often guide interpretations (Stübner et al., 2017). On the other hand, reliance on field observations introduces subjectivity and potentially inconsistent estimates. Furthermore, methods that depend on extreme values (i.e., selecting the youngest or oldest sample) can be skewed by a single outlier (Balco, 2011).

Beyond these conventional methods, other such as probabilistic approaches comparing modelled and observed age distributions offer additional insights (Balco, 2011).

5. Methods

5.1. Data compilation

5.1.1. Exposure age data

We reviewed the original papers listed in the global database of published ^{10}Be and ^{26}Al data from glacial samples (Expage, 2023) and compiled a database including only boulder, cobble and pebble samples from moraines, that comprised 526 publications (Table 2). The exposure ages in Expage database are recalculated using modified version of the CRONUS calculator (Balco et al., 2008) and we used these recalculated ages, not the age calculations as originally published. No additional snow-shielding correction was applied to the exposure ages. In regions with frequent snow cover, snow can reduce the cosmogenic nuclide production rate (Schildgen et al., 2005), and the absence of the snow cover correction can introduce some error in the calculated exposure ages. However, this does not significantly affect our analysis, focusing on the clustering of exposure ages for individual moraine sites.

For the clustering analysis, we used the internal uncertainty that considered only measurement uncertainty in the nuclide concentration (Balco et al., 2008). Unlike the external uncertainty, the internal uncertainty is the same for all scaling schemes and should be considered when comparing measurements from one site (Balco et al., 2008).

Other data used from the database were geographic coordinates, latitude and longitude, and elevation of samples. Elevation and latitude were used as some of the potential descriptors of the environment examined to assess possible relationship with moraine age scatter.

5.1.2. Data from the original publications

Based on the information in the original publications, moraine samples were identified and classified into moraine ridge groups, assuming each group represents a single deglaciation age. Moraine ridge was defined as a continuous crest and the classification was based on topography maps in the figurework of the published papers. Groups from multiple papers were not combined. The dataset comprised 10 083 samples categorized into 3243 moraine ridge groups. We also classified the type of ice mass that formed the moraines into four categories: (i) Ice sheet in low relief, (ii) Ice sheet in high relief, (iii) Icecap or icefield outlet glaciers, and (iv) Mountain glaciation, assuming that geomorphic processes affect the exposure age scatter differently for different size and shape of moraines.

The data were categorized into regions based on their geographic location. The main regions include Africa, Alaska, Antarctica, British Isles, Europe and western Asia (Eu. + W-Asia), Greenland, High Asia, Japan and Taiwan, North America (N-Am.), northeastern Asia (NE-Asia), northern South America (NS-Am.), Oceania, southern South America (SS-Am.) and Svalbard. For some analyses region and type of ice mass were combined (either grouping ice sheet and ice sheet in high relief or icefield/icecap and mountain glaciation). When referring to specific ice sheets we use their established names: Antarctic ice sheet (AIS), British-Irish Ice Sheet (BIIS), Cordilleran Ice Sheet (CIS), Laurentide Ice Sheet (LIS), Fennoscandian Ice Sheet (FIS), and Greenland Ice Sheet (GIS). The regionalisation is supposed to reflect the extent and configuration of past glaciations.

Table 2 List of publications with moraine samples dated with ^{10}Be included in the database

Abbühl et al., 2009	Balco et al., 2002	Batbaatar & Gillespie, 2016
Abramowski, 2004	Balco et al., 2009	Becker et al., 2018
Abramowski et al., 2006	Balco et al., 2014	Benn et al., 2006
Ackert et al., 2007	Balco et al., 2016	Benson et al., 2004
Ackert. et al., 2008	Balco & Schaefer, 2006	Benson et al., 2007
Akçar et al., 2007	Ballantyne et al., 2008	Bentley et al., 2007
Akçar et al., 2014	Ballantyne et al., 2009	Bentley et al., 2017
Akçar et al., 2020	Ballantyne et al., 2013	Bichler et al., 2016
Alexanderson & Fabel, 2015	Ballantyne et al., 2014	Biette et al., 2020
Alexanderson & Håkansson, 2014	Balter-Kennedy et al., 2020	Blard et al., 2013
Alloway et al., 2018	Barnard et al., 2006	Blomdin et al., 2018
Amidon et al., 2013	Barnard et al., 2004a	Böhlert et al., 2011
Amos et al., 2010	Barnard et al., 2004b	Boxleitner et al., 2017
Anderson et al., 2017	Baroni et al., 2017	Boxleitner et al., 2018
Anderson et al., 2020	Baroni et al., 2018	Boxleitner et al., 2019a
Anjar et al., 2014	Baroni et al., 2021	Boxleitner et al., 2019
Anjar et al., 2021	Barrows et al., 2001	Braakhekke et al., 2020
Aoki, 2000	Barrows et al., 2002	Bradwell et al., 2008
Aoki, 2003	Barrows et al., 2007	Bradwell et al., 2021a
Arzhannikov et al., 2012	Barrows et al., 2013	Bradwell et al., 2021b
Badding et al., 2013	Barth et al., 2016	Braucher et al., 2006
Bai et al., 2018	Barth et al., 2018	Braumann et al., 2020
Bakke et al., 2021	Batbaatar et al., 2018	Briner, 2009
Balbas et al., 2017	Batbaatar et al., 2020	Briner et al., 2003

Briner et al., 2005
Briner et al., 2007
Briner et al., 2014
Briner et al., 2017
Briner & Hormes, 2018
Bromley et al., 2015
Bromley et al, 2016
Bromley et al, 2020
Brook et al., 2008
Brook et al., 1993
Brook et al., 1995
Brook et al., 2008
Brown et al., 1991
Brown et al., 2002
Brugger, 2007
Brugger et al., 2019a
Brugger et al., 2019b
Carcaillet et al., 2013
Carlson et al., 2014
Carrasco et al., 2013
Carrasco et al., 2015
Ceperley et al., 2019
Clark et al., 2003
Clark et al., 2009a
Clark et al., 2009b
Cogez et al., 2018
Colgan et al., 2006
Corbett et al., 2015
Cossart et al., 2012
Crest et al., 2017
Crump et al., 2017
Crump et al., 2019
Crump et al., 2020
Cunningham et al., 2018
Dahms et al., 2018
D'Arcy et al., 2019
Darvill et al., 2018
Davies et al., 2017
Davies et al., 2018
Davis et al., 1999
Davis et al., 2015
Delmas et al., 2008
Delmas et al., 2011
Denton et al., 2021
Di Nicola et al., 2009
Dieleman et al., 2018
Dong et al., 2014
Dong et al., 2016
Dong et al., 2017a
Dong et al., 2017b
Dong et al., 2018
Dong et al., 2020
Dong et al., 2022
Dortch et al., 2013
Dortch et al., 2010a
Dortch et al., 2010b
Dortch et al., 2010c
Doughty et al., 2015
Douglass et al., 2005
Douglass et al., 2006
Dowling et al., 2021
Dühnforth & Anderson, 2011
Egli et al., 2020
Engel et al., 2011
Engel et al., 2014
Engel et al., 2015
Engel et al., 2017
Everest et al., 2006
Everest & Kubik, 2006
Fabel et al., 2004
Fabel et al., 2006
Fame et al., 2018
Farber et al., 2005
Favilli et al., 2009
Federici et al., 2008
Federici et al., 2012
Fernández et al., 2022
Fernández-Fernández et al., 2017
Fink et al., 2006
Finkel et al., 2003
Finlayson et al., 2011
Finlayson et al., 2014
Fleming, 2019
Fogwill, 2003
Fogwill et al., 2014
Fu et al., 2013
Ganyushkin et al., 2018
García et al., 2012
García et al., 2018
García et al., 2019
García et al., 2020
García-Ruiz et al., 2020
Gayer et al., 2004
Gheorghiu et al., 2012
Gheorghiu et al., 2015
Gianotti et al., 2008
Gillespie et al., 2008
Glasser et al., 2006
Glasser et al., 2009
Glasser et al., 2011
Glasser et al., 2012
Glasser et al., 2014
Goehring et al., 2010
Goehring et al., 2012
Gosse et al., 1995a
Gosse et al., 1995b
Graf et al., 2008
Grant, 2016
Gribenski et al., 2016
Gribenski et al., 2018
Grin et al., 2016
Gump et al., 2017
Håkansson et al., 2007
Hall et al., 2009
Hall et al., 2016
Hall et al., 2020
Harrison et al., 2010
Heath et al., 2020
Chen et al., 2015
Chenet et al., 2016
Chevalier et al., 2011
Chevalier et al., 2016
Chevalier et al., 2018
Chevalier et al., 2022
Chevalier & Replumaz, 2019
Hebenstreit et al., 2011
Hedrick et al., 2011
Hedrick et al., 2017
Hein et al., 2009
Hein et al., 2010
Hein et al., 2011a
Hein et al., 2011b
Hein et al., 2016a
Hein et al., 2016b
Hein et al., 2017
Heine et al., 2009
Henriksen et al., 2014
Heyman et al., 2011a
Hodgson et al., 2012
Hofmann, 2018
Hormes et al., 2008
Houmark-Nielsen et al., 2012
Howle et al., 2012
Hu et al., 2017
Hubert-Ferrari et al., 2005
Hughes et al., 2014
Hughes et al., 2018
Ivy-Ochs et al., 1996
Ivy-Ochs et al., 1999
Ivy-Ochs et al., 2004
Ivy-Ochs et al., 2006a
Ivy-Ochs et al., 2006b
Ivy-Ochs et al., 2008
Ivy-Ochs et al., 2018
Jackson et al., 1997
Jackson et al., 2019
Jackson et al., 2020
Johnsen et al., 2009
Johnsen et al., 2010
Jomelli et al., 2011
Jomelli et al., 2014
Jones et al., 2021
Joy et al., 2017
Kaplan et al., 2004
Kaplan et al., 2005
Kaplan et al., 2007
Kaplan et al., 2008
Kaplan et al., 2010
Kaplan et al., 2011
Kaplan et al., 2013
Kaplan et al., 2016
Kawamata et al., 2020
Kelley et al., 2014
Kelly et al., 2004
Kelly et al., 2008
Kelly et al., 2014
Kelly et al., 2015

Kerschner et al., 2006
Khandsuren et al., 2019
Kiernan et al., 2004
Kiernan et al., 2010
Kiernan et al., 2014
Kiernan et al., 2017
Kirkbride et al., 2014
Kleman et al., 2020
Koester et al., 2017
Koffman et al., 2017
Kohut, 2011
Kong et al., 2009a
Kong et al., 2009b
Koppes et al., 2008
Kronig et al., 2018
Kuhlemann et al., 2009
Kuhlemann et al., 2013a
Kuhlemann et al., 2013b
Laabs et al., 2007
Laabs et al., 2011
Laabs et al., 2013
Laabs et al., 2020
Landvik et al., 2003
Lane et al., 2020
Larsen et al., 2012
Larsen et al., 2014
Larsen et al., 2016
Larsen et al., 2021
Lasserre et al., 2002
Le Roy et al., 2017
Lee et al., 2014
Leger et al., 2021
Leonard et al., 2017
Lesnek & Briner, 2018
Levy et al., 2012
Levy et al., 2014
Levy et al., 2016
Levy et al., 2018
Levy et al., 2020
Li et al., 2011
Li et al., 2014
Li et al., 2016
Licciardi et al., 2001
Licciardi et al., 2004
Licciardi et al., 2009
Licciardi & Pierce, 2008
Licciardi & Pierce, 2018
Lifton et al., 2014
Liu et al., 2017
Liu et al., 2018
Lowell et al., 2013
Luna et al., 2018
Makos et al., 2016
Makos et al., 2018
Mangerud et al., 2008
Mangerud et al., 2013
Marcott et al., 2019
Margold et al., 2016
Margreth et al., 2017
Marsella et al., 2000
Martin et al., 2018
Martin et al., 2020
Martini et al., 2017
Mathers, 2014
Matmon et al., 2006
Matmon et al., 2010
Mattas, 2021
Matthews et al., 2008
May et al., 2011
McCarthy et al., 2008
Mendelová et al., 2020
Menounos et al., 2013a
Menounos et al., 2013b
Menounos et al., 2017
Mentlík et al., 2013
Mériaux et al., 2004
Mey et al., 2020
Meyer et al., 2020
Möller et al., 2010
Moore et al., 2022
Moran et al., 2016a
Moran et al., 2016b
Moran et al., 2017
Moreiras et al., 2017
Moreno et al., 2009
Munroe et al., 2006
Murari et al., 2014
Murray et al., 2012
Nimick et al., 2016
Nishiizumi et al., 1993
Norris et al., 2022
Oberholzer et al., 2003
O'Hara et al., 2017
Oliva et al., 2021
Orr et al., 2017
Orr et al., 2018
Owen et al., 2002
Owen et al., 2005
Owen et al., 2006a
Owen et al., 2006b
Owen et al., 2009
Owen et al., 2010
Owen et al., 2012
Owen et al., 2003a
Owen et al., 2003b
Owen et al., 2003c
Palacios et al., 2019
Palacios et al., 2020
Pallàs et al., 2006
Pallàs et al., 2010
Pendleton et al., 2015
Pendleton et al., 2017
Peng et al., 2019
Peng et al., 2020
Phillips et al., 2000
Phillips et al., 2016
Philipps et al., 2017
Pierce et al., 2017
Pötsch, 2017
Pratt-Sitaula et al., 2011
Protin, 2019
Protin et al., 2019
Protin et al., 2021
Putnam et al., 2010
Putnam et al., 2012
Putnam et al., 2013a
Putnam et al., 2013b
Putnam et al., 2019
Quirk et al., 2018
Quirk et al., 2020
Quirk et al., 2022
Reber et al., 2014a
Reber et al., 2014b
Refsnider et al., 2008
Regnéll et al., 2022
Reitner et al., 2016
Reusche et al., 2014
Reusche et al., 2018
Reuther et al., 2007
Reuther et al., 2011
Reynhout et al., 2019
Reynhout et al., 2022
Ribolini et al., 2018
Rinterknecht et al., 2004
Rinterknecht et al., 2006
Rinterknecht et al., 2009
Rinterknecht et al., 2012a
Rinterknecht et al., 2012b
Rinterknecht et al., 2014
Roberts et al., 2013
Rodríguez-Rodríguez et al., 2014
Rodríguez-Rodríguez et al., 2016
Rodríguez-Rodríguez et al., 2017
Rodríguez-Rodríguez et al., 2018
Röhringer et al., 2012
Romundset et al., 2017
Rood et al., 2011
Rother, 2006
Rother et al., 2014a
Rother et al., 2014b
Rother et al., 2017
Ruleman et al., 2018
Ruszkiczay-Rüdiger et al., 2016
Ruszkiczay-Rüdiger et al., 2021
Sagredo et al., 2011
Sagredo et al., 2017
Sagredo et al., 2018
Saha et al., 2016
Saha et al., 2018
Saha et al., 2019
Schaefer et al., 2006
Schaefer et al., 2008
Schaefer et al., 2009
Schaefer et al., 2015
Schäfer et al., 2002
Scherler et al., 2010
Scherler et al., 2014

Schimmelpfennig et al., 2012
Schimmelpfennig et al., 2014
Schindelwig et al., 2012
Schweinsberg et al., 2019
Schweinsberg et al., 2020
Seong et al., 2007
Seong et al., 2009
Shakesby et al., 2008
Shakun et al., 2015
Shulmeister et al., 2005
Shulmeister et al., 2010
Shulmeister et al., 2018
Siame et al., 2007
Sinclair, 2019
Small et al., 2012
Small et al., 2017
Small et al., 2021
Small & Fabel, 2016
Smith et al., 2005a
Smith et al., 2005b
Smith et al., 2011
Smith et al., 2016
Smith & Rodbell, 2010
Søndergaard et al., 2019
Standell, 2014
Stansell et al., 2015
Stansell et al., 2017
Steig et al., 1998
Steinemann et al., 2020
Storey et al., 2010 Strand et al., 2019
Strand et al., 2022
Strasky et al., 2009a
Strasky, 2009b
Strelin et al., 2014
Stroeven et al., 2010
Stroeven et al., 2014
Stroup et al., 2014
Stroup et al., 2015
Stübner et al., 2017
Suganuma et al., 2014
Sutherland et al., 2007
Svendsen et al., 2019
Terrizzano et al., 2017
Thorndycraft et al., 2019
Tielidze et al., 2020
Todd et al., 2010
Tschudi et al., 2003
Tulenko et al., 2018
Ullman et al., 2015
Ullman et al., 2016
Valentino et al., 2021
Valletta et al., 2017
Voisine et al., 2020
Wang et al., 2006
Wang et al., 2013
Wang et al., 2020
Ward et al., 2015
Ward & Anderson, 2011
Wesnousky et al., 2012
Wesnousky et al., 2016
Wilson et al., 2013
Wilson et al., 2018
Wilson et al., 2019
Wilson et al., 2020
Winkler, 2014
Winsor et al., 2014
Winsor et al., 2015
Wittmeier et al., 2020
Wüthrich et al., 2018
Xu et al., 201
Xu et al., 2020
Young et al., 2009
Young et al., 2011
Young et al., 2011
Young et al., 2012
Young et al., 2013
Young et al., 2015
Young et al., 2019
Young et al., 2020
Young et al., 2021
Young et al., 2021
Zahno et al., 2009
Zahno et al., 2010
Zasadni et al., 2020
Zech, J. et al., 2009
Zech, J. et al., 2010
Zech, J. et al., 2017
Zech, R., 2012
Zech, R. et al., 2005
Zech, R. et al., 2006
Zech, R. et al., 2007a
Zech, R. et al., 2007b
Zech, R. et al., 2009
Zech, R. et al., 2011
Zech, R. et al., 2013
Zeng et al., 2021
Zhang et al., 2016
Zhang et al., 2018
Zhou et al., 2007

5.1.3. Climate and terrain variables from other datasets

The topographic and climate variables selected for the analysis (summarised in Table 3) are assumed to influence the intensity of geomorphic processes and hence the rate of denudation, or to sufficiently characterize the environments (e.g. Conrad continentality index – CCI, elevation). Relative topography should reflect the surrounding landscape dynamics, assuming more active geomorphic processes for higher relative topography (Barr and Lowell, 2014). Climate controls like temperature, precipitation or temperature ranges are linked to weathering processes (e. g., Ovlmo, 2010; Hall, 1999), while being simple and easily accessible, reducing potential cumulative errors.

Table 3 Examined variables

Variable		Source dataset
Exposure age Elevation Latitude		*Expage database*
Ice Mass		*Original publications*
Landscape relief (Demek et al., 1971)	(within a buffer of 2 km)	*ASTER GDEM v3, ArcticDEM, CryoSat-2 Antarctica 1km DEM*
Mean annual precipitation Mean annual 2 m air temperature Mean annual range of 2 m air temperature Mean diurnal range of 2 m air temperature Conrad's continentality index	(1951-2020)	*ERALClim*
Time spent in frost cracking window (-8 to -3 °C) Number of freeze-thaw cycles	(1951-2020)	*ERA5-Land Hourly*
Köppen-Trewartha climate classification	(1951-2020)	*Belda et al., 2014*

The Conrad continentality index, a function of latitude and annual mean temperature, and Trewartha climate classification (based on temperatures and precipitation) were included as alternative descriptors of climate conditions. The only more complex variables were simplified descriptors of frost weathering processes, included to provide an insight into this mechanism operating in periglacial environments.

The topographic relief and regional climate data were evaluated using Google Earth Engine for all samples. Based on the digital elevation models ASTER GDEM v3 (NASA, 2019) complemented by ArcticDEM (Porter et al., 2018) and CryoSat-2 Antarctica 1km DEM (Slater at al., 2018), the relative topography was calculated for each sample as a difference between the maximum and minimum elevation within a 2 km buffer zone (Demek et al., 1971).

Regional climate variables such as mean annual precipitation (P), mean annual 2 m air temperature (T), mean diurnal temperature range (DTR), and mean annual range of 2 m temperature (ATR) were derived from ERALClim (a database derived from ERA5-Land reanalysis data) that covers the period from 1951 to 2020 (Lea et al., 2024). Using these data, the Conrad continentality index (CCI) was determined to characterize the degree of continentality (Conrad, 1946).

Two parameters were used as proxies for frost weathering intensity: the time spent in the frost cracking window (FCW) (-8 °C to -3 °C) and the number of freeze-thaw (F-T) cycles (oscillation over 0 °C). Both metrics were calculated for the period 1951 to 2020 using skin temperature (temperature of the surface of the Earth) from ERA5-Land Hourly data (Muñoz Sabater, 2019).

To better capture the prevailing climate conditions, each sample was assigned a Trewartha climate classification category B to F (B: dry climates, C: subtropical climates,

D: temperate climates, E: boreal, F: polar climates) applied from 1951 to 1980 (Belda et al., 2014).

Before conducting the analysis, potential collinearity among the variables was evaluated. Several variable pairs show moderate to strong correlations—for example, continentality with diurnal (0.80) or annual temperature range (0.80) and elevation (0.61); diurnal temperature range with elevation (0.75) and freeze–thaw cycles (0.67); precipitation with annual temperature range (–0.71) and mean temperature (0.60); freeze–thaw cycles with elevation (0.68); and mean temperature with annual temperature range (–0.61) (see correlation matrix in Fig. 3). Some degree of correlation was expected, particularly because continentality is derived from latitude and temperature range.

To further assess multicollinearity, variance inflation factors (VIF) were calculated. After removing continentality and either annual or diurnal temperature range, all VIF values decreased to below 4 (see Tab. 4). Nevertheless, all variables were retained for subsequent analyses, as the primary aim was to identify the most relevant environmental descriptors that may explain variations in moraine age clustering (moraine degradation).

Figure 3 Correlation matrix for examined variables, correlation calculated with Spearman's rank correlation coefficient.

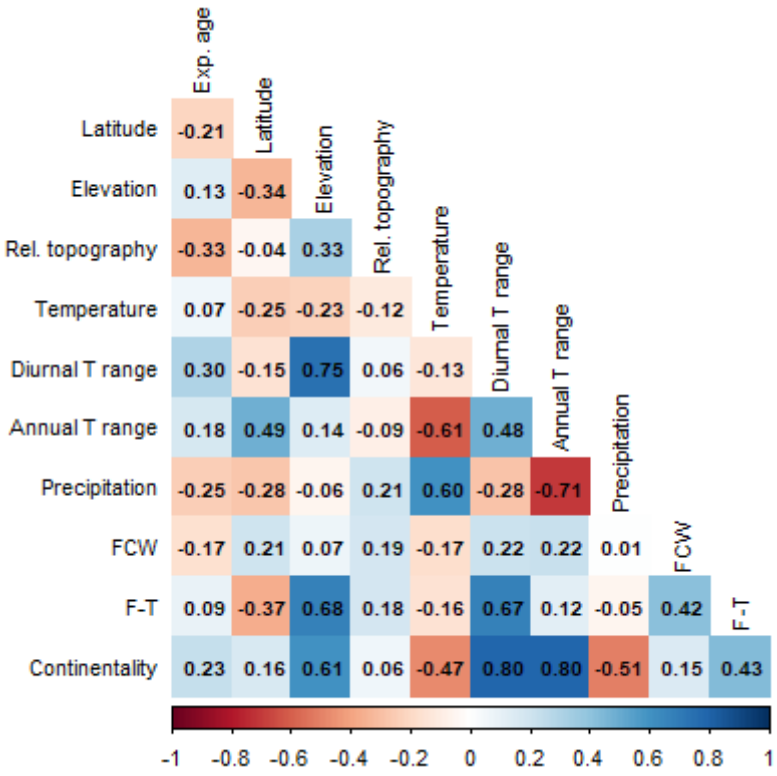

Table 4 Variance inflation factor values for examined variables.

Variables	**VIF**	**VIF**
Exposure age	1.18	1.17
Latitude	2.40	1.92
Elevation	9.62	3.00
Relative topography	1.57	1.51
Annual T	3.35	1.80
Diurnal T range	8.16	-
Annual T range	20.18	2.69
Precipitation	2.73	1.61
Time spent in FCW	2.28	2.12
Number of F-T cycles	3.71	3.54
Continentality	20.54	-

5.2. Data Analysis

To assess the quality of boulder group exposure ages, we evaluate their clustering, assuming that in theory (without prior or incomplete exposure), all boulders from a single moraine would

yield a single, well-clustered age. To quantify the clustering, we calculated the reduced chi-square value (χ_R^2) (or mean square weighted deviation – MSWD) for all boulder groups with at least three samples (Balco, 2011; Heyman et al., 2016):

$$\chi_R^2 = \frac{1}{n-1}\sum_{i=1}^{n}\left(\frac{t_i - \bar{t}}{\sigma_i}\right)^2$$

Where:

- t_i = individual apparent exposure ages
- $\bar{t}$ = group mean age
- σ_i = individual uncertainties (internal uncertainty – nuclide concentration measurement error; Balco et al., 2008)

The χ_R^2 is close to 1 if the only source of scatter is the measurement uncertainty, increasing with the exposure age scatter (Balco, 2011). We adopted the cut-off value of 2 for well-clustered ($\chi_R^2 < 2$) and scattered groups ($\chi_R^2 \geq 2$) following Heyman et al. (2011b). To get a better insight into the data for some analyses we also specified a "moderately clustered" category ($2 \leq \chi_R^2 < 3.5$). For instance, Blomdin et al. (2016) defined "moderately clustered" as $\chi_R^2 \geq 2$ with a standard deviation ≤ 15% of the mean exposure age. However, we did not adopt this approach because this criterion may not be meaningful prior to outlier removal, as even a few extreme values can disproportionately inflate the standard deviation and distort how well most of the samples cluster.

For the outlier identification a method based on an iterative reduced chi-squared approach was used, where the outliers with the highest deviation are removed sequentially (Dortch et al., 2022) until the χ_R^2 is lower than two or there are only three remaining samples in the group.

To investigate the influence of examined variables, we compared their values with both the χ_R^2 values and the ratio of well-clustered ages. For practical application, the χ_R^2 values were classified into three categories—well-clustered, moderately clustered, and scattered—rather than relying solely on the exact χ_R^2 values. In exposure dating, the optimal outcome is a well-clustered set of moraine ages (or, alternatively, moderately clustered). For scattered results, the precise χ_R^2 value offers limited additional information, as it mainly reflects poor or questionable clustering.

The dataset was analysed as a whole and also subdivided into several groups based on age type of ice mass or region. Because the data are not normally distributed, we used Spearman's rank correlation coefficient to assess statistical relationships, and did not apply linear regression.

In addition, skewness of the exposure age distribution was used as an indicator of nuclide inheritance (skew > 0.5) or incomplete exposure (skew < -0.5) (Applegate et al., 2010). In the final part of the analysis, we investigated how the number of samples per moraine influences clustering.

6. Results

The dataset contains 3243 globally distributed moraine ridge groups (Fig. 4A). However, only 1620 of these moraines contain at least three samples per ridge and are therefore suitable for further analysis (Fig. 4B). The decrease in the number of moraines with at least three samples is particularly evident in the Alps, New Zealand, Patagonia, and the Rocky Mountains of the USA.

Figure 4 Spatial distribution of moraine ridges dated with cosmogenic nuclides. A: all moraine ridges, B: moraine ridges with at least 3 samples.

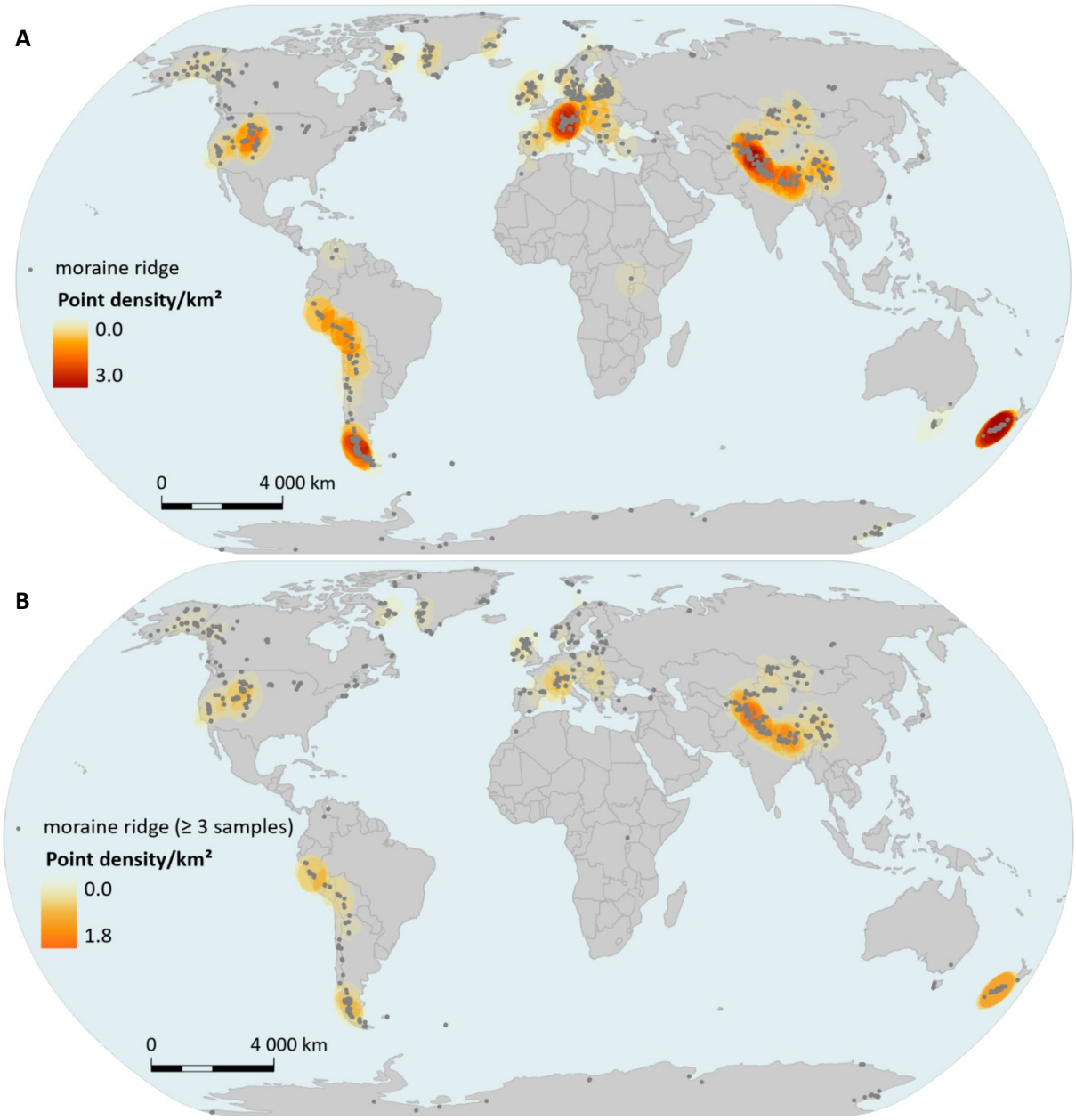

The subset with at least three samples per moraine spans a broad temporal range, with moraine ages ranging from 56 to 5.38 million years (Fig. 5A). Within this group, only 23 % (373 moraines) have well-clustered exposure ages (Fig. 5A, 5B). After removing outliers, the

proportion of well-clustered moraines increases to 46 % (748 moraines) (Fig. 5C, D). Moraines with mean ages between 10 and 20 ka tend to show the best clustering (Fig. 5B, D). The age scatter gradually increases with older moraine ages, and substantial scatter is also observed among the youngest moraines. Beyond 35 ka, only seven moraine groups are classified as well-clustered when outliers are included, but this number increases to 47 after outlier removal.

Figure 5 Exposure age MSWD versus mean exposure age for all moraines with at least three boulders per group; dotted line corresponds to a MSWD = 2. A: overview of the whole dataset, B: Moraines with mean exposure age < 65 ka, C: overview of the whole dataset after removing outliers, D: Moraines with mean exposure age < 65 ka after removing outliers; y-axes are shown with a logarithmic scale, x-axes on A, C are shown with logarithmic scale, YD – Younger Dryas, B-A – Bølling–Allerød, LGM – Last Glacial Maximum

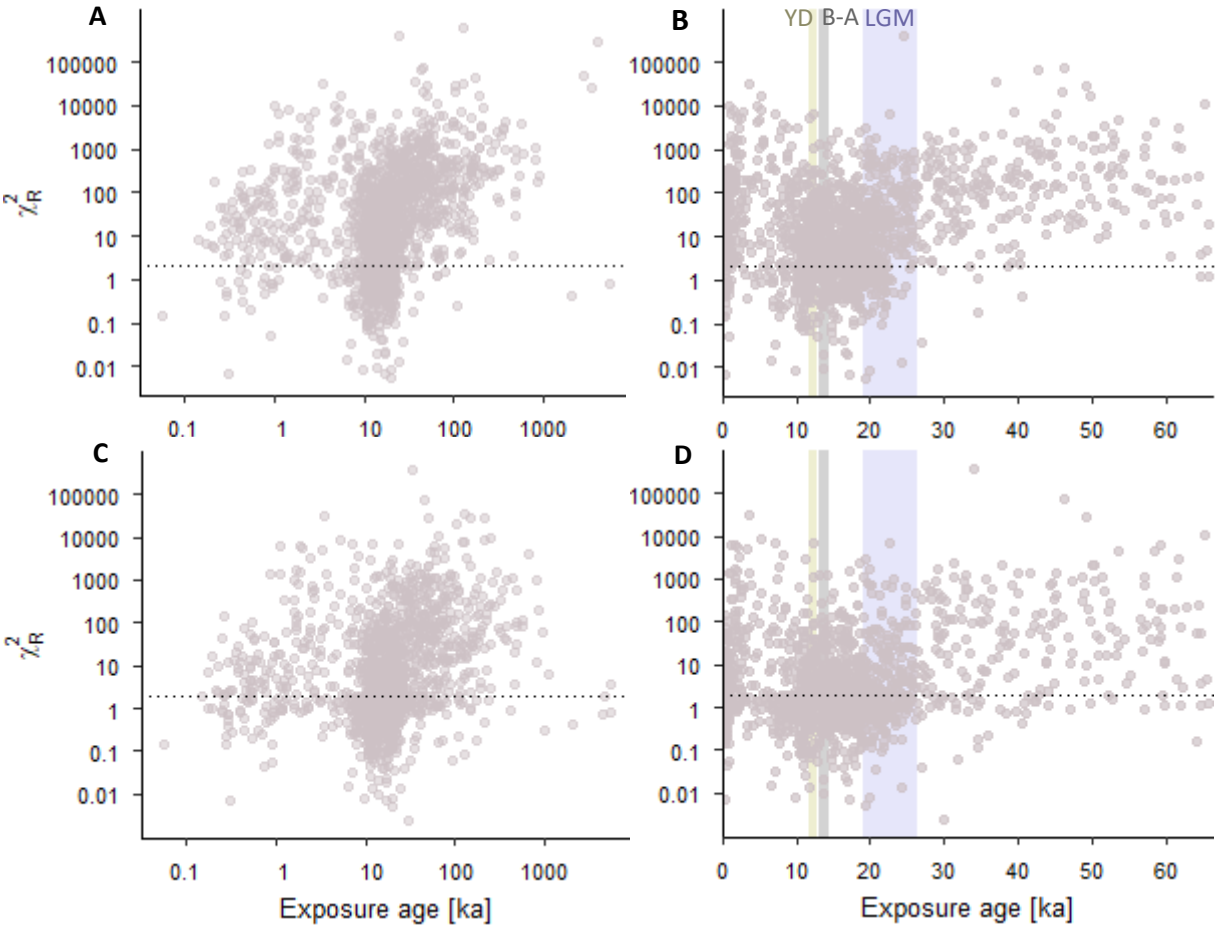

Although the MSWD values tend to increase with moraine mean ages, there is no significant overall trend for the entire dataset, with a Spearman's correlation coefficient of 0.33. However, stronger correlations, indicating potential trends, are observed in specific regions, including northeastern Asia (0.47), ice sheets in Alaska (0.69) and the Patagonian Ice Sheet (PIS) (0.65). When considering only moraines older than 10 ka, the correlation strength increases both globally (0.53) and regionally. In this "older than 10 ka" subset, higher values are observed for mountain glaciation or icefield/icecap category in Greenland (0.79), northern South America (0.72), Alaska (0.46) and Oceania (0.49) (see Table 5). The categories of the Alaskan and Patagonian Ice Sheets consist only of moraines older than 10 ka, thus, no change is observed in correlation values for these regions.

	Region	All data	Age > 10 ka
	Global	**0.33**	**0.53**
Icefield, icecap and mountain glaciation	High Asia	**0.36**	**0.46**
	Europe + W-Asia	-	**0.23**
	Greenland	-	**0.79**
	N-Am.	**0.15**	**0.27**
	Alaska	-	**0.46**
	NE-Asia	**0.47**	**0.49**
	NS-Am.	**0.14**	**0.72**
	Oceania	**0.19**	**0.49**
	SS-Am.	-	**0.32**
	FIS	**0.28**	**0.36**
Ice sheet and ice sheet in high relief	GIS	**0.28**	-
	CIS-LIS	**0.32**	**0.29**
	Alaska	**0.69**	**0.69**
	PIS	**0.65**	**0.65**

Table 5 Spearman's rank correlation coefficient for the relationship between moraine ridge exposure age clustering and age for the whole dataset and moraines older than 10 ka for significance level α=0.01, H_0: ρ=0, H_A: $\rho \neq 0$. Only statistically significant results are presented.

Figure 6 (or, in more detail, Table 6) presents an alternative approach, analysing only the proportion of well-clustered moraine ages within 5 ka age bins. The highest proportion of well-clustered ages occurs between 10 and 20 ka. When outliers are included, the highest percentage of well-clustered ages is 38 % (between 10 to 15 ka). After removing outliers, this percentage exceeds 60 % for the same interval. The proportion of scattered moraine groups increases towards the younger and older age intervals.

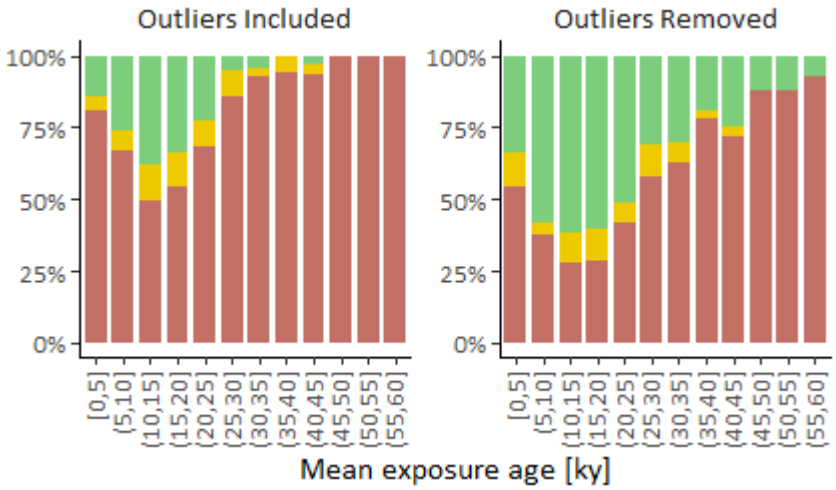

Figure 6 Proportion of well-clustered (green), moderately clustered (yellow) and scattered (red) moraine ridge groups within 5-ky age intervals. Moraine exposure ages clustering is calculated including outliers (left) and after removing outliers (right).

Table 6 Proportion of well—clustered (W-C) moraine ridge groups within 5-ky age intervals. OI: outliers included, OR: outliers removed.

	Mean exposure age [ka]											
	[0,5]	(5,10]	(10,15]	(15,20]	(20,25]	(25,30]	(30,35]	(35,40]	(40,45]	(45,50]	(50,55]	(55,60]
Moraine Ridges [n]	186	114	384	344	182	62	43	36	32	25	25	14
W-C (OI) [%]	14.5	26.3	38.0	34.0	22.5	4.8	4.7	0.0	3.1	0.0	0.0	0.0
W-C (OR) [%]	33.9	57.9	61.7	60.5	51.1	30.7	30.2	19.4	25.0	12.0	12.0	7.1

The assumption that moraine age skewness can indicate inheritance (skew > 0.5) or degradation (skew < -0.5), as proposed by Applegate et al. (2010), was also tested. Among moraines with MSWD ≥ 2, 26.6 % show signs of degradation, and 48.8 % signs of inheritance. However, no significant correlation was found between skewness (or its absolute value) and MSWD (r = 0.17). Independent age controls would be necessary to evaluate the influence of inheritance versus denudation.

6.1. Climate and terrain variables

To investigate the relationship between the MSWD and the other variables, Spearman's rank correlation coefficients were calculated for the whole dataset and its specific subsets grouped by age, type of ice mass and combination of region with type of ice mass (see Table 7, 8). Across the whole dataset, none of the variables showed strong correlations with MSWD. However, some subsets showed relatively higher values, suggesting a potential climate-driven influence (annual mean temperature, annual temperature range, diurnal temperature range or precipitation) on moraine age clustering. These included ice sheets in high relief, icefields and icecaps and the regions of Alaska (icefields, icecaps and mountain glaciation) and the Patagonian Ice Sheet.

Overall, moraine exposure age clustering tends to decrease (MSWD increases) with higher age, elevation, annual and diurnal temperature ranges or continentality, and lower mean annual temperatures, and precipitation (Table 7, 8). Nonetheless, there are some significant exceptions to these general trends. In Greenland (icefields, icecaps and mountain glaciation) the MSWD increases with lower annual temperature range and lower continentality. No significant relationship was found between the MSWD and time spent in frost-cracking window, number of freeze-thaw cycles and relative topography.

				Type of ice mass				*Hemisphere*	
	All data	All data (OR)	Age > 10 ka	Ice Sheet	Ice Sheet in HR	Icecap, Icefield	Mountain glaciation	South	North
Age	**0.33**	**0.28**	**0.53**	**0.53**	**0.33**	**0.36**	**0.28**	**0.38**	**0.31**
NS	**0.21**	**-0.19**	**0.20**	**0.24**	**0.25**	**0.18**	**0.22**	**0.23**	**0.20**
Elev.	**0.20**	**0.15**	**0.21**	**0.35**	**0.24**	**0.35**	**0.18**	-	**0.24**
Lat	-	-	-	**-0.25**	**-0.34**	**0.23**	-	-	**-0.14**
T	**-0.32**	**-0.25**	**-0.35**	-	**-0.51**	**-0.44**	**-0.25**	**-0.13**	**-0.33**
ATR	**0.27**	**0.21**	**0.31**	-	**0.24**	**0.45**	**0.21**	**0.11**	**0.32**
DTR	**0.21**	**0.16**	**0.24**	**0.45**	-	**0.34**	**0.17**	-	**0.25**
P	**-0.32**	**-0.24**	**-0.39**	**0.26**	**-0.49**	**-0.41**	**-0.27**	**-0.26**	**-0.31**
FCW	**-0.06**	-	**-0.06**	-	**-0.20**	-	**-0.11**	**-0.27**	-
F-T	**0.10**	**0.07**	**0.12**	**0.31**	**-0.29**	**0.13**	**0.13**	**-0.17**	**0.23**
RT	-	-	**-0.09**	-	-	**0.14**	**-0.14**	-	-
CCI	**0.29**	**0.21**	**0.33**	-	**0.21**	**0.46**	**0.23**	**0.21**	**0.35**

Table 7 Spearman's rank correlation coefficient for the relationship between moraine ridge groups exposure age clustering and the examined parameters for significance level α=0.05, H_0: ρ=0, H_A: $\rho \neq 0$. Only statistically significant results are presented. Only subsets with statistically significant results are included. OR: outliers removed, Age: mean boulder group exposure age, NS: number of samples per group, Elev.: elevation, Lat: latitude, FCW: time spent in FCW, F-T: number of F-T cycles, RT: relative topography.

Table 8 Spearman's rank correlation coefficient for the relationship between moraine ridge groups exposure age clustering and the examined parameters for significance level $\alpha=0.05$, H_0: $\rho=0$, H_A: $\rho\neq0$. Only statistically significant results are presented. Only subsets with statistically significant results are included.

	Icefield, icecap and mountain glaciation							*Ice sheet and ice sheet in high relief*			
	High Asia	British Isles	Eu. + W-Asia	Greenland	N-Am.	Alaska	NS-Am.	AIS	CIS-LIS	Alaska	PIS
NS	**0.21**	-	**0.21**	**0.58**	**0.19**	-	**0.33**	**0.37**	-	-	-
Elev.	**0.16**	**0.39**	**-0.16**	-	-	-	-	-	**0.40**	-	-
Lat	-	**-0.38**	-	-	-	**0.54**	-	-	-	**0.58**	-
T	**-0.16**	-	-	-	-	-	-	-	-	**-0.55**	-
ATR	**0.22**	-	-	**-0.41**	**-0.18**	**0.64**	-	-	**0.32**	**0.59**	**0.53**
DTR	**0.23**	**0.36**	**-0.17**	-	**-0.18**	**0.39**	**0.18**	-	-	-	**0.48**
P	**-0.21**	**-0.41**	-	-	**-0.18**	**-0.42**	**-0.22**	-	-	-	**-0.32**
FCW	-	-	-	-	-	**-0.33**	-	-	-	-	-
F-T	-	-	-	-	-	**-0.38**	-	-	-	-	-
RT	**-0.19**	-	-	**0.39**	-	-	-	-	-	-	-
CCI	**0.28**	-	-	**-0.39**	**-0.23**	**0.59**	**0.17**	-	**0.32**	-	**0.48**

Similar to the analysis of mean exposure age, the proportion of well-clustered moraine groups was assessed across binned intervals of remaining variables. As shown in Figure 7, the proportion of well-clustered moraines increases significantly with higher mean annual temperature and precipitation and with lower annual temperature range and continentality. A weaker effect is observed with a lower diurnal temperature range and lower elevation. In contrast, certain variables appear to have no effect on moraine age clustering, including time spent within the frost-cracking window, number of freeze-thaw cycles, latitude, and relative topography (Fig. 7).

Figure 7 Proportion of well-clustered (green), moderately clustered (yellow) and scattered (red) moraine ridge groups within bins of environmental and topographic variables.

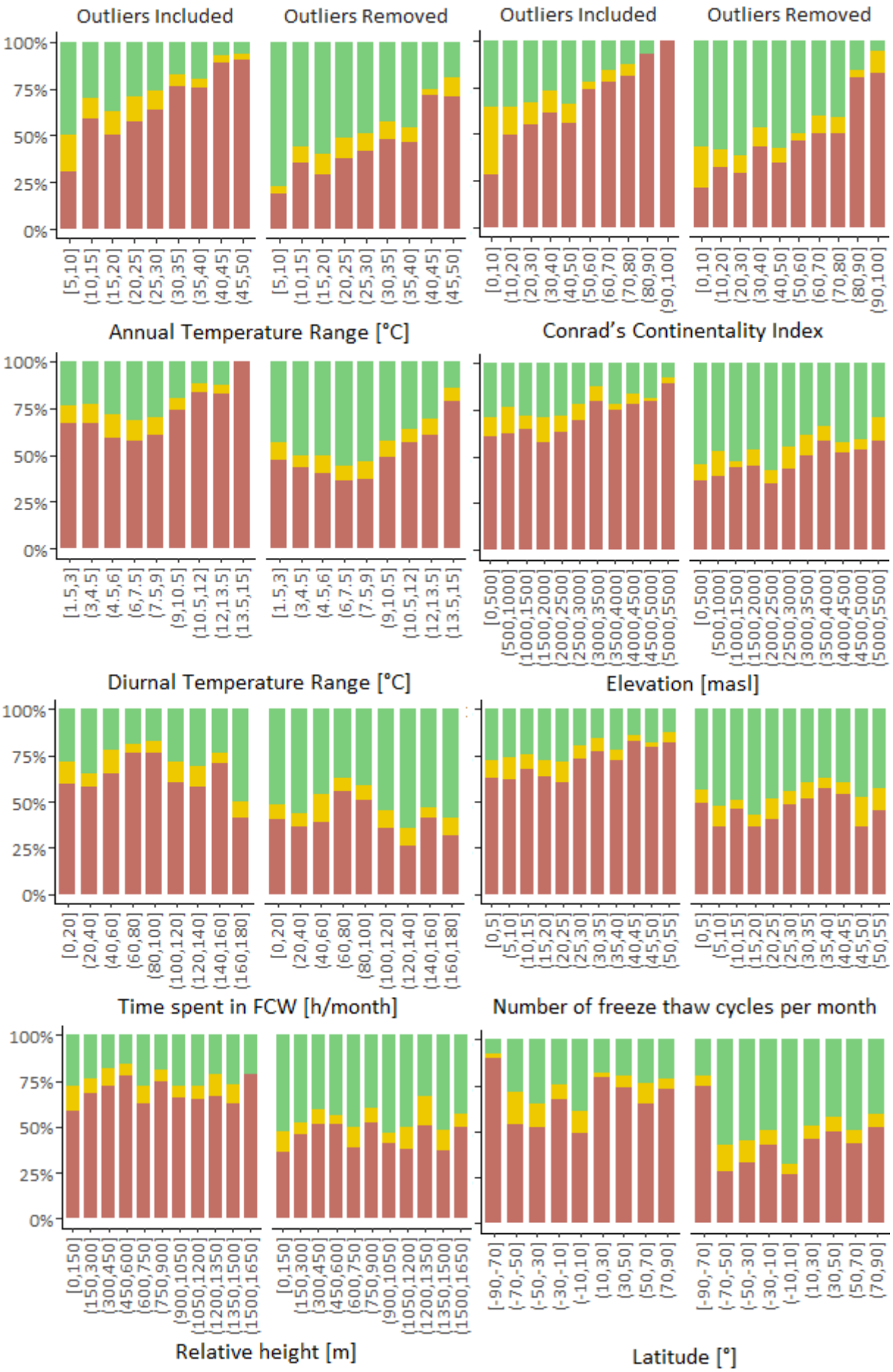
Outliers Included
Outliers Removed
Outliers Included
Outliers Removed
100%
75%
50%
25%
0%
[5,10]
(10,15]
(15,20]
(20,25]
(25,30]
(30,35]
(35,40]
(40,45]
(45,50]
[0,10]
(10,20]
(20,30]
(30,40]
(40,50]
(50,60]
(60,70]
(70,80]
(80,90]
(90,100]
Annual Temperature Range [°C]
Conrad's Continentality Index
[1.5,3]
(3,4.5]
(4.5,6]
(6,7.5]
(7.5,9]
(9,10.5]
(10.5,12]
(12,13.5]
(13.5,15]
[0,500]
(500,1000]
(1000,1500]
(1500,2000]
(2000,2500]
(2500,3000]
(3000,3500]
(3500,4000]
(4000,4500]
(4500,5000]
(5000,5500]
Diurnal Temperature Range [°C]
Elevation [masl]
[0,20]
(20,40]
(40,60]
(60,80]
(80,100]
(100,120]
(120,140]
(140,160]
(160,180]
[0,5]
(5,10]
(10,15]
(15,20]
(20,25]
(25,30]
(30,35]
(35,40]
(40,45]
(45,50]
(50,55]
Time spent in FCW [h/month]
Number of freeze thaw cycles per month
[0,150]
(150,300]
(300,450]
(450,600]
(600,750]
(750,900]
(900,1050]
(1050,1200]
(1200,1350]
(1350,1500]
(1500,1650]
[-90,-70]
(-70,-50]
(-50,-30]
(-30,-10]
(-10,10]
(10,30]
(30,50]
(50,70]
(70,90]
Relative height [m]
Latitude [°]

Finally, we examined the categorical variables, Trewartha climate classification and the type of ice mass. In the case of ice mass type, no significant differences in clustering were observed among the categories (Fig. 8, 9), and the improvement in clustering after outlier removal was similar for all types (Fig. 8, 9). Regarding climate classification, moraines formed in dry climates (B) exhibited the lowest proportion of well-clustered ages and showed the smallest improvement after outlier removal, likely reflecting the influence of low precipitation on age scatter. The proportion of well-clustered ages increased by more than 20 % for all remaining climate categories after removing outliers. Clustering was highest in subtropical climates (C) and progressively decreased toward colder climate types, consistent with the observed effect of decreasing annual temperature on moraine age clustering (Fig. 8, 9).

Figure 8 Moraine ridge exposure age clustering against the climate types and type of ice mass before removing outliers (red) and after removing outliers (blue). The black dotted horizontal line marks the MSWD=2. The y-axes are shown with a logarithmic scale.

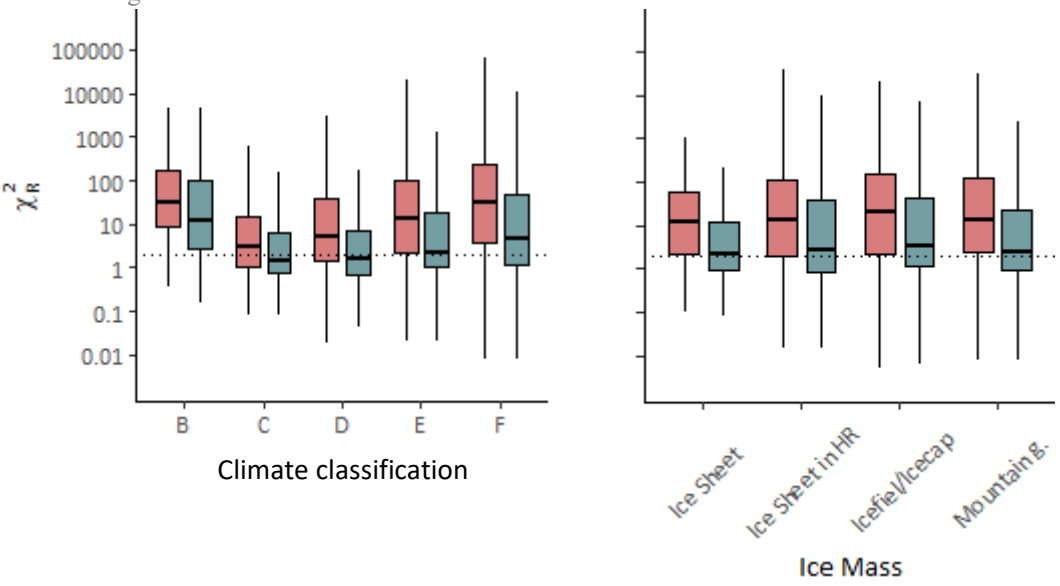

Figure 9 Proportion of well-clustered (green), moderately clustered (yellow) and scattered (red) moraine ridge groups for each category of climate classification and type of ice mass.

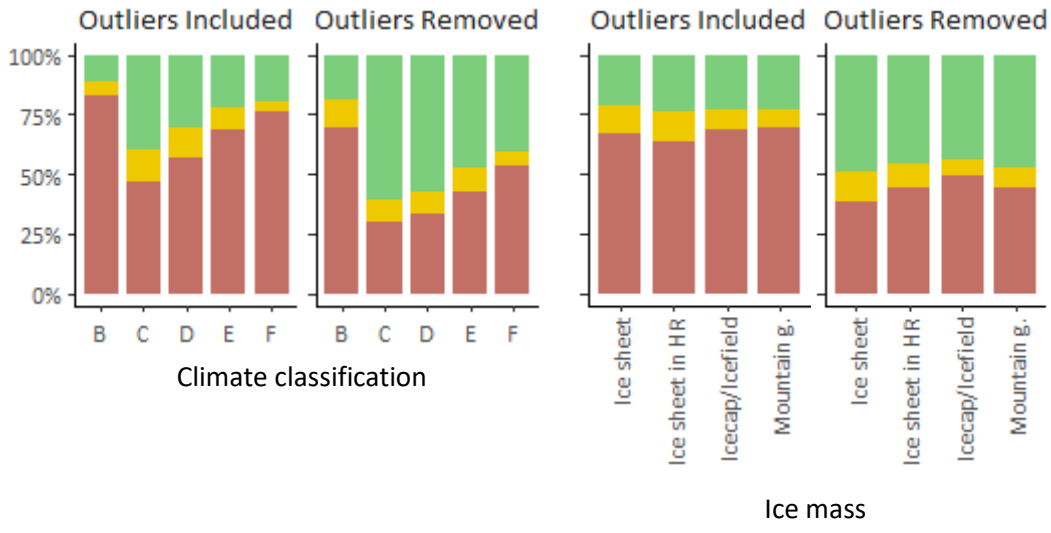

6.2. Clustering among different regions

Regionally, most of the examined moraine ridges were located in High Asia (440 ridges), North America (249) and Europe with western Asia (235) (Fig. 10). The highest proportions of well-clustered ages (after removing outliers) were observed in the regions of the British Isles (68 %), Europe and western Asia (60 %), Oceania (57 %), North America (55 %), and southern (53 %) and northern (52 %) South America. In contrast, the regions with the lowest proportion of well-clustered ages are northeastern Asia (21 % scattered ages), Antarctica (21 %) and High Asia (30 %).

Figure 10 Proportion of well-clustered (green), moderately clustered (yellow) and scattered (red) moraine ridge groups after removing outliers in examined regions.

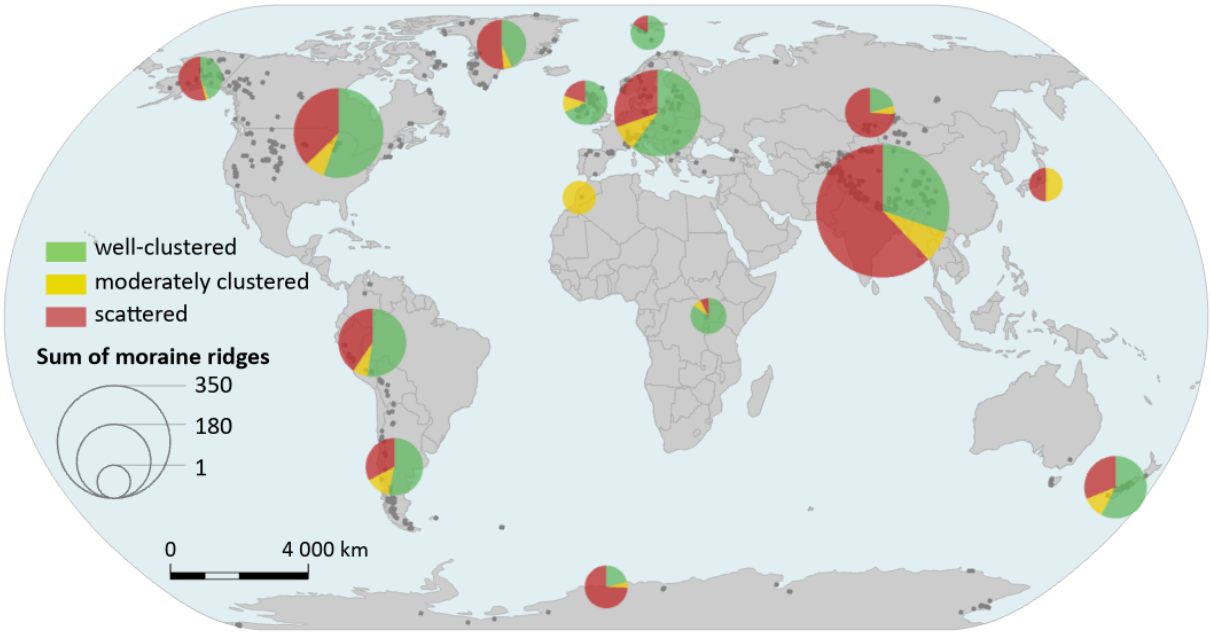

Clustering of moraine exposure ages was also examined across different regions in combination with ice mass type (Fig. 11). In several regions, outlier removal had minimal impact on clustering, and these can be divided into two categories: (1) regions with poor clustering regardless of outlier removal, including the AIS, Greenland (icefield/icecap and mountain glaciation), High Asia, and northeastern Asia; and (2) regions with consistently good clustering, such as Oceania. The most significant improvement after outlier removal was observed in North America (icefield/icecap and mountain glaciation), Alaska, GIS and PIS.

Figure 11 Proportion of well-clustered, moderately clustered, and scattered moraine ridge groups for different regions. OR: outliers removed.

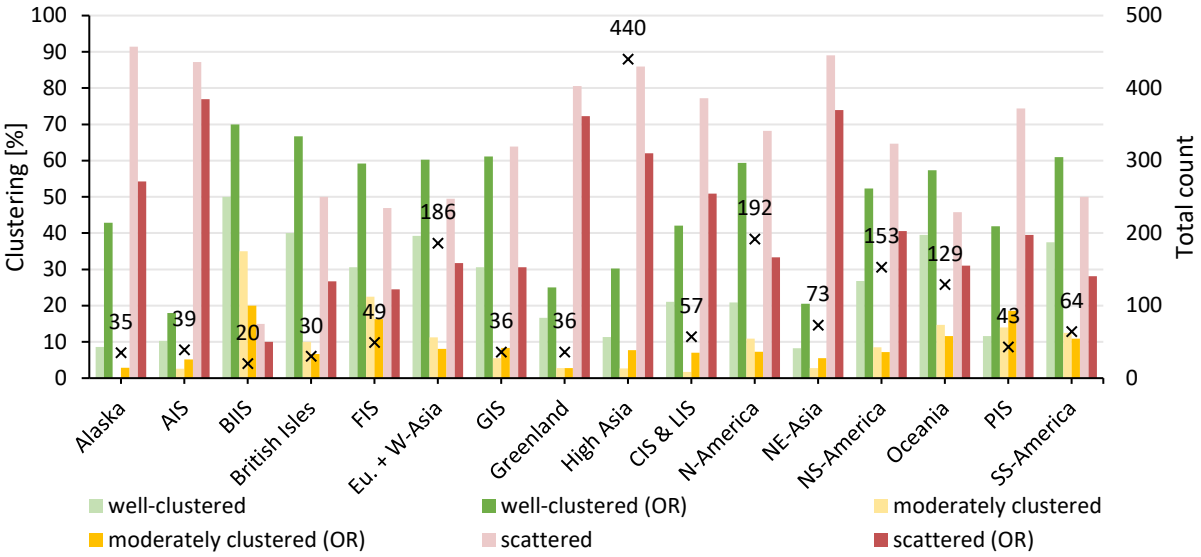

6.3. Sample size, outliers, and moraine exposure age clustering

The effect of varying sample sizes on the clustering of moraine exposure ages was examined to see whether a higher number of samples allowing for removing more outliers improves the clustering of ages. Table 9 summarizes the effect of outlier removal on the proportion of well-clustered ages. As expected, the success rate is lowest for groups with the fewest samples (three samples), gradually increasing with sample size. Notable shifts in success rates occur between groups with three and four samples (from 30 % to 50 %) and between groups with six and seven samples (from 53 % to 64 %). There is little difference between groups with four to six samples, seven, eight, and 10 samples, and 11 and 12 samples. The group with nine samples stands out with the highest success rate (85 %), which is higher than other groups. However, for larger sample sizes, the results become less clear for larger sample sizes due to the limited number of cases.

Table 9 Proportion [%] of well-clustered moraine age groups with respect to the number of samples per group and number of outliers removed. Percentage >50 % is in green.

number of samples per group (before removing outliers)	number of groups	number of outliers removed									
		0	1	2	3	4	5	6	7	8	9
3	587	**30.5**									
4	364	26.1	**50.0**								
5	299	15.7	35.5	**50.8**							
6	139	15.8	32.4	43.2	**53.2**						
7	91	16.5	30.8	42.9	51.6	**63.7**					
8	48	12.5	18.8	31.3	43.8	58.3	**66.7**				
9	26	19.2	23.1	30.8	46.2	53.8	65.4	**84.6**			
10	26	3.8	3.8	15.4	23.1	30.8	46.2	57.7	**69.2**		
11	9	11.1	11.1	11.1	44.4	66.7	66.7	66.7	77.8	**77.8**	
12	14	0.0	7.1	7.1	7.1	14.3	14.3	42.9	50.0	57.1	**78.6**

To further understand the effect of sample size on moraine age clustering, Figure 12 illustrates the relationship between the number of samples and the percentage of well-clustered ages, considering moraine ages. This figure clearly shows the effect of taking at least four samples per group, with a higher number of samples proving especially effective for younger moraines (at least seven samples) and older moraines (>20 ka: at least six samples; >30 ka: at least eight samples). However, results for older moraines should be interpreted with caution due to the limited number of cases. For moraines between 10 and 20 ka, the results for groups with five to seven samples are very similar.

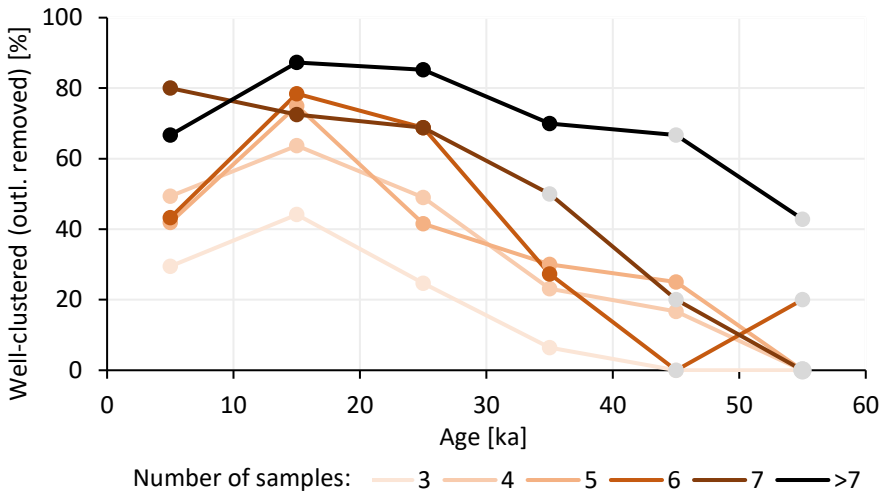

Figure 12 Proportion of well-clustered moraine groups (after removing outliers) with respect to mean moraine age and the number of samples taken per moraine. Grey dots: less than 10 moraines.

7. Discussion

7.1. Data overview

Compared to previous studies attempting to assess cosmogenic exposure ages on moraines, the dataset in this work is substantially larger. For instance, one of the more recent compilations by Heyman et al. (2016) comprised 579 boulder groups with at least three boulders. The overall trends and results related to clustering and moraine ages are very similar. As in the dataset in this work, Heyman et al. (2016) observed the highest proportion of well-clustered ages within the 10 to 15 ka range, 42 % of well-clustered ages (compared to 38 % in the dataset in this work) with the fraction of scattered increasing towards younger and older ages. Overall, Heyman´s dataset comprised 21 % of well-clustered ages, while this study contained a slightly higher proportion of 23 % of well-clustered ages.

Some previous studies used metrics different from MSWD to assess moraine age scatter, such as moraine boulder age range. Putkonen & Swanson (2003) quantified moraine age scatter using normalised age range – difference between maximum and minimum boulder ages divided by the maximum age of the moraine, resulting in values between 0 and 1. Their dataset's average normalised age range (comprising moraines younger than 100 ka) after removing old outliers was 0.38, indicating a substantial scatter among moraine boulders.

The average normalised age range of the dataset presented in this study (including moraines with at least two samples) is 0.31. After removing the old outliers, this value slightly

increases to 0.32, probably because while removing old outliers reduces the absolute age range, it also lowers the maximum boulder age, increasing the normalised age range. Applying the same age limit of 100 ka as Putkonen & Swanson (2003) to our dataset does not impact the average normalised age range, which remains 0.31.

Putkonen & O´Neil (2008) presented a different approach to age scatter, analysing the absolute age range (the difference between maximum and minimum moraine boulder ages). They found a positive correlation with moraine age, suggesting continuous moraine degradation over time. After excluding old outliers, the regression model for their dataset is $t_s = 0.45t + 2000$, where t_s is the absolute age range and t is moraine age.

Applying the same approach to the dataset in this work (for moraines with at least two samples after removing old outliers) yielded a considerably steeper relationship: $t_s = 0.87t - 3124$. Because the oldest moraine in the dataset of Putkonen & O´Neil (2008) is 582 ka, the same upper limit was also applied to the dataset in this paper resulting in even steeper regression: $t_s = 1.03t - 9619$ (see Fig. 13). Overall, the substantially steeper slopes observed in this dataset indicate stronger time-dependent increase in age scatter and hence more significant moraine degradation over time. However, moraines older than 582 ka appear to have relatively lower absolute age scatter than expected from the regression for the younger ages.

In summary, the average scatter expressed by the normalised age range is slightly lower than in the dataset of Putkonen & Swanson (2003). However, the linear regression shows a substantially higher increase in absolute age scatter with moraine age than reported in the previous study by Putkonen & O´Neil (2008). This suggests that despite more consistent relative ages, post-depositional processes might play a more important role with increasing moraine age in this dataset.

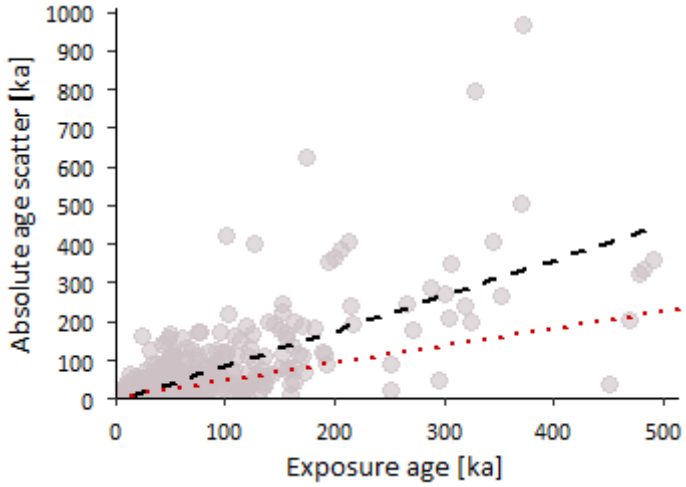

Figure 13 Absolute age scatter compared to mean moraine age, datapoints older than 500 ka were excluded from the graph, but are included in the regression calculation. Black dashed line: the linear regression of the dataset; the red dotted line: linear regression of Putkonen & O'Neal's (2003) dataset.

7.2. Clustering for different moraine ages

The scatter in moraine ages is generally supposed to increase with moraine age due to moraine degradation (Putkonen & Swanson, 2003; Putkonen & O´Neil, 2008). However, as shown in previous studies (Heyman et al., 2016), the youngest moraines do not show the highest fraction

of well-clustered ages. In this work, the highest proportion of well-clustered ages is observed in the 10 to 15 ka interval, gradually decreasing toward older ages. There is also a significant fraction of scattered ages for the youngest moraines (0-5 ka), with only 14.5 % (33.9 % after removing outliers) of well-clustered ages.

Potential environmental influences were examined to gain better insight into the high scatter observed among the youngest moraines. As demonstrated in Figure 14, these youngest moraines with high scatter do not appear to be associated with any specific environmental conditions. In contrast, older moraines (> 25 ka) with higher scatter show more expected relationships between their MSWD values and the examined variables (see section 1.1.). For instance, a high fraction of the scattered older moraines is located in regions with low precipitation, large diurnal and annual temperature ranges or high continentality. Also, the moraines at the lowest temperatures are almost exclusively associated with the old moraine group (in the AIS region).

Figure 14 MSWD and examined variables, outliers included. Red: young moraines (0-5 ka), blue: older moraines (> 25 ka). The precipitation was cut at 5000 mm (max. 18 000 mm).

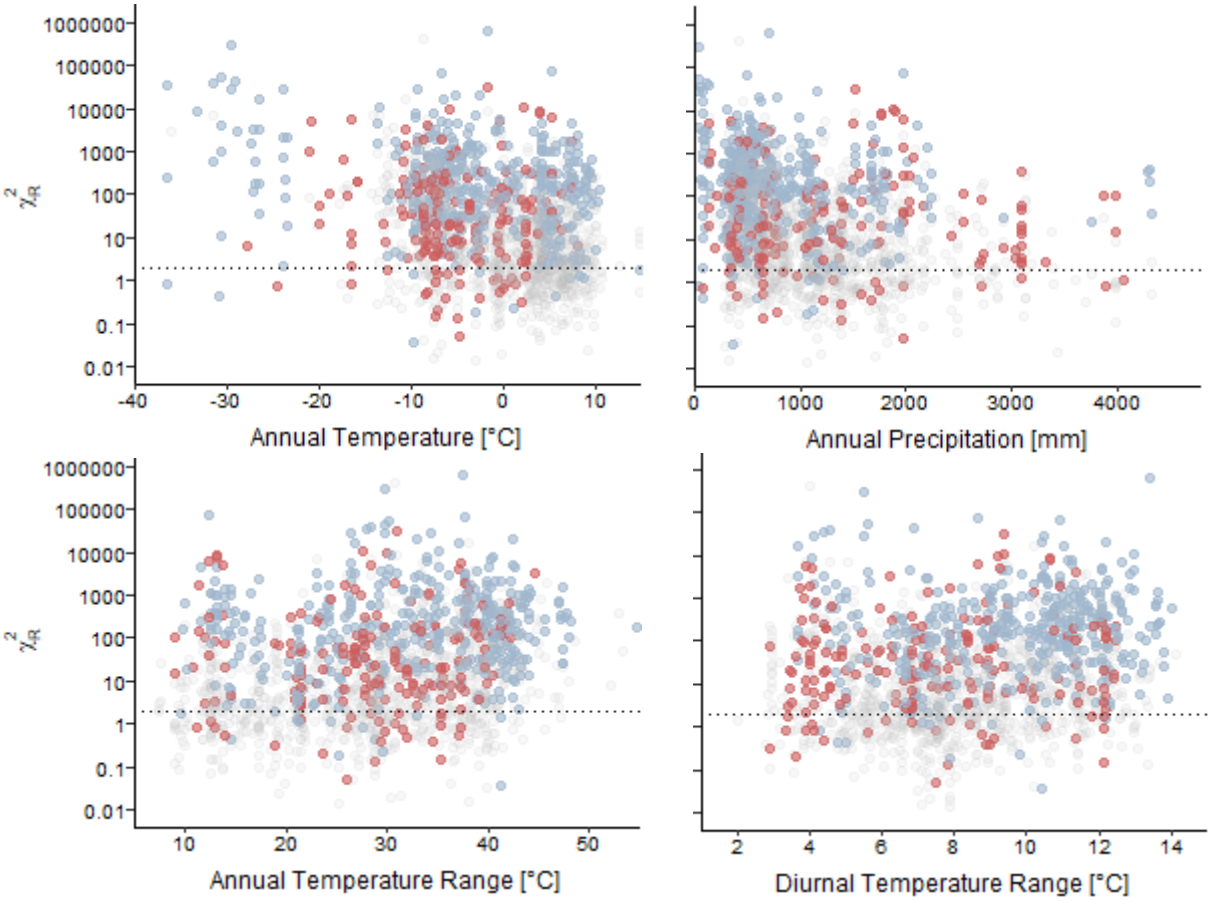

Unlike the older moraines, the youngest moraines seem to reflect the general distribution of the whole dataset, suggesting different causes for the observed scatter. This supports the assumption that denudation should have a negligible effect on the scattering among young moraines. Another cause might be nuclide inheritance. Assuming skewness > 0.5 indicates

inheritance and < -0.5 degradation (Applegate et al., 2010), then inheritance might significantly contribute to scatter among the youngest ages. Based on skewness data, 60 % of the scattered (MSWD ≥ 2) young moraines likely suffer from inheritance, while 21 % from incomplete exposure. Additionally, the relationship between MSWD and skewness is slightly stronger (0.34) compared to the whole dataset (0.19).

Another possible contributor to scatter among young moraines (≤ 5 ka) is uncertainty related to blank concentration—background contamination introduced during sample preparation (Balco et al., 2008; Balco, 2011). However, no correction could be applied since blank data are not available in this dataset.

Fig. 15 also reveals regional patterns. Young, scattered moraines are concentrated in areas like Greenland, southern part of High Asia, and northern South America.

Figure 15 Regional distribution of scattered, young (≤ 5 ka, red) and old (> 25 ka, blue) moraines.

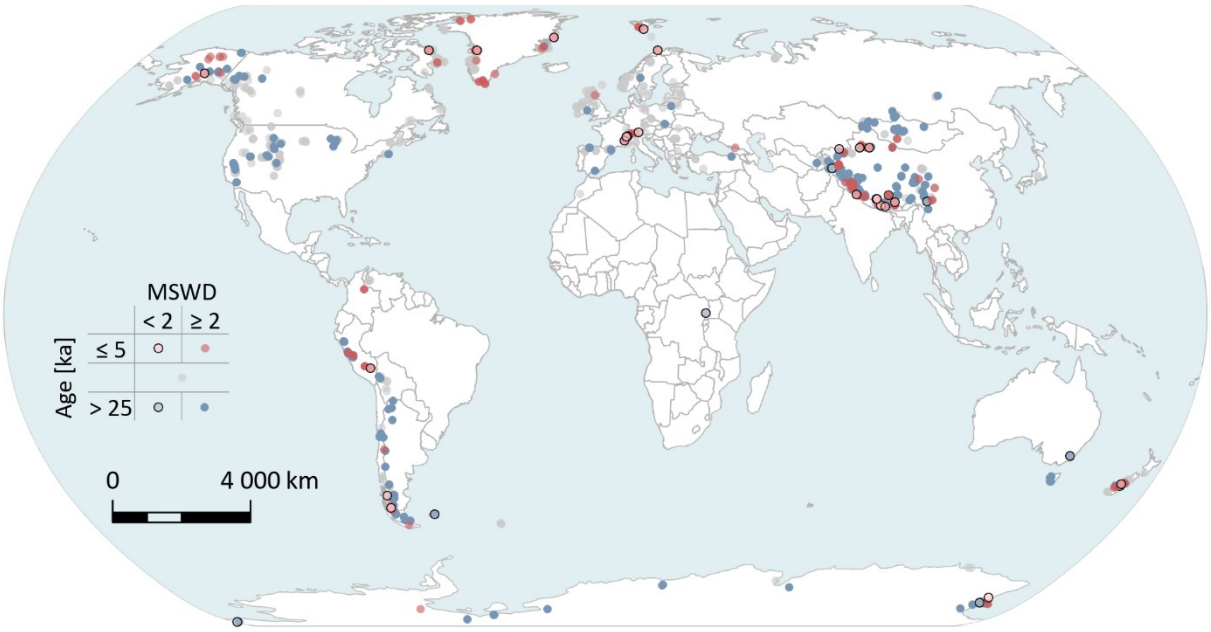

Beyond 35 ka, only seven moraine groups are classified as well-clustered when outliers are included, and 47 groups after outlier removal. These old, well-clustered moraines were examined for common trends, but no patterns were found. Both groups span a wide range of climatic and topographic conditions across different regions. They can be found in arid, cold polar climates as well as in boreal or temperate climates with higher precipitation and temperatures, at various elevations, and in continental, oceanic or moderate climates.

The seven well-clustered (outliers included) are located in Antarctica, High Asia, southern South America and Oceania. The group of 47 well-clustered groups (outliers removed) is distributed across Antarctica, High Asia, North America, Oceania, all regions of South America, and includes one moraine in northeastern Asia. Some regions are not represented due to the absence of moraines older than 35 ka (BIIS, British Isles, Greenland, GIS), or because there are only a few of these moraines (FIS, Europe and western Asia, and likely CIS and LIS).

7.3. Regional patterns

As shown in section 1.2. the clustering in several regions was only slightly affected by outlier removal, suggesting either overall poorly clustered regions or consistently well-clustered regions. The first group includes the AIS, Greenland (icefield/icecap and mountain glaciation), High Asia, and northeastern Asia. Oceania is the only region representing the second group with consistently well-clustered moraines. Some of the climate or topography-related characteristics of these regions (with a comparison of the whole dataset) are shown in Fig. 16.

Figure 16 Boxplots for selected variables. Categories: regions with MSWD only slightly affected by outlier removal and boxplots of GIS and the whole dataset for comparison.

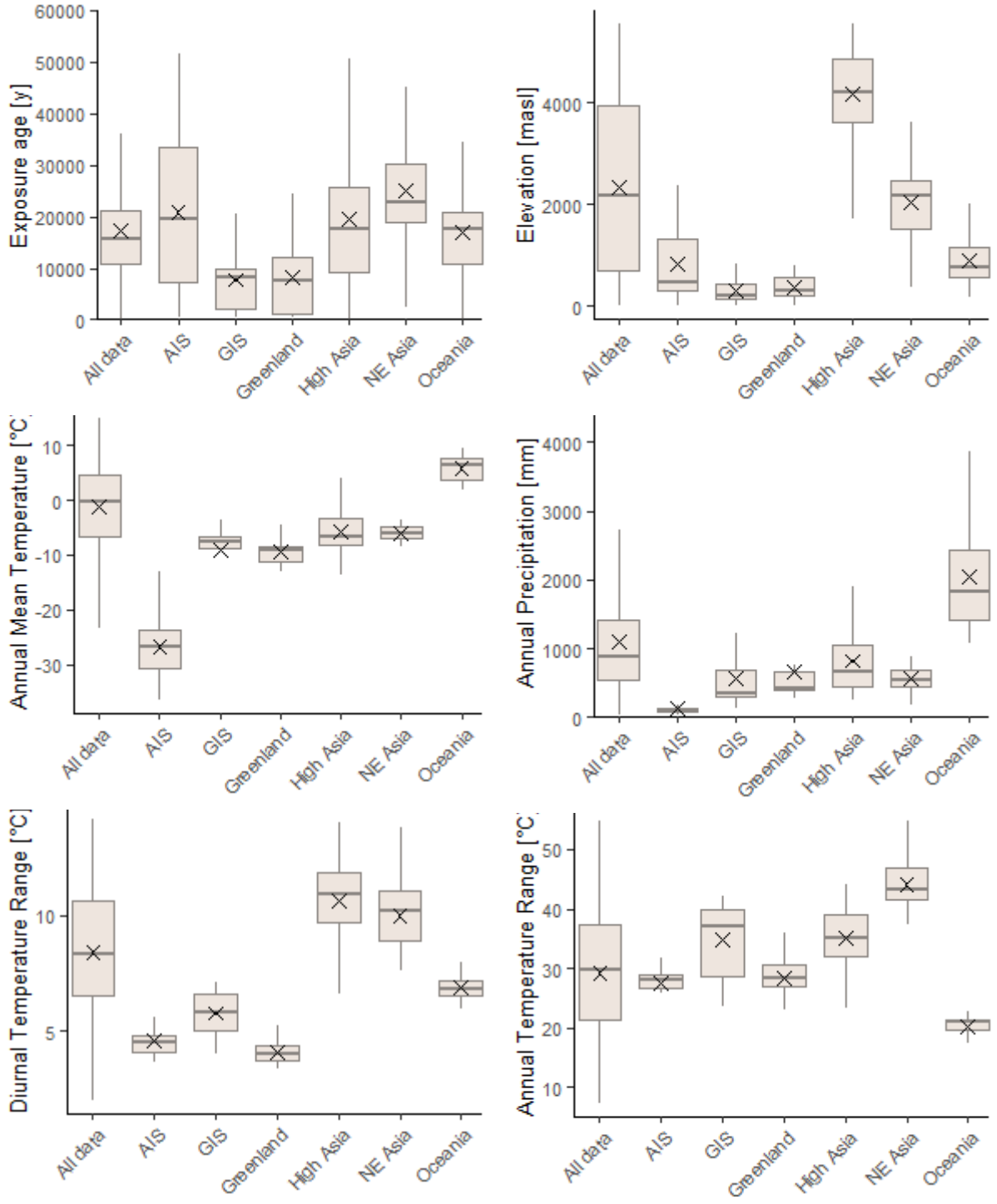

As shown in Fig 16. the moraines of the AIS are located in extremely cold and arid environments. They represent the group of moraines with the lowest mean temperatures and precipitation in the entire dataset (Fig. 17). These extremely cold and arid climate conditions might indicate non-erosive cold-based ice. The periods of burial by cold-based ice might limit the accuracy of cosmogenic nuclide dating in Antarctica (Bentley et al., 2017; Di Nicola et al., 2007; Strasky et al., 2009a). Another source of scatter in Antarctica may include post-depositional reworking of boulders causing overturning or rearrangement of boulders (Strasky et al., 2009a) or the presence of reworked clasts with inherited nuclides (Bentley et al., 2017). Several studies suggest that the poor clustering might reflect complex exposure histories (Bentley et al., 2017; Strasky et al., 2009a).

In terms of inheritance vs. incomplete exposure, there is a slightly higher, though still very weak, correlation between MSWD and skewness (0.33) compared to the full dataset (0.17). Among the scattered AIS moraines, 31.4% exhibit signs of incomplete exposure and 48.6% inheritance, which is similar to the full dataset (26.6% and 48.8%, respectively).

Figure 17 The relationship between mean annual temperature or precipitation and the MSWD for the whole dataset. The points representing AIS are in dark red.

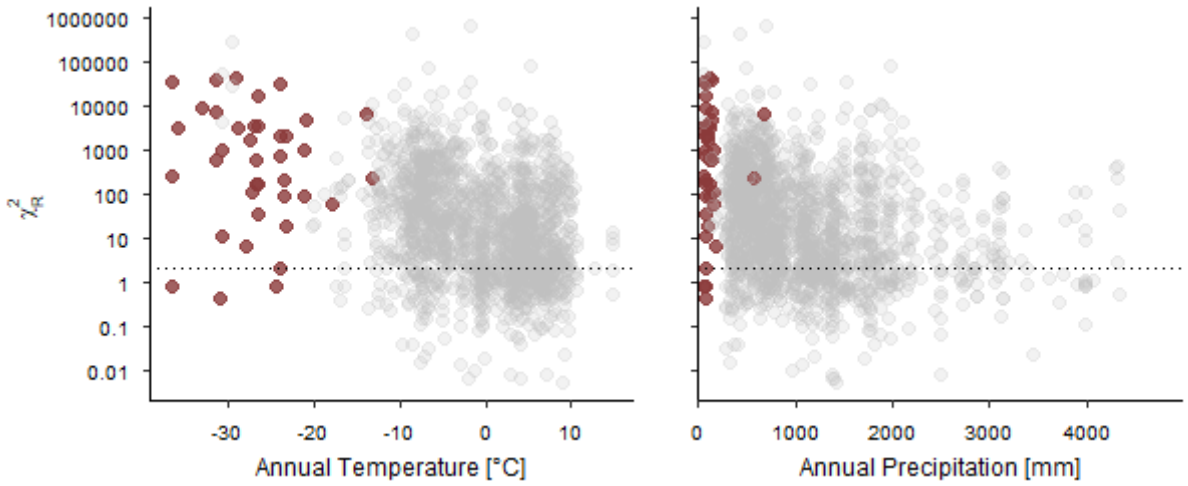

The next poorly clustered region is Greenland (icefield/icecap and mountain glaciation). While the environmental conditions in Greenland and the GIS are very similar (Fig 16), the GIS shows substantially better clustering (see Fig. 11), probably reflecting different glacial dynamics. The GIS moraines in this dataset are post-LGM, corresponding to recessional positions. According to Larsen et al. (2021), the GIS recessional moraines yield more consistent exposure ages due to intense glacial erosion during LGM that removed the nuclides from previous episodes of exposure. In contrast, moraines deposited by mountain glaciers are often highly scattered with signs of inheritance and exhumation (Larsen et al., 2021). This may be caused by a higher frequency of Holocene glacier readvances of mountain glaciers (Larsen et al., 2021).

Interestingly, the skewness analysis of moraine age distributions (before outlier removal) suggests that 72.0 % of the scattered GIS moraines exhibit inheritance and only 16.0 % incomplete exposure. For Greenland mountain glaciers, these values are 56.7 % (inheritance) and 23.3 % (incomplete exposure).

The third region with poorly clustered ages is northeastern Asia. This region is characterized by lower mean annual precipitation and temperature (Fig. 16) and notably the highest annual temperature range among the whole dataset (Fig. 18), reflecting the strongly continental climate. Moraines in this region are generally older and often predate the Last Glacial Maximum (LGM). Given the observed relationship between clustering and moraine age, this may reflect a greater influence of post-depositional processes or inheritance, possibly driven by complex glacial histories involving multiple glacier readvances (Blomdin et al., 2018; Gillespie et al., 2008). The skewness-based classification of scattered moraine groups in northeastern Asia is consistent with the results for the whole dataset with 53.7 % showing inheritance and 22.4 % incomplete exposure.

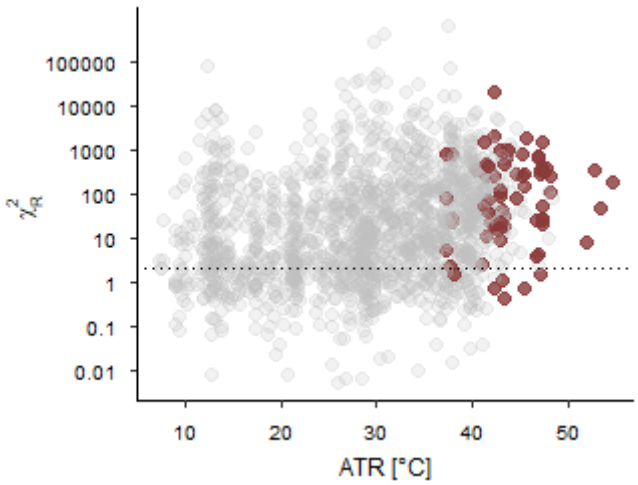

Figure 18 The relationship between MSWD and ATR (annual temperature range) for the whole dataset. The points representing NE-Asia are in dark red.

The last of the poorly clustered regions is High Asia**.** In terms of climate characteristics, mean annual temperatures are lower, with relatively high annual and diurnal temperature ranges, but apart from the DTR, no climatic variable stands out (Fig. 16). The region also features the highest elevations and a wide range of moraine ages. Heyman (2014) and Blomdin et al. (2016) have reported similar patterns of poor clustering even after removing outliers in this region. Many moraines predate the LGM, which may increase their susceptibility to post-depositional processes and reflect complex glacial histories with multiple glacier readvances (Heyman, 2014).

The skewness-based classification of the scattered moraine groups is very similar to that of northeastern Asia (and the whole dataset), with 49.7 % indicating inheritance and 21.8 % incomplete exposure.

Oceania is the only region where outlier removal had a small effect on clustering, and which overall shows good clustering. As shown in the Fig. 16, the characteristics of this region

correspond to the general trends associated with better clustering discussed in section 1.1. These include lower elevations, high mean temperatures and precipitation, and lower ATR and DTR. In contrast to the previously discussed regions (and the overall dataset), which show a higher proportion of scattered groups indicating inheritance, Oceania shows an equal proportion of groups indicating inheritance and incomplete exposure, both at 39.7 %.

7.4. Implications for sampling strategies

Previous studies have shown that sampling taller boulders increases the proportion of well-clustered ages, likely due to their more probable continuous exposure to cosmic radiation (Heyman et al., 2016). However, our work did not focus on specific characteristics or moraine morphology (e.g., moraine height, slope angle, moraine shape or boulder height) but instead examined broader climatic and topographic controls.

The results support the assumption that moraine age is one of the main factors influencing the moraine age clustering (Heyman et al., 2016). However, the clustering does not always decrease with increasing age. While the proportion of well-clustered groups decreases from beyond about 15 ka, the youngest moraines (< 5 ka) show a significant scatter.

A key implication of this analysis is the relationship between the number of samples per moraine group and the likelihood of well-clustered results. Although at least three samples per moraine are generally recommended (Darvill, 2013), our results show that sampling more than three boulders per moraine consistently improves the results. Nevertheless, 36 % of groups with at least three samples only contain three boulders (Table 9).

To achieve a 50 % probability of obtaining well-clustered results within the "best " age interval 10-20 ka (interval with the highest proportion of well-clustered ages), at least four samples should be taken. More samples are required for similar accuracy for older and younger moraines: at least seven samples for moraines younger than 10 ka; at least six for 20–30 ka, and at least eight for moraines older than 30 ka.

Interestingly, increasing the number of samples per group does not always result in a proportional increase of well-clustered ages. For instance, taking four to six boulders from moraines younger than 10 ka makes a minor difference. In the 10-20 ka interval, clustering is comparable for groups with five to seven samples, and in the 30-40 ka interval, for four to six samples.

If moraine age estimates are not available prior to sampling, climate classification or regionalisation may offer some insight. From the subtropical or boreal towards colder climates, more samples are necessary for comparable likelihood of well-clustered moraine groups (Fig. 19A). Subtropical climates are the only category where three samples yield comparable results to moraines with four samples.

Regionally, taking only three samples most negatively affected North America and Oceania, while taking at least five samples significantly improved clustering in northeastern

Asia and Oceania. Sampling more than five boulders notably improved results in regions such as Antarctica and Alaska (Fig. 19B).

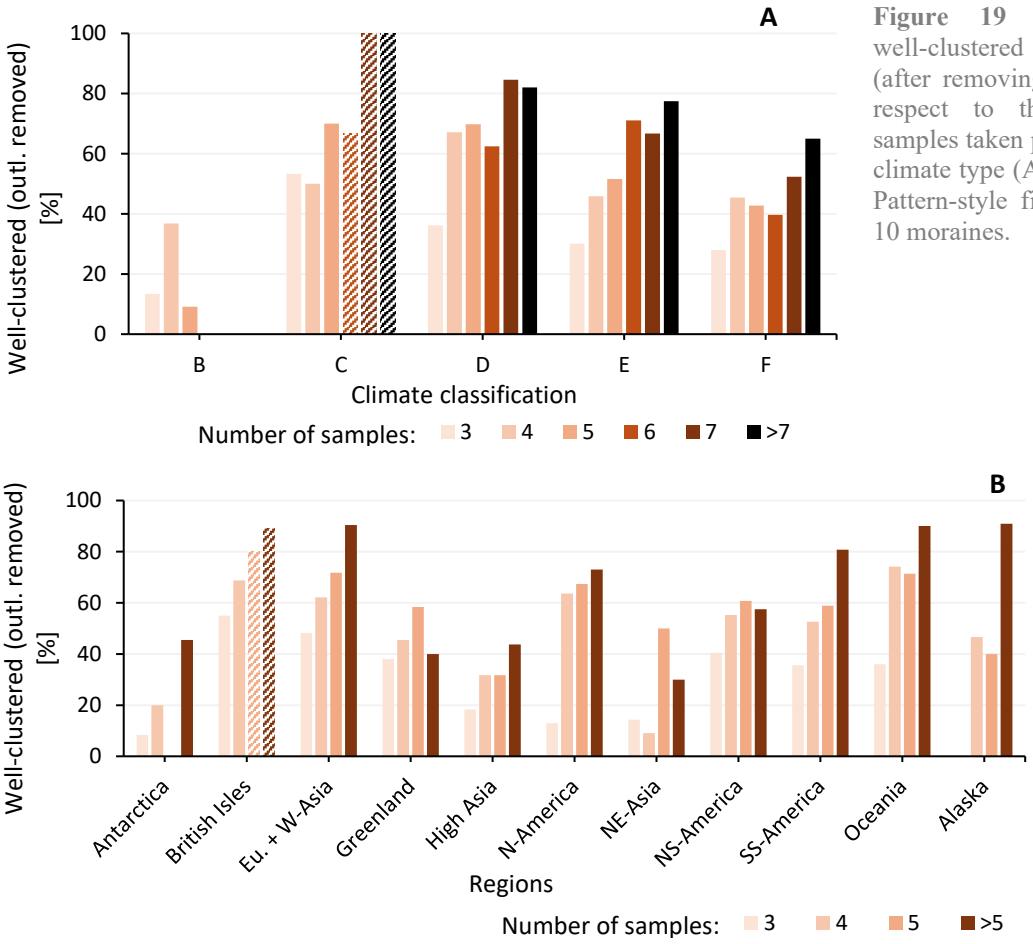

Figure 19 Proportion of well-clustered moraine groups (after removing outliers) with respect to the number of samples taken per moraine and climate type (A) or region (B). Pattern-style filling: less than 10 moraines.

The results do not support the expected influence of glacier type on clustering, based on the assumption of different moraine topography or the surrounding terrain (Barr and Lowell, 2014; Balco, 2011). This may suggest that ice mass type alone is not a reliable indicator of moraine morphology or associated post-depositional processes. However, combining with geographic regions may provide additional insights, reflecting distinct glacial histories and environmental conditions.

Regarding direct climatic or topographic controls, the most important variables for clustering are the annual mean temperature, precipitation, annual temperature range, and, to some extent, elevation or diurnal temperature range.

7.5. Implications for moraine denudation

Various climatic, topographic, and glaciological factors control moraine preservation. Degradation models indicate relatively high impacts of erosion (Putkonen & O'Neal, 2006; Putkonen et al., 2008). Putkonen and O'Neal (2006) modelled degradation of Pleistocene

moraines in western North America and suggested an average erosion depth of 25 % of the final moraine height.

Denudation patterns linked to climate conditions or lithology offer insight into weathering rate and surface stability (e.g., Olvmo, 2010; Summerfield et al., 1999). Weathering rates increase with higher temperature and moisture availability, enhancing chemical and mechanical weathering (Olvmo, 2010). Even in cold climates, some effective frost-weathering processes require water availability (Anderson, 1998; Hales and Roering, 2007). However, our dataset shows better clustering with higher precipitation or temperatures. This might suggest the importance of other weathering processes active in cold, arid regions (e. g., thermal stress fatigue, salt crystallisation (Hall, 1999; Matsuoka, 1995) or that weathering alone cannot sufficiently explain moraine age scatter and preservation patterns.

Moraine preservation is also influenced by self-censoring and external censoring processes, related to the topography and glacial history (Barr and Lowell, 2014). Self-censoring includes obliterative overlap, where glacier readvances partially or completely erase older landforms (Gibbons et al., 1984; Kirkbride & Winkler, 2012), and melting of ice-cored moraines, delaying their stabilisation (Kirkbride & Winkler, 2012; Lukas, 2011). External censoring, like post-depositional erosion, is more intense in dynamic terrain with steep slopes, in the proximity of, e.g. proglacial rivers or the aggrading outwash fans (Kirkbride & Winkler, 2012; Barr and Lowell, 2014).

The existing literature assumes that topographic controls vary with moraine morphology and ice mass type. While ice sheets are assumed to form moraines that are less prone to external censoring (Barr and Lowell, 2014), smaller, sharp-crested moraines deposited by mountain glaciers in topographically dynamic terrain should be more susceptible to reworking and erosion (Barr and Lowell, 2014; Putkonen and O´Neil, 2006). However, the analysis of moraine age scatter as an indicator of moraine degradation did not show any results that would suggest the influence of ice mass.

Moraine preservation potential reflects the interplay between climate, topography, lithology, and glacier dynamics. Climate influences weathering rates but also glacier behaviour, which subsequently plays a role in moraine preservation as well (Olvmo, 2010). The age scatter may reflect moraine denudation but also the intensity of other processes like post-depositional reworking, or inheritance or the intensity of pre-depositional glacial erosion (Larsen et al., 2021). However, the reliability of moraine age scatter to indicate the denudation may be questionable. For example, although very low denudation rates in Antarctica allow the preservation of old moraines (Summerfield et al., 1999, see Fig. 16), their exposure ages are among the most scattered of all examined regions (Fig. 11).

In conclusion, geomorphological controls on moraine preservation are interconnected and site-specific. Climate and topography provide broad constraints but cannot alone reliably predict the clustering of moraine exposure ages without considering glacial history and post-depositional processes – as has been shown, e.g. for Greenland mountain glaciation and

GIS. There are very similar environmental conditions in Greenland and the GIS, but the GIS moraines are better clustered, likely due to different glacial dynamics.

8. Conclusions

This work aimed to evaluate the controls on moraine preservation or denudation and derive implications for the reliability of exposure dating and sampling strategies.

For that, we compiled a global database from 526 publications, containing 10 083 moraine samples dated with ^{10}Be and grouped into 3243 moraine groups. Of these, only 1,620 groups with at least three samples per moraine were suitable for further analysis. As a measure of moraine exposure age quality, the MSWD was calculated and combined with various climatic and topographic data.

The examined 1620 moraine groups span a broad temporal range from 56 years to 5.38 million years. Only 23 % of moraines show well-clustered exposure ages, increasing to 46 % after removing outliers. Moraine age is one of the main factors influencing age clustering. However, the youngest age group does not show the best results. Moraines with mean ages between 10 and 15 ka show the best clustering. The likelihood of obtaining a well-clustered age significantly decreases for older and younger moraines.

Another limiting factor is the number of samples taken per moraine. Although a minimum of three samples is recommended to account for potential moraine degradation or inheritance, only half of the original moraine groups (3242) meet this requirement. Among the 1620 analysed moraines, 36 % contained only three samples. However, the results show that sampling at least four boulders per moraine consistently and significantly improves the likelihood of obtaining a well-clustered result. The optimal number of samples varies with moraine age: for the youngest moraines, at least seven are needed to achieve a 50 % likelihood of well-clustered results; for moraines between 10 to 20 ka four samples are sufficient. For older moraines, the optimal number of samples increases with age.

Among climatic and topographical factors, higher mean annual temperature and precipitation, lower annual temperature range, or lower continentality show better clustering. Similarly, with these results, a trend was observed for the climate classification, where moraines formed in dry climates exhibited the lowest proportion of well-clustered ages. The best clustering was observed for subtropical climates and decreased toward colder climate types.

Some regions exhibited very poor clustering overall, even after removing outliers. The worst results were found for the Antarctic Ice sheet, Greenland (mountain glaciation, icefields and icecaps category), northeastern Asia, and High Asia. In some regions, poor clustering corresponds with climatic variables, e.g., the very cold and arid environment of the Antarctic Ice Sheet or a large annual temperature range in northeastern Asia. However, the poor clustering is also likely influenced by complex glacial histories (Greenland) and the mean moraine ages (High Asia). This is particularly evident in Greenland, where the mountain glaciation and icefields or icecaps show significantly worse clustering than

the Greenland Ice Sheet despite comparable climatic conditions. This contrast probably reflects different glacial dynamics. The frequent Holocene readvances of mountain glaciers resulted in a more complex moraine record, whereas the ice sheet formed well-preserved recessional moraines.

Compared to the poorly clustered regions, the highest proportion of well-clustered moraines is found in regions sharing milder climates with relatively higher precipitation and temperatures. These include the British Isles, Europe and western Asia, Oceania, North America, and South America.

9. References

Abbühl, L. M., Akcar, N., Strasky, S., Graf, A. A., Ivy-Ochs, S., & Schlüchter, C. (2009). A zero-exposure time test on an erratic boulder: evaluating the problem of pre-exposure in surface exposure dating. Eiszeitalter und Gegenwart Quaternary Science Journal 58, 1-11.

Abramowski, U. (2004). The use of 10 Be surface exposure dating of erratic boulders in the reconstruction of the late Pleistocene glaciation history of mountainous regions, with examples from Nepal and Central Asia. Dissertation thesis, University of Bayreuth.

Abramowski, U., Bergau, A., Seebach, D., Zech, R., Glaser, B., Sosin, P., Kubik, P. W., & Zech, W. (2006). Pleistocene glaciations of Central Asia: results from 10Be surface exposure ages of erratic boulders from the Pamir (Tajikistan), and the Alay-Turkestan range (Kyrgyzstan). Quaternary Science Reviews, 25(9–10), 1080–1096.

Ackert Jr., R. P., Becker, R. A., Singer, B. S., Kurz, M. D., Caffee, M. W., & Mickelson, D. M. (2008). Patagonian Glacier Response During the Late Glacial–Holocene Transition. Science, 321(5887), 388–392.

Ackert, R. P., Mukhopadhyay, S., Parizek, B. R., & Borns, H. W. (2007). Ice elevation near the West Antarctic Ice Sheet divide during the Last Glaciation. Geophysical Research Letters, 34(21).

Akçar, N., Yavuz, V., Ivy-Ochs, S., Kubik, P. W., Vardar, M., & Schlüchter, C. (2007). Paleoglacial records from Kavron Valley, NE Turkey: Field and cosmogenic exposure dating evidence. Quaternary International, 164–165, 170–183.

Akçar, N., Yavuz, V., Ivy-Ochs, S., Reber, R., Kubik, P. W., Zahno, C., & Schlüchter, C. (2014). Glacier response to the change in atmospheric circulation in the eastern Mediterranean during the Last Glacial Maximum. Quaternary Geochronology, 19, 27–41.

Akçar, N., Yeşilyurt, S., Hippe, K., Christl, M., Vockenhuber, C., Yavuz, V., & Özsoy, B. (2020). Build-up and chronology of blue ice moraines in Queen Maud Land, Antarctica. Quaternary Science Advances, 2.

Alexanderson, H., & Fabel, D. (2015). Holocene Chronology of the Brattforsheden Delta and Inland Dune Field, Sw Sweden. Geochronometria, 42(1), 1–16.

Alexanderson, H., & Håkansson, L. (2014). Coastal glaciers advanced onto jameson land, east greenland during the late glacial-early holocene milne land stade. Polar Research, 33.

Alloway, B. V., Almond, P. C., Moreno, P. I., Sagredo, E., Kaplan, M. R., Kubik, P. W., & Tonkin, P. J. (2018). Mid-latitude trans-Pacific reconstructions and comparisons of coupled glacial/interglacial climate cycles based on soil stratigraphy of cover-beds. Quaternary Science Reviews, 189, 57–75.

Amidon, W. H., Bookhagen, B., Avouac, J. P., Smith, T., & Rood, D. (2013). Late Pleistocene glacial advances in the western Tibet interior. Earth and Planetary Science Letters, 381, 210–221.

Amos, C. B., Kelson, K. I., Rood, D. H., Simpson, D. T., & Rose, R. S. (2010). Late quaternary slip rate on the Kern Canyon fault at Soda Spring, Tulare County, California. Lithosphere, 2(6), 411–417.

Anderson, J. T. H., Wilson, G. S., Fink, D., Lilly, K., Levy, R. H., & Townsend, D. (2017). Reconciling marine and terrestrial evidence for post LGM ice sheet retreat in southern McMurdo Sound, Antarctica. Quaternary Science Reviews, 157, 1–13.

Anderson, J. T. H., Wilson, G. S., Jones, R. S., Fink, D., & Fujioka, T. (2020). Ice surface lowering of Skelton Glacier, Transantarctic Mountains, since the Last Glacial Maximum: Implications for retreat of grounded ice in the western Ross Sea. Quaternary Science Reviews, 237.

Anderson, R. S. (1998). Near-surface Thermal Profiles in Alpine Bedrock: Implications for the Frost Weathering of Rock. Arctic and Alpine Research, 30(4), 362–372.

Anjar, J., Akçar, N., Lakeman, T., Larsen, E. A., & Seiler, M. (2021). 10Be surface exposure dating of the deglaciation of northernmost Norway and Finland. Boreas, 50(2), 369–380.

Anjar, J., Larsen, N. K., Håkansson, L., Möller, P., Linge, H., Fabel, D., & Xu, S. (2014). A 10Be-based reconstruction of the last deglaciation in southern Sweden. Boreas, 43(1), 132–148.

Aoki, T. (2000). Chronometry of Glacial Deposits by the 10Be Exposure Dating Method. A Case Study in the Senjojiki and Nogaike Cirques, Northern Kiso Mountain Range, Central Japan. The Quaternary Research (Daiyonki-Kenkyu), 39(3), 189–198.

Aoki, T. (2003). younger Dryas glacial advances in Japan dated with in situ produced cosmogenic radionuclides. Transactions, Japanese Geomorphological Union, 24, 27–39.

Applegate, P. J., Urban, N. M., Laabs, B. J. C., Keller, K., & Alley, R. B. (2010). Geoscientific Model Development Modeling the statistical distributions of cosmogenic exposure dates from moraines. Geosci. Model Dev, 3.

Applegate, P. J., Urban, N. M., Keller, K., Lowell, T. V., Laabs, B. J. C., Kelly, M. A., & Alley, R. B. (2012). Improved moraine age interpretations through explicit matching of geomorphic process models to cosmogenic nuclide measurements from single landforms. Quaternary Research, 77(2), 293–304.

Arzhannikov, S. G., Braucher, R., Jolivet, M., Arzhannikova, A. V., Vassallo, R., Chauvet, A., Bourlès, D., & Chauvet, F. (2012). History of late Pleistocene glaciations in the central Sayan-Tuva Upland (southern Siberia). Quaternary Science Reviews, 49, 16–32.

Auqué, L. F., Puigdomenech, I., Tullborg, E. L., Gimeno, M. J., Grodzinsky, K., & Hogmalm, K. J. (2019). Chemical weathering in a moraine at the ice sheet margin at Kangerlussuaq, western Greenland. Arctic, Antarctic, and Alpine Research, 51(1), 440–459.

Badding, M. E., Briner, J. P., & Kaufman, D. S. (2013). 10Be ages of late Pleistocene deglaciation and Neoglaciation in the north-central Brooks Range, Arctic Alaska. Journal of Quaternary Science, 28(1), 95–102.

Bai, M., Chevalier, M. L., Pan, J., Replumaz, A., Leloup, P. H., Métois, M., & Li, H. (2018). Southeastward increase of the late Quaternary slip-rate of the Xianshuihe fault, eastern Tibet. Geodynamic and seismic hazard implications. Earth and Planetary Science Letters, 485, 19–31.

Bakke, J., Paasche, Ø., Schaefer, J. M., & Timmermann, A. (2021). Long-term demise of sub-Antarctic glaciers modulated by the Southern Hemisphere Westerlies. Scientific Reports, 11(1).

Balbas, A. M., Barth, A. M., Clark, P. U., Clark, J., Caffee, M., O'Connor, J., Baker, V. R., Konrad, K., & Bjornstad, B. (2017). 10Be dating of late pleistocene megafloods and cordilleran ice sheet retreat in the northwestern United States. Geology, 45(7), 583–586.

Balco, G. (2011). Contributions and unrealized potential contributions of cosmogenic-nuclide exposure dating to glacier chronology, 1990-2010. Quaternary Science Reviews, 30 (1–2), 3–27.

Balco, G. (2020). Glacier Change and Paleoclimate Applications of Cosmogenic-Nuclide Exposure Dating. Annual Review of Earth and Planetary Sciences, 48, 21-48.

Balco, G., Briner, J., Finkel, R. C., Rayburn, J. A., Ridge, J. C., & Schaefer, J. M. (2009). Regional beryllium-10 production rate calibration for late-glacial northeastern North America. Quaternary Geochronology, 4(2), 93–107.

Balco, G., & Schaefer, J. M. (2006). Cosmogenic-nuclide and varve chronologies for the deglaciation of southern New England. Quaternary Geochronology, 1(1), 15–28.

Balco, G., Stone, J. O. H., Porter, S. C., & Caffee, M. W. (2002). Cosmogenic-nuclide ages for New England coastal moraines, Martha's Vineyard and Cape Cod, Massachusetts, USA. Quaternary Science Reviews, 21.

Balco, G., Stone, J. O., Lifton, N. A., & Dunai, T. J. (2008). A complete and easily accessible means of calculating surface exposure ages or erosion rates from 10Be and 26Al measurements. Quaternary Geochronology, 3 (3), pp. 174–195.

Balco, G., Stone, J. O. H., Sliwinski, M. G., & Todd, C. (2014). Features of the glacial history of the Transantarctic Mountains inferred from cosmogenic 26Al, 10Be and 21Ne concentrations in bedrock surfaces. Antarctic Science, 26(6), 708–723.

Balco, G., Todd, C., Huybers, K., Campbell, S., Vermeulen, M., Hegland, M., Goehring, B. M., & Hillebrand, T. R. (2016). Cosmogenic-nuclide exposure ages from the Pensacola Mountains adjacent to the foundation ice stream, Antarctica. American Journal of Science, 316(6), 542–577.

Ballantyne, C. K., Rinterknecht, V., & Gheorghiu, D. M. (2013). Deglaciation chronology of the Galloway Hills Ice Centre, southwest Scotland. Journal of Quaternary Science, 28(4), 412–420.

Ballantyne, C. K., Schnabel, C., & Xu, S. (2009). Readvance of the last British-Irish Ice Sheet during Greenland Interstade 1 (GI-1): the Wester Ross Readvance, NW Scotland. Quaternary Science Reviews, 28(9–10), 783–789.

Ballantyne, C. K., Stone, J. O., & McCarroll, D. (2008). Dimensions and chronology of the last ice sheet in Western Ireland. Quaternary Science Reviews, 27(3–4), 185–200.

Ballantyne, C. K., Wilson, P., Gheorghiu, D., & Rodés, À. (2014). Enhanced rock-slope failure following ice-sheet deglaciation: Timing and causes. Earth Surface Processes and Landforms, 39(7), 900–913.

Balter-Kennedy, A., Bromley, G., Balco, G., Thomas, H., & Jackson, M. S. (2020). A 14.5-million-year record of East Antarctic Ice Sheet fluctuations from the central Transantarctic Mountains, constrained with cosmogenic 3He, 10Be, 21Ne, and 26Al. Cryosphere, 14(8), 2647–2672.

Barnard, P. L., Owen, L. A., & Finkel, R. C. (2004a). Style and timing of glacial and paraglacial sedimentation in a monsoon-influenced high Himalayan environment, the upper Bhagirathi Valley, Garhwal Himalaya. Sedimentary Geology, 165(3–4), 199–221.

Barnard, P. L., Owen, L. A., Sharma, M. C., & Finkel, R. C. (2004b). Late Quaternary (Holocene) landscape evolution of a monsoon-influenced high Himalayan valley, Gori Ganga, Nanda Devi, NE Garhwal. Geomorphology, 61(1–2), 91–110.

Barnard, P. L., Owen, L. A., Finkel, R. C., & Asahi, K. (2006). Landscape response to deglaciation in a high relief, monsoon-influenced alpine environment, Langtang Himal, Nepal. Quaternary Science Reviews, 25(17–18), 2162–2176.

Baroni, C., Casale, S., Salvatore, M. C., Ivy-Ochs, S., Christl, M., Carturan, L., Seppi, R., & Carton, A. (2017). Double response of glaciers in the Upper Peio Valley (Rhaetian Alps, Italy) to the Younger Dryas climatic deterioration. Boreas, 46(4), 783–798.

Baroni, C., Gennaro, S., Salvatore, M. C., Ivy-Ochs, S., Christl, M., Cerrato, R., & Orombelli, G. (2021). Last Lateglacial glacier advance in the Gran Paradiso Group reveals relatively drier climatic conditions established in the Western Alps since at least the Younger Dryas. Quaternary Science Reviews, 255.

Baroni, C., Guidobaldi, G., Salvatore, M. C., Christl, M., & Ivy-Ochs, S. (2018). Last glacial maximum glaciers in the Northern Apennines reflect primarily the influence of southerly storm-tracks in the western Mediterranean. Quaternary Science Reviews, 197, 352–367.

Barr, I. D., & Lovell, H. (2014). A review of topographic controls on moraine distribution. Geomorphology, 226, 44–64. Elsevier.

Barrows, T. T., Almond, P., Rose, R., Keith Fifield, L., Mills, S. C., & Tims, S. G. (2013). Late Pleistocene glacial stratigraphy of the Kumara-Moana region, West Coast of South Island, New Zealand. Quaternary Science Reviews, 74, 139–159.

Barrows, T. T., Lehman, S. J., Fifield, L. K., & De Drecker, P. (2007). Absence of Cooling in New Zealand and the Adjacent Ocean During the Younger Dryas Chronozone. Science, 318(5847), 86–89.

Barrows, T. T., Stone, J. O., Fifield, L. K., & Cresswell, R. G. (2001). Late pleistocene glaciation of the kosciouszko massif, snowy mountains, Australia. Quaternary Research, 55(2), 179–189.

Barrows, T. T., Stone, J. O., Fifield, L. K., & Cresswell, R. G. (2002). The timing of the Last Glacial Maximum in Australia. Quaternary Science Reviews, 21.

Barth, A. M., Clark, P. U., Clark, J., McCabe, A. M., & Caffee, M. (2016). Last Glacial Maximum cirque glaciation in Ireland and implications for reconstructions of the Irish Ice Sheet. Quaternary Science Reviews, 141, 85–93.

Barth, A. M., Clark, P. U., Clark, J., Roe, G. H., Marcott, S. A., Marshall McCabe, A., Caffee, M. W., He, F., Cuzzone, J. K., & Dunlop, P. (2018). Persistent millennial-scale glacier fluctuations in Ireland between 24 ka and 10 ka. Geology, 46(2), 151–154.

Batbaatar, J., & Gillespie, A. R. (2016). Outburst floods of the Maly Yenisei. Part II – new age constraints from Darhad basin. International Geology Review, 58(14), 1753–1779.

Batbaatar, J., Gillespie, A. R., Fink, D., Matmon, A., & Fujioka, T. (2018). Asynchronous glaciations in arid continental climate. Quaternary Science Reviews, 182, 1–19. Elsevier Ltd.

Batbaatar, J., Gillespie, A. R., Koppes, M., Clark, D. H., Chadwick, O. A., Fink, D., Matmon, A., & Rupper, S. (2020). Glacier development in continental climate regions of central Asia, in Waitt, R.B., Thackray, G.D., and Gillespie, A.R., eds., Untangling the Quaternary Period: A Legacy of Stephen C. Porter. Special Paper of the Geological Society of America, 548, 123–153.

Becker, R. A., Barth, A. M., Marcott, S. A., Tikoff, B., & Caffee, M. (2018). The last deglaciation along Mono Creek and the south fork of the San Joaquin River, Sierra Nevada, USA. In: Becker RA, Glacial geology and geomorphology of the west-central Sierra Nevada, USA. Dissertation thesis, University of Wisconsin-Madison.

Belda, M., Holtanová, E., Halenka, T., & Kalvová, J. (2014). Climate classification revisited: From Köppen to Trewartha. Climate Research, 59(1), 1–13.

Benn, D. I., Owen, L. A., Finkel, R. C., & Clemmens, S. (2006). Pleistocene lake outburst floods and fan formation along the eastern Sierra Nevada, California: implications for the interpretation of intermontane lacustrine records. Quaternary Science Reviews, 25(21–22), 2729–2748.

Benson, L., Madole, R., Kubik, P., & McDonald, R. (2007). Surface-exposure ages of Front Range moraines that may have formed during the Younger Dryas, 8.2 cal ka, and Little Ice Age events. Quaternary Science Reviews, 26(11–12), 1638–1649.

Benson, L., Madole, R., Phillips, W., Landis, G., Thomas, T., & Kubik, P. (2004). The probable importance of snow and sediment shielding on cosmogenic ages of north-central Colorado Pinedale and pre-Pinedale moraines. Quaternary Science Reviews, 23(1–2), 193–206.

Bentley, M. J., Evans, D. J. A., Fogwill, C. J., Hansom, J. D., Sugden, D. E., & Kubik, P. W. (2007). Glacial geomorphology and chronology of deglaciation, South Georgia, sub-Antarctic. Quaternary Science Reviews, 26(5–6), 644–677.

Bentley, M. J., Hein, A. S., Sugden, D. E., Whitehouse, P. L., Shanks, R., Xu, S., & Freeman, S. P. H. T. (2017). Deglacial history of the Pensacola Mountains, Antarctica from glacial geomorphology and cosmogenic nuclide surface exposure dating. Quaternary Science Reviews, 158, 58–76.

Bichler, M. G., Reindl, M., Reitner, J. M., Drescher-Schneider, R., Wirsig, C., Christl, M., Hajdas, I., & Ivy-Ochs, S. (2016). Landslide deposits as stratigraphical markers for a sequence-based glacial stratigraphy: a case study of a Younger Dryas system in the Eastern Alps. Boreas, 45(3), 537–551.

Biette, M., Jomelli, V., Chenet, M., Braucher, R., Rinterknecht, V., & Lane, T. (2020). Mountain glacier fluctuations during the Lateglacial and Holocene on Clavering Island (northeastern Greenland) from 10Be moraine dating. Boreas, 49(4), 873–885.

Blard, P. H., Braucher, R., Lavé, J., & Bourlès, D. (2013). Cosmogenic 10Be production rate calibrated against 3He in the high Tropical Andes (3800-4900 m, 20-22° S). Earth and Planetary Science Letters, 382, 140–149.

Blomdin, R., Stroeven, A. P., Harbor, J. M., Lifton, N. A., Heyman, J., Gribenski, N., Petrakov, D. A., Caffee, M. W., Ivanov, M. N., Hättestrand, C., Rogozhina, I., & Usubaliev, R. (2016).

Evaluating the timing of former glacier expansions in the Tian Shan: A key step towards robust spatial correlations. Quaternary Science Reviews, 153, 78–96.

Blomdin, R., Stroeven, A. P., Harbor, J. M., Gribenski, N., Caffee, M. W., Heyman, J., Rogozhina, I., Ivanov, M. N., Petrakov, D. A., Walther, M., Rudoy, A. N., Zhang, W., Orkhonselenge, A., Hättestrand, C., Lifton, N. A., & Jansson, K. N. (2018). Timing and dynamics of glaciation in the Ikh Turgen Mountains, Altai region, High Asia. Quaternary Geochronology, 47, 54–71.

Böhlert, R., Egli, M., Maisch, M., Brandová, D., Ivy-Ochs, S., Kubik, P. W., & Haeberli, W. (2011). Application of a combination of dating techniques to reconstruct the Lateglacial and early Holocene landscape history of the Albula region (eastern Switzerland). Geomorphology, 127(1–2), 1–13.

Boxleitner, M., Ivy-Ochs, S., Brandova, D., Christl, M., Egli, M., & Maisch, M. (2018). Piecing together the Lateglacial advance phases of the Reussgletscher (central Swiss Alps). Geographica Helvetica, 73(3), 241–252.

Boxleitner, M., Ivy-Ochs, S., Egli, M., Brandova, D., Christl, M., Dahms, D., & Maisch, M. (2019a). The 10Be deglaciation chronology of the Göschenertal, central Swiss Alps, and new insights into the Göschenen Cold Phases. Boreas, 48(4), 867–878.

Boxleitner, M., Ivy-Ochs, S., Egli, M., Brandova, D., Christl, M., & Maisch, M. (2019b). Lateglacial and Early Holocene glacier stages - New dating evidence from the Meiental in central Switzerland. Geomorphology, 340, 15–31.

Boxleitner, M., Musso, A., Waroszewski, J., Malkiewicz, M., Maisch, M., Dahms, D., Brandová, D., Christl, M., de Castro Portes, R., & Egli, M. (2017). Late Pleistocene – Holocene surface processes and landscape evolution in the central Swiss Alps. Geomorphology, 295, 306–322.

Braakhekke, J., Ivy-Ochs, S., Monegato, G., Gianotti, F., Martin, S., Casale, S., & Christl, M. (2020). Timing and flow pattern of the Orta Glacier (European Alps) during the Last Glacial Maximum. Boreas, 49(2), 315–332.

Bradwell, T., Fabel, D., Stoker, M., Mathers, H., McHargue, L., & Howe, J. (2008). Ice caps existed throughout the Lateglacial Interstadial in northern Scotland. Journal of Quaternary Science, 23(5), 401–407.

Bradwell, T., Fabel, D., Clark, C. D., Chiverrell, R. C., Small, D., Smedley, R. K., Saher, M. H., Moreton, S. G., Dove, D., Callard, S. L., Duller, G. A. T., Medialdea, A., Bateman, M. D., Burke, M. J., McDonald, N., Gilgannon, S., Morgan, S., Roberts, D. H., & Cofaigh, C. (2021a). Pattern, style and timing of British–Irish Ice Sheet advance and retreat over the last 45 000 years: evidence from NW Scotland and the adjacent continental shelf. Journal of Quaternary Science, 36(5), 871–933.

Bradwell, T., Small, D., Fabel, D., Clark, C. D., Chiverrell, R. C., Saher, M. H., Dove, D., Callard, S. L., Burke, M. J., Moreton, S. G., Medialdea, A., Bateman, M. D., Roberts, D. H., Golledge, N. R., Finlayson, A., Morgan, S., & Cofaigh, C. (2021b). Pattern, style and timing of British–Irish Ice Sheet retreat: Shetland and northern North Sea sector. Journal of Quaternary Science, 36(5), 681–722.

Braucher, R., Kalvoda, J., Bourlès, D., Brown, E., Engel, Z., & Mercier, J.-L. (2006). Late Pleistocene deglaciation in the Vosges and the Krkonoše mountains: correlation of cosmogenic 10Be exposure ages. Geografický Časopis, 58, 3–14.

Braumann, S. M., Schaefer, J. M., Neuhuber, S. M., Reitner, J. M., Lüthgens, C., & Fiebig, M. (2020). Holocene glacier change in the Silvretta Massif (Austrian Alps) constrained by a new 10Be chronology, historical records and modern observations. Quaternary Science Reviews, 245.

Briner, J. P. (2009). Moraine pebbles and boulders yield indistinguishable 10Be ages: A case study from Colorado, USA. Quaternary Geochronology, 4(4), 299–305.

Briner, J. P., & Hormes, A. (2018). 10Be dating the last deglaciation of Bjørnøya, Svalbard. Arktos, 4(1), 1–10.

Briner, J. P., Kaufman, D. S., Manley, W. F., Finkel, R. C., & Caffee, M. W. (2005). Cosmogenic exposure dating of late Pleistocene moraine stabilization in Alaska. Bulletin of the Geological Society of America, 117(7–8), 1108–1120.

Briner, J. P., Miller, G. H., Davis, P. T., Bierman, P. R., & Caffee, M. (2003). Last glacial maximum ice sheet dynamics in Arctic Canada inferred from young erratics perched on ancient tors. Quaternary Science Reviews, 22(5–7), 437–444.

Briner, J. P., Overeem, I., Miller, G., & Finkel, R. (2007). The deglaciation of Clyde Inlet, northeastern Baffin Island, Arctic Canada. Journal of Quaternary Science, 22(3), 223–232.

Briner, J. P., Svendsen, J. I., Mangerud, J., Lohne, Ø. S., & Young, N. E. (2014). A 10Be chronology of south-western Scandinavian Ice Sheet history during the Lateglacial period. Journal of Quaternary Science, 29(4), 370–380.

Briner, J. P., Tulenko, J. P., Kaufman, D. S., Young, N. E., Baichtal, J. F., & Lesnek, A. (2017). The last deglaciation of Alaska. Cuadernos de Investigacion Geografica, 43(2), 429–448.

Bromley, G. R. M., Hall, B. L., Thompson, W. B., Kaplan, M. R., Garcia, J. L., & Schaefer, J. M. (2015). Late glacial fluctuations of the Laurentide Ice Sheet in the White Mountains of Maine and New Hampshire, U.S.A. Quaternary Research (United States), 83(3), 522–530.

Bromley, G. R. M., Hall, B. L., Thompson, W. B., & Lowell, T. V. (2020). Age of the Berlin moraine complex, New Hampshire, USA, and implications for ice sheet dynamics and climate during Termination 1. Quaternary Research (United States), 94, 80–93.

Bromley, G. R. M., Schaefer, J. M., Hall, B. L., Rademaker, K. M., Putnam, A. E., Todd, C. E., Hegland, M., Winckler, G., Jackson, M. S., & Strand, P. D. (2016). A cosmogenic 10Be chronology for the local last glacial maximum and termination in the Cordillera Oriental, southern Peruvian Andes: Implications for the tropical role in global climate. Quaternary Science Reviews, 148, 54–67.

Brook, E. J., Kurz, M. D., Ackert, R. P., Denton, G. H., Brown, E. T., Raisbeck, G. M., & Tiou, F. (1993). Chronology of Taylor Glacier advances in Arena Valley, Antarctica, using in situ cosmogenic 3He and 10Be. Quaternary Research, 39, 11–23.

Brook, E. J., Kurz, M. D., Ackert, R. P., Raisbeck, G., & Yiou, F. (1995). Cosmogenic nuclide exposure ages and glacial history of late Quaternary Ross Sea drift in McMurdo Sound, Antarctica. EPSL Earth and Planetary Science Letters, 131.

Brook, M. S., Shulmeister, J., Crow, T. V. H., & Zondervan, A. (2008). First cosmogenic 10Be constraints on LGM glaciation on New Zealand's North Islands: Park Valley, Tararua Range. Journal of Quaternary Science, 23(8), 707–712.

Brown, E. T., Edmond, J. M., Raisbeck, G. M., Yiou, F., Kurz, M. D., & Brook, E. J. (1991). Examination of surface exposure ages of Antarctic moraines using in situ produced "Be and 26Al. Geochimica et Cosmochimica Acta 55, 2269-2283.

Brown, E. T., Bendick, R., Bourlès, D. L., Gaur, V., Molnar, P., Raisbeck, G. M., & Yiou, F. (2002). Slip rates of the Karakorum fault, Ladakh, India, determined using cosmic ray exposure dating of debris flows and moraines. Journal of Geophysical Research: Solid Earth, 107(B9).

Brugger, K. A. (2007). Cosmogenic 10Be and 36Cl ages from Late Pleistocene terminal moraine complexes in the Taylor River drainage basin, central Colorado, USA. Quaternary Science Reviews, 26(3–4), 494–499.

Brugger, K. A., Laabs, B., Reimers, A., & Bensen, N. (2019a). Late Pleistocene glaciation in the Mosquito Range, Colorado, USA: chronology and climate. Journal of Quaternary Science, 34(3), 187–202.

Brugger, K. A., Ruleman, C. A., Caffee, M. W., & Mason, C. C. (2019b). Climate during the last glacial maximum in the Northern Sawatch range, Colorado, USA. Quaternary, 2(4).

Carcaillet, J., Angel, I., Carrillo, E., Audemard, F. A., & Beck, C. (2013). Timing of the last deglaciation in the Sierra Nevada of the Mérida Andes, Venezuela. Quaternary Research (United States), 80(3), 482–494.

Carlson, A. E., Winsor, K., Ullman, D. J., Brook, E. J., Rood, D. H., Axford, Y., Legrande, A. N., Anslow, F. S., & Sinclair, G. (2014). Earliest Holocene south Greenland ice sheet retreat within its late Holocene extent. Geophysical Research Letters, 41(15), 5514–5521.

Carrasco, R. M., Pedraza, J., Domínguez-Villar, D., Villa, J., & Willenbring, J. K. (2013). The plateau glacier in the Sierra de Béjar (Iberian Central System) during its maximum extent. Reconstruction and chronology. Geomorphology, 196, 83–93.

Carrasco, R. M., Pedraza, J., Domínguez-Villar, D., Willenbring, J. K., & Villa, J. (2015). Sequence and chronology of the Cuerpo de Hombre paleoglacier (Iberian Central System) during the last glacial cycle. Quaternary Science Reviews, 129, 163–177.

Ceperley, E. G., Marcott, S. A., Rawling, J. E., Zoet, L. K., & Zimmerman, S. R. H. (2019). The role of permafrost on the morphology of an MIS 3 moraine from the southern Laurentide Ice Sheet. Geology, 47(5), 440–444.

Chen, Y., Li, Y., Wang, Y., Zhang, M., Cui, Z., Yi, C., & Liu, G. (2015). Late Quaternary glacial history of the Karlik Range, easternmost Tian Shan, derived from 10Be surface exposure and optically stimulated luminescence datings. Quaternary Science Reviews, 115, 17–27.

Chenet, M., Brunstein, D., Jomelli, V., Roussel, E., Rinterknecht, V., Mokadem, F., Biette, M., Robert, V., & Léanni, L. (2016). 10Be cosmic-ray exposure dating of moraines and rock avalanches in the Upper Romanche valley (French Alps): Evidence of two glacial advances during the Late Glacial/Holocene transition. Quaternary Science Reviews, 148, 209–221.

Chevalier, M. L., Hilley, G., Tapponnier, P., Van Der Woerd, J., Liu-Zeng, J., Finkel, R. C., Ryerson, F. J., Li, H., & Liu, X. (2011). Constraints on the late Quaternary glaciations in Tibet

from cosmogenic exposure ages of moraine surfaces. Quaternary Science Reviews, 30(5–6), 528–554.

Chevalier, M. L., Leloup, P. H., Replumaz, A., Pan, J., Liu, D., Li, H., Gourbet, L., & Métois, M. (2016). Tectonic-geomorphology of the Litang fault system, SE Tibetan Plateau, and implication for regional seismic hazard. Tectonophysics, 682, 278–292.

Chevalier, M. L., Leloup, P. H., Replumaz, A., Pan, J., Métois, M., & Li, H. (2018). Temporally constant slip rate along the Ganzi fault, NW Xianshuihe fault system, eastern Tibet. Bulletin of the Geological Society of America, 130(3–4), 396–410.

Chevalier, M. L., & Replumaz, A. (2019). Deciphering old moraine age distributions in SE Tibet showing bimodal climatic signal for glaciations: Marine Isotope Stages 2 and 6. Earth and Planetary Science Letters, 507, 105–118.

Chevalier, M. L., Replumaz, A., Wang, S., Pan, J., Bai, M., Li, K., & Li, H. (2022). Limit of monsoonal precipitation in southern Tibet during the Last Glacial Maximum from relative moraine extents. Geomorphology, 397.

Clark, P. U., Brook, E. J., Raisbeck, G. M., Yiou, F., & Clark, J. (2003). Cosmogenic 10 Be ages of the Saglek Moraines, Torngat Mountains, Labrador. Geology, 31(7), 617-620.

Clark, J., Marshall Mccabe, A., Schnabel, C., Clark, P. U., Freeman, S., Maden, C., & BOREAS Clark, S. X. (2009a). 10Be chronology of the last deglaciation of County Donegal, northwestern Ireland. Boreas, 38, 111–118.

Clark, J., McCabe, A. M., Schnabel, C., Clark, P. U., McCarron, S., Freeman, S. P. H. T., Maden, C., & Xu, S. (2009b). Cosmogenic 10Be chronology of the last deglaciation of western Ireland, and implications for sensitivity of the Irish ice sheet to climate change. Bulletin of the Geological Society of America, 121(1–2), 3–16.

Cogez, A., Herman, F., Pelt, É., Reuschlé, T., Morvan, G., Darvill, C. M., Norton, K. P., Christl, M., Märki, L., & Chabaux, F. (2018). U-Th and 10Be constraints on sediment recycling in proglacial settings, Lago Buenos Aires, Patagonia. Earth Surface Dynamics, 6(1), 121–140.

Colgan, P. M., Munroe, J. S., & Shangzhe, Z. (2006). Cosmogenic radionuclide evidence for the limited extent of last glacial maximum glaciers in the Tanggula Shan of the central Tibetan Plateau. Quaternary Research, 65(2), 336–339.

Conrad, V. (1946): Usual formulas for continentality and their limits of validity. American Geophysical Union Transactions, 27, 663–664.

Corbett, L. B., Bierman, P. R., Lasher, G. E., & Rood, D. H. (2015). Landscape chronology and glacial history in Thule, northwest Greenland. Quaternary Science Reviews, 109, 57–67.

Corbett, L. B., Bierman, P. R., & Rood, D. H. (2016). An approach for optimizing in situ cosmogenic 10Be sample preparation. Quaternary Geochronology, 33, 24–34.

Cossart, E., Fort, M., Bourlès, D., Braucher, R., Perrier, R., & Siame, L. (2012). Deglaciation pattern during the Lateglacial/Holocene transition in the southern French Alps. Chronological data and geographical reconstruction from the Clarée Valley (upper Durance catchment, southeastern France). Palaeogeography, Palaeoclimatology, Palaeoecology, 315–316, 109–123.

Crest, Y., Delmas, M., Braucher, R., Gunnell, Y., & Calvet, M. (2017). Cirques have growth spurts during deglacial and interglacial periods: Evidence from 10Be and 26Al nuclide inventories in the central and eastern Pyrenees. Geomorphology, 278, 60–77.

Crump, S. E., Anderson, L. S., Miller, G. H., & Anderson, R. S. (2017). Interpreting exposure ages from ice-cored moraines: a Neoglacial case study on Baffin Island, Arctic Canada. Journal of Quaternary Science, 32(8), 1049–1062.

Crump, S. E., Miller, G. H., Power, M., Sepúlveda, J., Dildar, N., Coghlan, M., & Bunce, M. (2019). Arctic shrub colonization lagged peak postglacial warmth: Molecular evidence in lake sediment from Arctic Canada. Global Change Biology, 25(12), 4244–4256.

Crump, S. E., Young, N. E., Miller, G. H., Pendleton, S. L., Tulenko, J. P., Anderson, R. S., & Briner, J. P. (2020). Glacier expansion on Baffin Island during early Holocene cold reversals. Quaternary Science Reviews, 241.

Cunningham, M. T., Stark, C. P., Kaplan, M. R., & Schaefer, J. M. (2019). Glacial buzzcutting limits the height of tropical mountains. Earth Surface Dynamics, 7, 147-169.

Dahms, D., Egli, M., Fabel, D., Harbor, J., Brandová, D., de Castro Portes, R., & Christl, M. (2018). Revised Quaternary glacial succession and post-LGM recession, southern Wind River Range, Wyoming, USA. Quaternary Science Reviews, 192, 167–184.

D'Arcy, M., Schildgen, T. F., Strecker, M. R., Wittmann, H., Duesing, W., Mey, J., Tofelde, S., Weissmann, P., & Alonso, R. N. (2019). Timing of past glaciation at the Sierra de Aconquija, northwestern Argentina, and throughout the Central Andes. Quaternary Science Reviews, 204, 37–57.

Darvill, C. M. (2013). Cosmogenic nuclide analysis. British Society for Geomorphology.

Darvill, C. M., Menounos, B., Goehring, B. M., Lian, O. B., & Caffee, M. W. (2018). Retreat of the Western Cordilleran Ice Sheet Margin During the Last Deglaciation. Geophysical Research Letters, 45(18), 9710–9720.

Davies, B. J. (2022). Cryospheric Geomorphology: Dating Glacial Landforms II: Radiometric Techniques. Treatise on Geomorphology, 249–280. Elsevier.

Davies, B. J., Hambrey, M. J., Glasser, N. F., Holt, T., Rodés, A., Smellie, J. L., Carrivick, J. L., & Blockley, S. P. E. (2017). Ice-dammed lateral lake and epishelf lake insights into Holocene dynamics of Marguerite Trough Ice Stream and George VI Ice Shelf, Alexander Island, Antarctic Peninsula. Quaternary Science Reviews, 177, 189–219.

Davies, B. J., Thorndycraft, V. R., Fabel, D., & Martin, J. R. V. (2018). Asynchronous glacier dynamics during the Antarctic Cold Reversal in central Patagonia. Quaternary Science Reviews, 200, 287–312.

Davis, P. T., Bierman, P. R., Corbett, L. B., & Finkel, R. C. (2015). Cosmogenic exposure age evidence for rapid Laurentide deglaciation of the Katahdin area, west-central Maine, USA, 16 to 15ka. Quaternary Science Reviews, 116, 95–105.

Davis, P. T., Bierman, P. R., Marsella, K. A., Caffee, M. W., & Southon, J. R. (1999). Cosmogenic analysis of glacial terrains in the eastern Canadian Arctic: A test for inherited nuclides and the effectiveness of glacial erosion. Annals of Glaciology, 28, 181–188.

Delmas, M., Calvet, M., Gunnell, Y., Braucher, R., & Bourlès, D. (2011). Palaeogeography and 10Be exposure-age chronology of Middle and Late Pleistocene glacier systems in the northern Pyrenees: Implications for reconstructing regional palaeoclimates. Palaeogeography, Palaeoclimatology, Palaeoecology, 305(1–4), 109–122.

Delmas, M., Gunnell, Y., Braucher, R., Calvet, M., & Bourlès, D. (2008). Exposure age chronology of the last glaciation in the eastern Pyrenees. Quaternary Research, 69(2), 231–241.

Demek, J., Aristarkhova, L.B., Verstappen, H.T., Bashenina, N.V., BélangerJ.R. (1971). Manual of detailed geomorphological mapping. Czechoslovak Academy of Sciences, Institute of Geography. Brno. 435.

Denton, G. H., Putnam, A. E., Russell, J. L., Barrell, D. J. A., Schaefer, J. M., Kaplan, M. R., & Strand, P. D. (2021). The Zealandia Switch: Ice age climate shifts viewed from Southern Hemisphere moraines. Quaternary Science Reviews, 257.

Di Nicola, L., Strasky, S., Schlüchter, C., Salvatore, M. C., Kubik, P. W., Ivy-Ochs, S., Wieler, R., Akçar, N., & Baroni, C. (2007). Complex exposure history of pre-LGM glacial drifts in Terra Nova Bay, Victoria Land, using a multiple cosmogenic nuclide approach. In A. K. Cooper & C. R. et al. Raymond (Eds.), Antarctica: A Keystone in a Changing World – Online Proceedings of the 10th ISAES X. USGS Open-File Report 2007-1047.

Di Nicola, L., Strasky, S., Schlüchter, C., Salvatore, M. C., Akçar, N., Kubik, P. W., Christl, M., Kasper, H. U., Wieler, R., & Baroni, C. (2009). Multiple cosmogenic nuclides document complex Pleistocene exposure history of glacial drifts in Terra Nova Bay (northern Victoria Land, Antarctica). Quaternary Research, 71(1), 83–92.

Dieleman, C., Ivy-Ochs, S., Hippe, K., Kronig, O., Kober, F., & Christl, M. (2018). Reconsidering the origin of the Sedrun fans (Graubünden, Switzerland). E and G Quaternary Science Journal, 67(1), 17–23.

Dixon, J. C., & Thorn, C. E. (2005). Chemical weathering and landscape development in mid-latitude alpine environments. Geomorphology, 67(1-2 SPEC. ISS.), 127–145.

Dong, G. C., Yi, C. L., & Caffee, M. (2014). 10Be dating of boulders on moraines from the last glacial period in the Nyainqentanglha mountains, Tibet. Science China Earth Sciences, 57(2), 221–231.

Dong, G., Huang, F., Yi, C., Liu, X., Zhou, W., & Caffee, M. W. (2016). Mid-late Pleistocene glacial evolution in the Grove Mountains, East Antarctica, constraints from cosmogenic 10Be surface exposure dating of glacial erratic cobbles. Quaternary Science Reviews, 145, 71–81.

Dong, G., Xu, X., Zhou, W., Fu, Y., Zhang, L., & Li, M. (2017a). Cosmogenic 10Be surface exposure dating and glacier reconstruction for the Last Glacial Maximum in the Quemuqu Valley, western Nyainqentanglha Mountains, south Tibet. Journal of Quaternary Science, 32(5), 639–652.

Dong, G., Zhou, W., Yi, C., Zhang, L., Li, M., Fu, Y., & Zhang, Q. (2017b). Cosmogenic 10Be surface exposure dating of 'Little Ice Age' glacial events in the Mount Jaggang area, central Tibet. Holocene, 27(10), 1516–1525.

Dong, G., Zhou, W., Yi, C., Fu, Y., Zhang, L., & Li, M. (2018). The timing and cause of glacial activity during the last glacial in central Tibet based on 10Be surface exposure dating east of Mount Jaggang, the Xainza range. Quaternary Science Reviews, 186, 284–297.

Dong, G., Zhou, W., Fu, Y., Zhang, L., Zhao, G., & Li, M. (2020). The last glaciation in the headwater area of the Xiaokelanhe River, Chinese Altai: Evidence from 10Be exposure-ages. Quaternary Geochronology, 56.

Dong, G., Zhou, W., Xian, F., Fu, Y., Zhang, L., Ding, P., Zhao, G., & Li, M. (2022). Timing and climatic drivers for the MIS 6 glaciation in the central Himalaya: 10Be surface exposure dating of hummocky moraine northwest of Mt. Gang Benchhen, Paiku Gangri. Palaeogeography, Palaeoclimatology, Palaeoecology, 605.

Dortch, J. M., Owen, L. A., & Caffee, M. W. (2010a). Quaternary glaciation in the Nubra and Shyok valley confluence, northernmost Ladakh, India. Quaternary Research, 74(1), 132–144.

Dortch, J. M., Owen, L. A., Caffee, M. W., & Brease, P. (2010b). Late Quaternary glaciation and equilibrium line altitude variations of the McKinley River region, central Alaska Range. Boreas, 39(2), 233–246.

Dortch, J. M., Owen, L. A., Caffee, M. W., Li, D., & Lowell, T. V. (2010c). Beryllium-10 surface exposure dating of glacial successions in the Central Alaska Range. Journal of Quaternary Science, 25(8), 1259–1269.

Dortch, J. M., Owen, L. A., & Caffee, M. W. (2013). Timing and climatic drivers for glaciation across semi-arid western Himalayan-Tibetan orogen. Quaternary Science Reviews, 78, 188–208.

Dortch, J. M., Tomkins, M. D., Saha, S., Murari, M. K., Schoenbohm, L. M., & Curl, D. (2022). A tool for the ages: The Probabilistic Cosmogenic Age Analysis Tool (P-CAAT). Quaternary Geochronology, 71.

Doughty, A. M., Schaefer, J. M., Putnam, A. E., Denton, G. H., Kaplan, M. R., Barrell, D. J. A., Andersen, B. G., Kelley, S. E., Finkel, R. C., & Schwartz, R. (2015). Mismatch of glacier extent and summer insolation in Southern Hemisphere mid-latitudes. Geology, 43(5), 407–410.

Douglass, D. C., Singer, B. S., Kaplan, M. R., Ackert, R. P., Mickelson, D. M., & Caffee, M. W. (2005). Evidence of early Holocene glacial advances in southern South America from cosmogenic surface-exposure dating. Geology, 33(3), 237–240.

Douglass, D. C., Singer, B. S., Kaplan, M. R., Mickelson, D. M., & Caffee, M. W. (2006). Cosmogenic nuclide surface exposure dating of boulders on last-glacial and late-glacial moraines, Lago Buenos Aires, Argentina: Interpretive strategies and paleoclimate implications. Quaternary Geochronology, 1(1), 43–58.

Dowling, L., Eaves, S., Norton, K., Mackintosh, A., Anderson, B., Hidy, A., Lorrey, A., Vargo, L., Ryan, M., & Tims, S. (2021). Local summer insolation and greenhouse gas forcing drove warming and glacier retreat in New Zealand during the Holocene. Quaternary Science Reviews, 266.

Dühnforth, M., & Anderson, R. (2011). Reconstructing the glacial history of green lakes valley, North Boulder Creek, Colorado front range. Arctic, Antarctic, and Alpine Research, 43(4), 527–542.

Dunai, T. J. (2000). Scaling factors for production rates of in situ produced cosmogenic nuclides: a critical reevaluation. Earth and Planetary Science Letters, 176(1), 157–169.

Dunai, T. J., & Lifton, N. A. (2014). The nuts and bolts of cosmogenic nuclide production. Elements, 10(5), 347–350.

Egli, M., Dahms, D., Dumitrescu, M., Derakhshan-Babaei, F., Christl, M., & Tikhomirov, D. (2020). Landscape evolution, post-LGM surface denudation and soil weathering processes from Dickinson Park mire, Wind River Range, Wyoming (USA). Geomorphology, 371.

Engel, Z., Braucher, R., Traczyk, A., Laetitia, L., Arnold, M., Aumaître, G., Bourlès, D., & Keddadouche, K. (2014). 10Be exposure age chronology of the last glaciation in the Krkonoše Mountains, Central Europe. Geomorphology, 206, 107–121.

Engel, Z., Křížek, M., Mentlík, P., Pluháčková, M., Braucher, R., Arnold, M., Aumaître, G., Bourlès, D., & Keddadouche, K. (2017). 10Be exposure age chronology of the last glaciation of the Roháčská Valley in the Western Tatra Mountains, central Europe. Geomorphology, 293, 130–142.

Engel, Z., Mentlík, P., Braucher, R., Minár, J., Léanni, L., Arnold, M., Aumaître, G., Bourlès, D., Keddadouche, K., & Aster Team. (2015). Geomorphological evidence and 10Be exposure ages for the Last Glacial Maximum and deglaciation of the Velká and Malá Studená dolina valleys in the High Tatra Mountains, central Europe. Quaternary Science Reviews, 124, 106–123.

Engel, Z., Traczyk, A., Braucher, R., Woronko, B., & Křížek, M. (2011). Use of10Be exposure ages and Schmidt hammer data for correlation of moraines in the Krkonoše Mountains, Poland/Czech Republic. Zeitschrift Fur Geomorphologie, 55(2), 175–196.

Etienne, S. (2002). The role of biological weathering in periglacial areas: a study of weathering rinds in south Iceland. Geomorphology, 47, 75-86.

Everest, J. D., Bradwell, T., Fogwill, C. J., & Kubik, P. W. (2006). Cosmogenic 10BE age constraints for the Wester Ross Readvance moraine: Insights into British Ice-Sheet behaviour. Geografiska Annaler, Series A: Physical Geography, 88(1), 9–17.

Everest, J., & Kubik, P. (2006). The deglaciation of eastern Scotland: Cosmogenic 10Be evidence for a Lateglacial stillstand. Journal of Quaternary Science, 21(1), 95–104.

Expage. (2023). A global compilation of glacial 10Be and 26Al data. In https://expage.github.io/index.html.

Fabel, D., Fink, D., Fredin, O., Harbor, J., Land, M., & Stroeven, A. P. (2006). Exposure ages from relict lateral moraines overridden by the Fennoscandian ice sheet. Quaternary Research, 65(1), 136–146.

Fabel, D., Harbor, J., Dahms, D., James, A., Elmore, D., Horn, L., Daley, K., & Steele, C. (2004). Spatial patterns of glacial erosion at a valley scale derived from terrestrial cosmogenic 10Be and 26Al concentrations in rock. Annals of the Association of American Geographers, 94(2), 241–255.

Fame, M. L., Owen, L. A., Spotila, J. A., Dortch, J. M., & Caffee, M. W. (2018). Tracking paraglacial sediment with cosmogenic 10Be using an example from the northwest Scottish Highlands. Quaternary Science Reviews, 182, 20–36.

Farber, D. L., Hancock, G. S., Finkel, R. C., & Rodbell, D. T. (2005). The age and extent of tropical alpine glaciation in the Cordillera Blanca, Peru. Journal of Quaternary Science, 20(7–8), 759–776.

Favilli, F., Egii, M., Brandova, D., Ivy-Ochs, S., Kubik, P. W., Maisch, M., Cherubini, P., & Haeberli, W. (2009). Combination of numerical dating techniques using 10be in rock boulders and 14C of resilient soil organic matter for reconstructing the chronology of glacial and periglacial processes in a high alpine catchment during the late Pleistocene and early Holocene. Radiocarbon, 51(2), 537–552.

Federici, P. R., Granger, D. E., Pappalardo, M., Ribolino, A., Spagnolo, M., & Cyr, A. J. (2008). Exposure age dating and Equilibrium Line Altitude reconstruction of an Egesen moraine in the Maritime Alps, Italy. Boreas, 37(2), 245–253.

Federici, P. R., Granger, D. E., Ribolini, A., Spagnolo, M., Pappalardo, M., & Cyr, A. J. (2012). Last Glacial Maximum and the Gschnitz stadial in the Maritime Alps according to 10Be cosmogenic dating. Boreas, 41(2), 277–291.

Fernández, H., García, J. L., Nussbaumer, S. U., Geiger, A. J., Gärtner-Roer, I., Pérez, F., Tikhomirov, D., Christl, M., & Egli, M. (2022). De-icing landsystem model for the Universidad Glacier (34° S) in the Central Andes of Chile during the past ~660 years. Geomorphology, 400, 108096.

Fernández-Fernández, J. M., Palacios, D., García-Ruiz, J. M., Andrés, N., Schimmelpfennig, I., Gómez-Villar, A., Santos-González, J., Álvarez-Martínez, J., Arnáez, J., Úbeda, J., Léanni, L., & ASTER Team. (2017). Chronological and geomorphological investigation of fossil debris-covered glaciers in relation to deglaciation processes: A case study in the Sierra de La Demanda, northern Spain. Quaternary Science Reviews, 170, 232–249.

Fink, D., McKelvey, B., Hambrey, M. J., Fabel, D., & Brown, R. (2006). Pleistocene deglaciation chronology of the Amery Oasis and Radok Lake, northern Prince Charles Mountains, Antarctica. Earth and Planetary Science Letters, 243(1–2), 229–243.

Finkel, R. C., Owen, L. A., Barnard, P. L., & Caffee, M. W. (2003). Beryllium-10 dating of Mount Everest moraines indicates a strong monsoon influence and glacial synchroneity throughout the Himalaya. Geology, 31, 561-564.

Finlayson, A., Fabel, D., Bradwell, T., & Sugden, D. (2014). Growth and decay of a marine terminating sector of the last British-Irish Ice Sheet: A geomorphological reconstruction. Quaternary Science Reviews, 83, 28–45.

Finlayson, A., Golledge, N., Bradwell, T., & Fabel, D. (2011). Evolution of a Lateglacial mountain icecap in northern Scotland. Boreas, 40(3), 536–554.

Fleming, K. C. (2019). Cosmogenic 10Be surface exposure dating and numerical modeling of late Pleistocene glaciers and lakes in northwestern Nevada. Ms Thesis, North Dakota State University.

Fogwill, C. (2003). The application of cosmogenic exposure dating to glacial landforms: Examples from Antarctica and Patagonia. Dissertation thesis, University of Edinburgh.

Fogwill, C. J., Turney, C. S. M., Golledge, N. R., Rood, D. H., Hippe, K., Wacker, L., Wieler, R., Rainsley, E. B., & Jones, R. S. (2014). Drivers of abrupt Holocene shifts in West Antarctic

ice stream direction determined from combined ice sheet modelling and geologic signatures. Antarctic Science, 26(6), 674–686.

Fu, P., Stroeven, A. P., Harbor, J. M., Hättestrand, C., Heyman, J., Caffee, M. W., & Zhou, L. (2013). Paleoglaciation of Shaluli Shan, southeastern Tibetan Plateau. Quaternary Science Reviews, 64, 121–135.

Ganyushkin, D., Chistyakov, K., Volkov, I., Bantcev, D., Kunaeva, E., Brandová, D., Raab, G., Christl, M., & Egli, M. (2018). Palaeoclimate, glacier and treeline reconstruction based on geomorphic evidences in the Mongun-Taiga massif (south-eastern Russian Altai) during the Late Pleistocene and Holocene. Quaternary International, 470, 26–37.

Ganyushkin, D. A., Lessovaia, S. N., Vlasov, D. Y., Kopitsa, G. P., Almásy, L., Chistyakov, K. V., Panova, E. G., Derkach, E., & Alekseeva, A. (2021). Application of rock weathering and colonization by biota for the relative dating of moraines from the arid part of the Russian Altai mountains. Geosciences (Switzerland), 11(8).

García, J. L., Hall, B. L., Kaplan, M. R., Gómez, G. A., De Pol-Holz, R., García, V. J., Schaefer, J. M., & Schwartz, R. (2020). 14C and 10Be dated Late Holocene fluctuations of Patagonian glaciers in Torres del Paine (Chile, 51°S) and connections to Antarctic climate change. Quaternary Science Reviews, 246.

García, J. L., Hein, A. S., Binnie, S. A., Gómez, G. A., González, M. A., & Dunai, T. J. (2018). The MIS 3 maximum of the Torres del Paine and Última Esperanza ice lobes in Patagonia and the pacing of southern mountain glaciation. Quaternary Science Reviews, 185, 9–26.

García, J. L., Kaplan, M. R., Hall, B. L., Schaefer, J. M., Vega, R. M., Schwartz, R., & Finkel, R. (2012). Glacier expansion in Southern Patagonia throughout the Antarctic cold reversal. Geology, 40(9), 859–862.

García, J. L., Maldonado, A., De Porras, M. E., Delaunay, A. N., Reyes, O., Ebensperger, C. A., Binnie, S. A., Lüthgens, C., & Méndez, C. (2019). Early deglaciation and paleolake history of Río Cisnes Glacier, Patagonian Ice Sheet (44°S). Quaternary Research (United States), 91(1), 194–217.

García-Ruiz, J. M., Palacios, D., Fernández-Fernández, J. M., Andrés, N., Arnáez, J., Gómez-Villar, A., Santos-González, J., Álvarez-Martínez, J., Lana-Renault, N., & Léanni, L. (2020). Glacial stages in the Peña Negra valley, Iberian Range, northern Iberian Peninsula: Assessing the importance of the glacial record in small cirques in a marginal mountain area. Geomorphology, 362.

Gayer, E., Pik, R., Lavé, J., France-Lanord, C., Bourlès, D., & Marty, B. (2004). Cosmogenic 3He in Himalayan garnets indicating an altitude dependence of the 3He/10Be production ratio. Earth and Planetary Science Letters, 229(1–2), 91–104.

Gheorghiu, D. M., Fabel, D., Hansom, J. D., & Xu, S. (2012). Lateglacial surface exposure dating in the Monadhliath Mountains, Central Highlands, Scotland. Quaternary Science Reviews, 41, 132–146.

Gheorghiu, D. M., Hosu, M., Corpade, C., & Xu, S. (2015). Deglaciation constraints in the Parâng Mountains, Southern Romania, using surface exposure dating. Quaternary International, 388, 156–167.

Gianotti, F., Forno, M. G., Ivy-Ochs, S., & Kubik, P. W. (2008). New chronological and stratigraphical data on the Ivrea amphitheatre (Piedmont, NW Italy). Quaternary International, 190(1), 123–135.

Gibbons, A. B., Megeath, J. D., & Pierce, K. L. (1984). Probability of moraine survival in a succession of glacial advances. Geology, *12*(6), 327–330.

Gillespie, A. R., Burke, R. M., Komatsu, G., & Bayasgalan, A. (2008). Late Pleistocene glaciers in Darhad Basin, northern Mongolia. Quaternary Research, 69(2), 169–187.

Glasser, N. F., Clemmens, S., Schnabel, C., Fenton, C. R., & McHargue, L. (2009). Tropical glacier fluctuations in the Cordillera Blanca, Peru between 12.5 and 7.6 ka from cosmogenic 10Be dating. Quaternary Science Reviews, 28(27–28), 3448–3458.

Glasser, N. F., Davies, B. J., Carrivick, J. L., Rodés, A., Hambrey, M. J., Smellie, J. L., & Domack, E. (2014). Ice-stream initiation, duration and thinning on James Ross Island, northern Antarctic Peninsula. Quaternary Science Reviews, 86, 78–88.

Glasser, N. F., Harrison, S., Ivy-Ochs, S., Duller, G. A. T., & Kubik, P. W. (2006). Evidence from the Rio Bayo valley on the extent of the North Patagonian Icefield during the Late Pleistocene-Holocene transition. Quaternary Research, 65(1), 70–77.

Glasser, N. F., Harrison, S., Schnabel, C., Fabel, D., & Jansson, K. N. (2012). Younger Dryas and early Holocene age glacier advances in Patagonia. Quaternary Science Reviews, 58, 7–17.

Glasser, N. F., Jansson, K. N., Goodfellow, B. W., de Angelis, H., Rodnight, H., & Rood, D. H. (2011). Cosmogenic nuclide exposure ages for moraines in the Lago San Martin Valley, Argentina. Quaternary Research, 75(3), 636–646.

Goehring, B. M., Kelly, M. A., Schaefer, J. M., Finkel, R. C., & Lowell, T. V. (2010). Dating of raised marine and lacustrine deposits in east Greenland using beryllium-10 depth profiles and implications for estimates of subglacial erosion. Journal of Quaternary Science, 25(6), 865–874.

Goehring, B. M., Lohne, Ø. S., Mangerud, J., Svendsen, J. I., Gyllencreutz, R., Schaefer, J., & Finkel, R. (2012). Late glacial and holocene 10Be production rates for western Norway. Journal of Quaternary Science, 27(1), 89–96.

Gosse, J. C., Evenson, E. B., Klein, J., Lawn, B., & Middleton, R. (1995a). Precise cosmogenic 10 Be measurements in western North America: Support for a global Younger Dryas cooling event. Geology, 23, 877–880.

Gosse, J. C., Klein, J., Evenson, E. B., Lawn, B., & Middleton, R. (1995b). Beryllium-10 Dating of the Duration and Retreat of the Last Pinedale Glacial Sequence. New Series, 268(5215).

Gosse, J. C., & Phillips, F. M. (2001). Terrestrial in situ cosmogenic nuclides: theory and application. Quaternary Science Reviews, 20.

Graf, A. A., Strasky, S., Zhao, Z. Z., Akçar, N., Ivy-Ochs, S., Kubik, P. W., Christl, M., Kasper, H. U., Wieler, R., & Schlüchter, C. (2008). Glacier extension on the eastern Tibetan Plateau in response to MIS 2 cooling, with a contribution to 10Be and 21Ne methodology. In: Strasky S, Glacial response to global climate changes: cosmogenic nuclide chronologies from high and low latitudes. Dissertation thesis, ETH Zürich.

Grant, O. R. (2016). The deglaciation of Kongsfjorden, Svalbard-based on surface exposure dating of glacial erratics and Quaternary geological mapping of Blomstrandhalvøya. Ms thesis, University of Bergen.

Gribenski, N., Jansson, K. N., Lukas, S., Stroeven, A. P., Harbor, J. M., Blomdin, R., Ivanov, M. N., Heyman, J., Petrakov, D. A., Rudoy, A., Clifton, T., Lifton, N. A., & Caffee, M. W. (2016). Complex patterns of glacier advances during the late glacial in the Chagan Uzun Valley, Russian Altai. Quaternary Science Reviews, 149, 288–305.

Gribenski, N., Jansson, K. N., Preusser, F., Harbor, J. M., Stroeven, A. P., Trauerstein, M., Blomdin, R., Heyman, J., Caffee, M. W., Lifton, N. A., & Zhang, W. (2018). Re-evaluation of MIS 3 glaciation using cosmogenic radionuclide and single grain luminescence ages, Kanas Valley, Chinese Altai. Journal of Quaternary Science, 33(1), 55–67.

Grin, E., Ehlers, T. A., Schaller, M., Sulaymonova, V., Ratschbacher, L., & Gloaguen, R. (2016). 10Be surface-exposure age dating of the Last Glacial Maximum in the northern Pamir (Tajikistan). Quaternary Geochronology, 34, 47–57.

Gump, D. J., Briner, J. P., Mangerud, J., & Svendsen, J. I. (2017). Deglaciation of Boknafjorden, south-western Norway. Journal of Quaternary Science, 32(1), 80–90.

Håkansson, L., Graf, A., Strasky, S., Ivy-Ochs, S., Kubik, P. W., Hjort, C., & Shlüchter, C. (2007). Cosmogenic 10Be-Ages from the Store Koldewey Island, NE Greenland. Geografiska Annaler. Series A, Physical Geography, 89(3), 195-202.

Hales, T. C., & Roering, J. J. (2007). Climatic controls on frost cracking and implications for the evolution of bedrock landscapes. Journal of Geophysical Research: Earth Surface, 112(2).

Hall, K. (1999). The role of thermal stress fatigue in the breakdown of rock in cold regions. Geomorphology, 31.

Hall, A. M., Binnie, S. A., Sugden, D., Dunai, T. J., & Wood, C. (2016). Late readvance and rapid final deglaciation of the last ice sheet in the Grampian Mountains, Scotland. Journal of Quaternary Science, 31(8), 869–878.

Hall, B. L., Lowell, T. V., & Brickle, P. (2020). Multiple glacial maxima of similar extent at ~20–45 ka on Mt. Usborne, East Falkland, South Atlantic region. Quaternary Science Reviews, 250.

Hall, S. R., Farber, D. L., Ramage, J. M., Rodbell, D. T., Finkel, R. C., Smith, J. A., Mark, B. G., & Kassel, C. (2009). Geochronology of Quaternary glaciations from the tropical Cordillera Huayhuash, Peru. Quaternary Science Reviews, 28(25–26), 2991–3009.

Hallet, B., & Putkonen, J. (1994). Surface Dating of Dynamic Landforms: Young Boulders on Aging Moraines. New Series, 265(5174).

Harrison, S., Glasser, N., Anderson, E., Ivy-Ochs, S., & Kubik, P. W. (2010). Late Pleistocene mountain glacier response to North Atlantic climate change in southwest Ireland. Quaternary Science Reviews, 29(27–28), 3948–3955.

Heath, S. L., Lowell, T. V., & Hall, B. L. (2020). Surface exposure dating of the Pierre Sublobe of the James Lobe, laurentide ice sheet. Quaternary Research (United States), 97, 88–98.

Hebenstreit, R., Ivy-Ochs, S., Kubik, P. W., Schlüchter, C., & Böse, M. (2011). Lateglacial and early Holocene surface exposure ages of glacial boulders in the Taiwanese high mountain range. Quaternary Science Reviews, 30(3–4), 298–311.

Hedrick, K. A., Owen, L. A., Chen, J., Robinson, A., Yuan, Z., Yang, X., Imrecke, D. B., Li, W., Caffee, M. W., Schoenbohm, L. M., & Zhang, B. (2017). Quaternary history and landscape evolution of a high-altitude intermountain basin at the western end of the Himalayan-Tibetan orogen, Waqia Valley, Chinese Pamir. Geomorphology, 284, 156–174.

Hedrick, K. A., Seong, Y. B., Owen, L. A., Caffee, M. W., & Dietsch, C. (2011). Towards defining the transition in style and timing of Quaternary glaciation between the monsoon-influenced Greater Himalaya and the semi-arid Transhimalaya of Northern India. Quaternary International, 236(1–2), 21–33.

Hein, A. S., Hulton, N. R. J., Dunai, T. J., Schnabel, C., Kaplan, M. R., Naylor, M., & Xu, S. (2009). Middle Pleistocene glaciation in Patagonia dated by cosmogenic-nuclide measurements on outwash gravels. Earth and Planetary Science Letters, 286(1–2), 184–197.

Hein, A. S., Hulton, N. R. J., Dunai, T. J., Sugden, D. E., Kaplan, M. R., & Xu, S. (2010). The chronology of the Last Glacial Maximum and deglacial events in central Argentine Patagonia. Quaternary Science Reviews, 29(9–10), 1212–1227.

Hein, A. S., Dunai, T. J., Hulton, N. R. J., & Xu, S. (2011a). Exposure dating outwash gravels to determine the age of the greatest Patagonian glaciations. Geology, 39(2), 103–106.

Hein, A. S., Fogwill, C. J., Sugden, D. E., & Xu, S. (2011b). Glacial/interglacial ice-stream stability in the Weddell Sea embayment, Antarctica. Earth and Planetary Science Letters, 307(1–2), 211–221.

Hein, A. S., Marrero, S. M., Woodward, J., Dunning, S. A., Winter, K., Westoby, M. J., Freeman, S. P. H. T., Shanks, R. P., & Sugden, D. E. (2016a). Mid-Holocene pulse of thinning in the Weddell Sea sector of the West Antarctic ice sheet. Nature Communications, 7.

Hein, A. S., Woodward, J., Marrero, S. M., Dunning, S. A., Steig, E. J., Freeman, S. P. H. T., Stuart, F. M., Winter, K., Westoby, M. J., & Sugden, D. E. (2016b). Evidence for the stability of the West Antarctic Ice Sheet divide for 1.4 million years. Nature Communications, 7.

Hein, A. S., Cogez, A., Darvill, C. M., Mendelova, M., Kaplan, M. R., Herman, F., Dunai, T. J., Norton, K., Xu, S., Christl, M., & Rodés, Á. (2017). Regional mid-Pleistocene glaciation in central Patagonia. Quaternary Science Reviews, 164, 77–94.

Heine, K., Reuther, A. U., Thieke, H. U., Schulz, R., Schlaak, N., & Kubik, P. W. (2009). Timing of Weichselian ice marginal positions in Brandenburg (northeastern Germany) using cosmogenic in situ 10Be. Zeitschrift Fur Geomorphologie, 53(4), 433–454.

Henriksen, M., Alexanderson, H., Landvik, J. Y., Linge, H., & Peterson, G. (2014). Dynamics and retreat of the Late Weichselian Kongsfjorden ice stream, NW Svalbard. Quaternary Science Reviews, 92, 235–245.

Heyman, J., Stroeven, A. P., Caffee, M. W., Hättestrand, C., Harbor, J. M., Li, Y., Alexanderson, H., Zhou, L., & Hubbard, A. (2011a). Palaeoglaciology of Bayan Har Shan, NE Tibetan Plateau: Exposure ages reveal a missing LGM expansion. Quaternary Science Reviews, 30(15–16), 1988–2001.

Heyman, J., Stroeven, A. P., Harbor, J. M., & Caffee, M. W. (2011b). Too young or too old: Evaluating cosmogenic exposure dating based on an analysis of compiled boulder exposure ages. Earth and Planetary Science Letters, 302(1–2), 71–80.

Heyman, J. (2014). Paleoglaciation of the Tibetan Plateau and surrounding mountains based on exposure ages and ELA depression estimates. Quaternary Science Reviews, 91.

Heyman, J., Applegate, P. J., Blomdin, R., Gribenski, N., Harbor, J. M., & Stroeven, A. P. (2016). Boulder height - exposure age relationships from a global glacial 10Be compilation. Quaternary Geochronology, 34, 1–11.

Hodgson, D. A., Bentley, M. J., Schnabel, C., Cziferszky, A., Fretwell, P., Convey, P., & Xu, S. (2012). Glacial geomorphology and cosmogenic 10Be and 26Al exposure ages in the northern Dufek Massif, Weddell Sea embayment, Antarctica. Antarctic Science, 24(4), 377–394.

Hofmann, F. M. (2018). Glacial history of the upper Drac Blanc catchment (Écrins massif, French Alps). E&G Quaternary Science Journal, 67, 37–40.

Hormes, A., Ivy-Ochs, S., Kubik, P. W., Ferreli, L., & Maria Michetti, A. (2008). 10Be exposure ages of a rock avalanche and a late glacial moraine in Alta Valtellina, Italian Alps. Quaternary International, 190(1), 136–145.

Houmark-Nielsen, M., Linge, H., Fabel, D., Schnabel, C., Xu, S., Wilcken, K. M., & Binnie, S. (2012). Cosmogenic surface exposure dating the last deglaciation in Denmark: Discrepancies with independent age constraints suggest delayed periglacial landform stabilisation. Quaternary Geochronology, 13, 1–17.

Howle, J. F., Bawden, G. W., Schweickert, R. A., Finkel, R. C., Hunter, L. E., Rose, R. S., & von Twistern, B. (2012). Airborne lidar analysis and geochronology of faulted glacial moraines in the Tahoe-Sierra frontal fault zone reveal substantial seismic hazards in the Lake Tahoe region, California-Nevada, USA. Bulletin of the Geological Society of America, 124(7–8), 1087–1101.

Hu, G., Yi, C., Zhang, J., Dong, G., Liu, J., Xu, X., & Jiang, T. (2017). Extensive glacial advances during the Last Glacial Maximum near the eastern Himalayan syntaxis. Quaternary International, 443, 1–12.

Hubert-Ferrari, A., Suppe, J., Van Der Woerd, J., Wang, X., & Lu, H. (2005). Irregular earthquake cycle along the southern Tianshan front Aksu area, China. Journal of Geophysical Research: Solid Earth, 110(6), 1–18.

Hughes, P. D., Fink, D., Fletcher, W. J., & Hannah, G. (2014). Catastrophic rock avalanches in a glaciated valley of the High Atlas, Morocco: 10Be exposure ages reveal a 4.5 ka seismic event. Bulletin of the Geological Society of America, 126(7–8), 1093–1104.

Hughes, P. D., Fink, D., Rodés, Á., Fenton, C. R., & Fujioka, T. (2018). Timing of Pleistocene glaciations in the High Atlas, Morocco: New 10Be and 36Cl exposure ages. Quaternary Science Reviews, 180, 193–213.

ICE-D. (2024). Informal cosmogenic-nuclide exposure-age database. Https://Www.Ice-d.Org/.

Ivy-Ochs, S., & Briner, J. P. (2014). Dating disappearing ice with cosmogenic nuclides. Elements, 10(5), 351–356.

Ivy-Ochs, S., Schlüchter, C., Kubik, P. W., Synal, H.-A., Beer, J., & Kerschner, H. (1996). The exposure age of an Egesen moraine at Julier Pass, Switzerland, measured with the cosmogenic radionuclides 10Be, 26A1 and 36Cl. Eclogae Geologicae Helvetiae, 89, 1049-1063.

Ivy-Ochs, S., Schluchter, C., Kubik, P. W., & Denton, G. H. (1999). Moraine Exposure Dates Imply Synchronous Younger Dryas Glacier Advances in the European Alps and in the Southern Alps of New Zealand. Geografiska Annaler, Series A: Physical Geography, 81(2), 313–323.

Ivy-Ochs, S., Schäfer, J., Kubik, P. W., Synal, H. A., & Schlüchter, C. (2004). Timing of deglaciation on the northern Alpine foreland (Switzerland). Eclogae Geologicae Helvetiae, 97(1), 47–55.

Ivy-Ochs, S., Kerschner, H., Kubik, P. W., & Schlüchter, C. (2006a). Glacier response in the European Alps to Heinrich Event 1 cooling: The Gschnitz stadial. Journal of Quaternary Science, 21(2) 115–130.

Ivy-Ochs, S., Kerschner, H., Reuther, A., Maisch, M., Sailer, R., Schaefer, J., Kubik, P. W., Synal, H. A., & Schlüchter, C. (2006b). The timing of glacier advances in the northern European Alps based on surface exposure dating with cosmogenic 10 Be, 26 Al, 36 Cl, and 21 Ne. Special Paper of the Geological Society of America, 415, 43–60.

Ivy-Ochs, S., Kerschner, H., Reuther, A., Preusser, F., Heine, K., Maisch, M., Kubik, P. W., & Schlüchter, C. (2008). Chronology of the last glacial cycle in the European Alps. Journal of Quaternary Science, 23(6–7), 559–573.

Ivy-Ochs, S., Lucchesi, S., Baggio, P., Fioraso, G., Gianotti, F., Monegato, G., Graf, A. A., Akçar, N., Christl, M., Carraro, F., Forno, M. G., & Schlüchter, C. (2018). New geomorphological and chronological constraints for glacial deposits in the Rivoli-Avigliana end-moraine system and the lower Susa Valley (Western Alps, NW Italy). Journal of Quaternary Science, 33(5), 550–562.

Jackson, L. E., Phillips, F. M., Shimamura, K., & Little, E. C. (1997). Cosmogenic 36Cl dating of the Foothills erratics train. Geology, 25(3), 195–198.

Jackson, M. S., Kelly, M. A., Russell, J. M., Doughty, A. M., Howley, J. A., Chipman, J. W., Cavagnaro, D. A., Baber, M. B., Zimmerman, S. R. H., & Nakileza, B. (2020). Glacial fluctuations in tropical Africa during the last glacial termination and implications for tropical climate following the Last Glacial Maximum. Quaternary Science Reviews, 243.

Jackson, M. S., Kelly, M. A., Russell, J. M., Doughty, A. M., Howley, J. A., Chipman, J. W., Cavagnaro, D., Nakileza, B., & Zimmerman, S. R. H. (2019). High-latitude warming initiated the onset of the last deglaciation in the tropics. Sci. Adv., 5.

Johnsen, T. F., Alexanderson, H., Fabel, D., & Freeman, S. P. H. T. (2009). New 10be cosmogenic ages from the vimmerby moraine confirm the timing of scandinavian ice sheet deglaciation in southern Sweden. Geografiska Annaler, Series A: Physical Geography, 91(2), 113–120.

Johnsen, T. F., Fabel, D., & Stroeven, A. P. (2010). High-elevation cosmogenic nuclide dating of the last deglaciation in the central Swedish mountains: implications for the timing of tree establishment. In: Johnsen TF, Late Quaternary ice sheet history and dynamics in central and southern Scandinavia. Dissertation thesis, Stockholm University.

Jomelli, V., Favier, V., Vuille, M., Braucher, R., Martin, L., Blard, P. H., Colose, C., Brunstein, D., He, F., Khodri, M., Bourlès, D. L., Leanni, L., Rinterknecht, V., Grancher, D., Francou, B., Ceballos, J. L., Fonseca, H., Liu, Z., & Otto-Bliesner, B. L. (2014). A major advance of tropical Andean glaciers during the Antarctic cold reversal. Nature, 513(7517), 224–228.

Jomelli, V., Khodri, M., Favier, V., Brunstein, D., Ledru, M. P., Wagnon, P., Blard, P. H., Sicart, J. E., Braucher, R., Grancher, D., Bourlès, D. L., Braconnot, P., & Vuille, M. (2011). Irregular tropical glacier retreat over the Holocene epoch driven by progressive warming. Nature, 474(7350), 196–199.

Jones, R. S., Whitmore, R. J., Mackintosh, A. N., Norton, K. P., Eaves, S. R., Stutz, J., & Christl, M. (2021). Regional-Scale abrupt Mid-Holocene Ice sheet thinning in the Western Ross Sea, Antarctica. Geology, 49(3), 278–282.

Joy, K., Fink, D., Storey, B., De Pascale, G. P., Quigley, M., & Fujioka, T. (2017). Cosmogenic evidence for limited local LGM glacial expansion, Denton Hills, Antarctica. Quaternary Science Reviews, 178, 89–101.

Kaplan, M. R., Ackert, R. P., Singer, B. S., Douglass, D. C., & Kurz, M. D. (2004). Cosmogenic nuclide chronology of millennial-scale glacial advances during O-isotope stage 2 in Patagonia. Bulletin of the Geological Society of America, 116(3–4), 308–321.

Kaplan, M. R., Coronato, A., Hulton, N. R. J., Rabassa, J. O., Kubik, P. W., & Freeman, S. P. H. T. (2007). Cosmogenic nuclide measurements in southernmost South America and implications for landscape change. Geomorphology, 87(4), 284–301.

Kaplan, M. R., Douglass, D. C., Singer, B. S., Ackert, R. P., & Caffee, M. W. (2005). Cosmogenic nuclide chronology of pre-last glacial maximum moraines at Lago Buenos Aires, 46°S, Argentina. Quaternary Research, 63(3), 301–315.

Kaplan, M. R., Fogwill, C. J., Sugden, D. E., Hulton, N. R. J., Kubik, P. W., & Freeman, S. P. H. T. (2008). Southern Patagonian glacial chronology for the Last Glacial period and implications for Southern Ocean climate. Quaternary Science Reviews, 27(3–4), 284–294.

Kaplan, M. R., Schaefer, J. M., Denton, G. H., Barrell, D. J. A., Chinn, T. J. H., Putnam, A. E., Andersen, B. G., Finkel, R. C., Schwartz, R., & Doughty, A. M. (2010). Glacier retreat in New Zealand during the Younger Dryas stadial. Nature, 467(7312), 194–197.

Kaplan, M. R., Schaefer, J. M., Denton, G. H., Doughty, A. M., Barrell, D. J. A., Chinn, T. J. H., Putnam, A. E., Andersen, B. G., Mackintosh, A., Finkel, R. C., Schwartz, R., & Anderson, B. (2013). The anatomy of long-term warming since 15 ka in New Zealand based on net glacier snowline rise. Geology, 41(8), 887–890.

Kaplan, M. R., Schaefer, J. M., Strelin, J. A., Denton, G. H., Anderson, R. F., Vandergoes, M. J., Finkel, R. C., Schwartz, R., Travis, S. G., Garcia, J. L., Martini, M. A., & Nielsen, S. H. H. (2016). Patagonian and southern South Atlantic view of Holocene climate. Quaternary Science Reviews, 141, 112–125.

Kaplan, M. R., Strelin, J. A., Schaefer, J. M., Denton, G. H., Finkel, R. C., Schwartz, R., Putnam, A. E., Vandergoes, M. J., Goehring, B. M., & Travis, S. G. (2011). In-situ cosmogenic 10Be production rate at Lago Argentino, Patagonia: Implications for late-glacial climate chronology. Earth and Planetary Science Letters, 309(1–2), 21–32.

Kawamata, M., Suganuma, Y., Doi, K., Misawa, K., Hirabayashi, M., Hattori, A., & Sawagaki, T. (2020). Abrupt Holocene ice-sheet thinning along the southern Soya Coast, Lützow-Holm Bay, East Antarctica, revealed by glacial geomorphology and surface exposure dating. Quaternary Science Reviews, 247.

Kellerer-Pirklbauer, A. (2017). Potential weathering by freeze-thaw action in alpine rocks in the European Alps during a nine year monitoring period. Geomorphology, 296, 113–131.

Kelley, S. E., Kaplan, M. R., Schafer, J. M., Andersen, B. G., Barrell, D. J. A., Putnam, A. E., Denton, G. H., Schwartz, R., Finkel, R. C., & Doughty, A. M. (2014). High-precision 10Be chronology of moraines in the Southern Alps indicates synchronous cooling in Antarctica and New Zealand 42,000 years ago. Earth and Planetary Science Letters, 405, 194–206.

Kelly, M. A., Kubik, P. W., Von Blanckenburg, F., & Schlüchter, C. (2004). Surface exposure dating of the Great Aletsch Glacier Egesen moraine system, western Swiss Alps, using the cosmogenic nuclide 10Be. Journal of Quaternary Science, 19(5), 431–441.

Kelly, M. A., Lowell, T. V., Applegate, P. J., Phillips, F. M., Schaefer, J. M., Smith, C. A., Kim, H., Leonard, K. C., & Hudson, A. M. (2015). A locally calibrated, late glacial 10Be production rate from a low-latitude, high-altitude site in the Peruvian Andes. Quaternary Geochronology, 26(1), 70–85.

Kelly, M. A., Lowell, T. V., Hall, B. L., Schaefer, J. M., Finkel, R. C., Goehring, B. M., Alley, R. B., & Denton, G. H. (2008). A 10Be chronology of lateglacial and Holocene mountain glaciation in the Scoresby Sund region, east Greenland: implications for seasonality during lateglacial time. Quaternary Science Reviews, 27(25–26), 2273–2282.

Kelly, M. A., Russell, J. M., Baber, M. B., Howley, J. A., Loomis, S. E., Zimmerman, S., Nakileza, B., & Lukaye, J. (2014). Expanded glaciers during a dry and cold last glacial maximum in equatorial East Africa. Geology, 42(6), 519–522.

Kerschner, H., Hertl, A., Gross, G., Ivy-Ochs, S., & Kubik, P. W. (2006). Surface exposure dating of moraines in the Kromer valley (Silvretta Mountains, Austria) - Evidence for glacial response to the 8.2 ka event in the Eastern Alps? Holocene, 16(1), 7–15.

Khandsuren, P., Seong, Y. B., Oh, J. S., Rhee, H. H., Sandag, K., & Yu, B. Y. (2019). Late Quaternary glacial history of Khentey Mountains, Central Mongolia. Boreas, 48(3), 779–799.

Kiernan, K., Fifield, L. K., & Chappell, J. (2004). Cosmogenic nuclide ages for Last Glacial Maximum moraine at Schnells Ridge, Southwest Tasmania. Quaternary Research, 61(3), 335–338.

Kiernan, K., Fink, D., Greig, D., & Mifud, C. (2010). Cosmogenic radionuclide chronology of pre-last glacial cycle moraines in the Western Arthur range, Southwest Tasmania. Quaternary Science Reviews, 29(23–24), 3286–3297.

Kiernan, K., Fink, D., & McConnell, A. (2017). Cosmogenic 10Be and 26Al exposure ages of glaciations in the Frankland Range, southwest Tasmania reveal a limited MIS-2 ice advance. Quaternary Science Reviews, 157, 141–151.

Kiernan, K., McMinn, M. S., & Fink, D. (2014). Topographic and microclimatic impacts on glaciation of the Denison Range, southwest Tasmania. Quaternary Science Reviews, 97, 136–147.

Kirkbride, M. P., & Winkler, S. (2012). Correlation of Late Quaternary moraines: Impact of climate variability, glacier response, and chronological resolution. Quaternary Science Reviews, 46, 1–29.

Kirkbride, M., Everest, J., Benn, D., Gheorghiu, D., & Dawson, A. (2014). Late-Holocene and Younger Dryas glaciers in the northern Cairngorm Mountains, Scotland. Holocene, 24(2), 141–148.

Kleman, J., Hättestrand, M., Borgström, I., Preusser, F., & Fabel, D. (2020). The Idre marginal moraine – An anchor point for Middle and Late Weichselian ice sheet chronology. Quaternary Science Advances, 2.

Koester, A. J., Shakun, J. D., Bierman, P. R., Davis, P. T., Corbett, L. B., Braun, D., & Zimmerman, S. R. (2017). Rapid thinning of the Laurentide Ice Sheet in coastal Maine, USA, during late Heinrich Stadial 1. Quaternary Science Reviews, 163, 180–192.

Koffman, T. N. B., Schaefer, J. M., Putnam, A. E., Denton, G. H., Barrell, D. J. A., Rowan, A. V., Finkel, R. C., Rood, D. H., Schwartz, R., Plummer, M. A., & Brocklehurst, S. H. (2017). A beryllium-10 chronology of late-glacial moraines in the upper Rakaia valley, Southern Alps, New Zealand supports Southern-Hemisphere warming during the Younger Dryas. Quaternary Science Reviews, 170, 14–25.

Kohut, D. L. (2011). Glacial chronology of a high altitude moraine series, Tamarack Bench/Francis Canyon, Sierra Nevada, California. Ms Thesis, University of California, Riverside.

Kong, P., Fink, D., Na, C., & Huang, F. (2009a). Late Quaternary glaciation of the Tianshan, Central Asia, using cosmogenic 10Be surface exposure dating. Quaternary Research, 72(2), 229–233.

Kong, P., Na, C., Fink, D., Zhao, X., & Xiao, W. (2009b). Moraine dam related to late Quaternary glaciation in the Yulong Mountains, southwest China, and impacts on the Jinsha River. Quaternary Science Reviews, 28(27–28), 3224–3235.

Koppes, M., Gillespie, A. R., Burke, R. M., Thompson, S. C., & Stone, J. (2008). Late Quaternary glaciation in the Kyrgyz Tien Shan. Quaternary Science Reviews, 27(7–8), 846–866.

Kronig, O., Ivy-Ochs, S., Hajdas, I., Christl, M., Wirsig, C., & Schlüchter, C. (2018). Holocene evolution of the Triftje- and the Oberseegletscher (Swiss Alps) constrained with 10Be exposure and radiocarbon dating. Swiss Journal of Geosciences, 111(1–2), 117–131.

Kuhlemann, J., Milivojević, M., Krumrei, I., & Kubik, P. W. (2009). Last glaciation of the Šara Range (Balkan peninsula) increasing dryness from the LGM to the Holocene. Austrian Journal of Earth Sciences, 102, 146–158.

Kuhlemann, J., Dobre, F., Urdea, P., Krumrei, I., Gachev, E., Kubik, P., & Rahn, M. (2013a). Last glacial maximum glaciation of the central south Carpathian range (Romania). Austrian Journal of Earth Sciences, 106, 50–62.

Kuhlemann, J., Gachev, E., Gikov, A., Nedkov, S., Krumrei, I., & Kubik, P. (2013b). Glaciation in the Rila mountains (Bulgaria) during the Last Glacial Maximum. Quaternary International, 293, 51–62.

Laabs, B. J. C., Licciardi, J. M., Leonard, E. M., Munroe, J. S., & Marchetti, D. W. (2020). Updated cosmogenic chronologies of Pleistocene Mountain glaciation in the western United States and associated paleoclimate inferences. Quaternary Science Reviews, 242, Elsevier Ltd.

Laabs, B. J. C., Marchetti, D. W., Munroe, J. S., Refsnider, K. A., Gosse, J. C., Lips, E. W., Becker, R. A., Mickelson, D. M., & Singer, B. S. (2011). Chronology of latest Pleistocene mountain glaciation in the western Wasatch Mountains, Utah, U.S.A. Quaternary Research, 76(2), 272–284.

Laabs, B. J. C., Munroe, J. S., Best, L. C., & Caffee, M. W. (2013). Timing of the last glaciation and subsequent deglaciation in the Ruby Mountains, Great Basin, USA. Earth and Planetary Science Letters, 361, 16–25.

Laabs, B. J. C., Munroe, J. S., Rosenbaum, J. G., Refsnider, K. A., Mickelson, D. M., Singer, B. S., & Caffee, M. W. (2007). Chronology of the last glacial maximum in the upper Bear River Basin, Utah. Arctic, Antarctic, and Alpine Research, 39(4), 537–548.

Lal, D. (1991). Cosmic ray labeling of erosion surfaces: in situ nuclide production rates and erosion models. Earth and Planetary Science Letters, 104.

Landvik, J. Y., Brook, E. J., & Salvigsen, O. (2003). Northwest Svalbard during the last glaciation: Ice-free areas existed. Geology, 31, 905-908.

Lane, T. P., Paasche, Kvisvik, B., Adamson, K. R., Rodés, Patton, H., Gomez, N., Gheorghiu, D., Bakke, J., & Hubbard, A. (2020). Elevation Changes of the Fennoscandian Ice Sheet Interior During the Last Deglaciation. Geophysical Research Letters, 47(14).

Larsen, N. K., Funder, S., Kjær, K. H., Kjeldsen, K. K., Knudsen, M. F., & Linge, H. (2014). Rapid early Holocene ice retreat in West Greenland. Quaternary Science Reviews, 92, 310–323.

Larsen, N. K., Funder, S., Linge, H., Möller, P., Schomacker, A., Fabel, D., Xu, S., & Kjær, K. H. (2016). A Younger Dryas re-advance of local glaciers in north Greenland. Quaternary Science Reviews, 147, 47–58.

Larsen, N. K., Linge, H., Håkansson, L., & Fabel, D. (2012). Investigating the last deglaciation of the Scandinavian Ice Sheet in southwest Sweden with 10Be exposure dating. Journal of Quaternary Science, 27(2), 211–220.

Larsen, N. K., Søndergaard, A. S., Levy, L. B., Laursen, C. H., Bjørk, A. A., Kjeldsen, K. K., Funder, S., Strunk, A., Olsen, J., & Kjær, K. H. (2021). Cosmogenic nuclide inheritance in Little Ice Age moraines - A case study from Greenland. Quaternary Geochronology, 65.

Lasserre, C., Gaudemer, Y., Tapponnier, P., Mériaux, A. -S., Van der Woerd, J., Daoyang, Y., Ryerson, F. J., Finkel, R. C., & Caffee, M. W. (2002). Fast late Pleistocene slip rate on the Leng Long Ling segment of the Haiyuan fault, Qinghai, China. Journal of Geophysical Research: Solid Earth, 107(B11).

Lea, J. M., Fitt, R.N.L., Brough, S., Carr, G., Dick, J., Jones, N., Webster, R.J. (2024). Making climate reanalysis and CMIP6 data processing easy: two “point-and-click” cloud based user interfaces for environmental and ecological studies. Frontiers in Environmental Science. 12.

Le Roy, M., Deline, P., Carcaillet, J., Schimmelpfennig, I., & Ermini, M. (2017). 10Be exposure dating of the timing of Neoglacial glacier advances in the Ecrins-Pelvoux massif, southern

French Alps. Quaternary Science Reviews, 178, 118–138. https://doi.org/10.1016/j.quascirev.2017.10.010

Lee, S. Y., Seong, Y. B., Owen, L. A., Murari, M. K., Lim, H. S., Yoon, H. Il, & Yoo, K. C. (2014). Late Quaternary glaciation in the Nun-Kun massif, northwestern India. Boreas, 43(1), 67–89.

Leger, T. P. M., Hein, A. S., Bingham, R. G., Rodés, Á., Fabel, D., & Smedley, R. K. (2021). Geomorphology and 10Be chronology of the Last Glacial Maximum and deglaciation in northeastern Patagonia, 43°S-71°W. Quaternary Science Reviews, 272.

Leonard, E. M., Laabs, B. J. C., Plummer, M. A., Kroner, R. K., Brugger, K. A., Spiess, V. M., Refsnider, K. A., Xia, Y., & Caffee, M. W. (2017). Late Pleistocene glaciation and deglaciation in the Crestone Peaks area, Colorado Sangre de Cristo Mountains, USA – chronology and paleoclimate. Quaternary Science Reviews, 158, 127–144.

Lesnek, A. J., & Briner, J. P. (2018). Response of a land-terminating sector of the western Greenland Ice Sheet to early Holocene climate change: Evidence from 10Be dating in the Søndre Isortoq region. Quaternary Science Reviews, 180, 145–156.

Levy, L. B., Kelly, M. A., Applegate, P. A., Howley, J. A., & Virginia, R. A. (2018). Middle to late Holocene chronology of the western margin of the Greenland Ice Sheet: A comparison with Holocene temperature and precipitation records. Arctic, Antarctic, and Alpine Research, 50(1).

Levy, L. B., Kelly, M. A., Howley, J. A., & Virginia, R. A. (2012). Age of the Ørkendalen moraines, Kangerlussuaq, Greenland: Constraints on the extent of the southwestern margin of the Greenland Ice Sheet during the Holocene. Quaternary Science Reviews, 52, 1–5.

Levy, L. B., Kelly, M. A., Lowell, T. V., Hall, B. L., Hempel, L. A., Honsaker, W. M., Lusas, A. R., Howley, J. A., & Axford, Y. L. (2014). Holocene fluctuations of Bregne ice cap, Scoresby Sund, east Greenland: A proxy for climate along the Greenland Ice Sheet margin. Quaternary Science Reviews, 92, 357–368.

Levy, L. B., Kelly, M. A., Lowell, T. V., Hall, B. L., Howley, J. A., & Smith, C. A. (2016). Coeval fluctuations of the Greenland ice sheet and a local glacier, central East Greenland, during late glacial and early Holocene time. Geophysical Research Letters, 43(4), 1623–1631.

Levy, L. B., Larsen, N. K., Knudsen, M. F., Egholm, D. L., Bjørk, A. A., Kjeldsen, K. K., Kelly, M. A., Howley, J. A., Olsen, J., Tikhomirov, D., Zimmerman, S. R. H., & Kjær, K. H. (2020). Multi-phased deglaciation of south and southeast Greenland controlled by climate and topographic setting. Quaternary Science Reviews, 242.

Li, Y., Li, Y., Harbor, J., Liu, G., Yi, C., & Caffee, M. W. (2016). Cosmogenic 10Be constraints on Little Ice Age glacial advances in the eastern Tian Shan, China. Quaternary Science Reviews, 138, 105–118.

Li, Y., Liu, G., Chen, Y., Li, Y., Harbor, J., Stroeven, A. P., Caffee, M., Zhang, M., Li, C., & Cui, Z. (2014). Timing and extent of Quaternary glaciations in the Tianger Range, eastern Tian Shan, China, investigated using 10Be surface exposure dating. Quaternary Science Reviews, 98, 7–23.

Li, Y., Liu, G., Kong, P., Harbor, J., Chen, Y., & Caffee, M. (2011). Cosmogenic nuclide constraints on glacial chronology in the source area of the Urumqi River, Tian Shan, China. Journal of Quaternary Science, 26(3), 297–304.

Licciardi, J. M., Clark, P. U., Brook, E. J., Elmore, D., & Sharma, P. (2004). Variable responses of western U.S. glaciers during the last deglaciation. Geology, 32(1), 81–84.

Licciardi, J. M., Clark, P. U., Brook, E. J., Pierce, K. L., Kurz, M. D., Elmore, D., & Sharma, P. (2001). Cosmogenic 3He and 10Be chronologies of the late Pinedale northern Yellowstone ice cap, Montana, USA. Geology, 29, 1095-1098.

Licciardi, J. M., & Pierce, K. L. (2008). Cosmogenic exposure-age chronologies of Pinedale and Bull Lake glaciations in greater Yellowstone and the Teton Range, USA. Quaternary Science Reviews, 27(7–8), 814–831.

Licciardi, J. M., & Pierce, K. L. (2018). History and dynamics of the Greater Yellowstone Glacial System during the last two glaciations. Quaternary Science Reviews, 200, 1–33. Elsevier Ltd.

Licciardi, J. M., Schaefer, J. M., Taggart, J. R., & Lund, D. C. (2009). Holocene Glacier Fluctuations in the Peruvian Andes Indicate Northern Climate Linkages. Science, 325(2), 1677–1679.

Lifton, N., Beel, C., Hättestrand, C., Kassab, C., Rogozhina, I., Heermance, R., Oskin, M., Burbank, D., Blomdin, R., Gribenski, N., Caffee, M., Goehring, B. M., Heyman, J., Ivanov, M., Li, Y., Li, Y., Petrakov, D., Usubaliev, R., Codilean, A. T., … Stroeven, A. P. (2014). Constraints on the late Quaternary glacial history of the Inylchek and Sary-Dzaz valleys from in situ cosmogenic 10Be and 26Al, eastern Kyrgyz Tian Shan. Quaternary Science Reviews, 101, 77–90.

Liu, B., Cui, Z., Peng, X., Han, Y., & Liu, G. (2018). Using 10Be exposure dating to constrain glacial advances during the late glacial and Holocene on Mount Xuebaoding, eastern Tibetan Plateau. Quaternary Research (United States), 90(2), 348–359.

Liu, J., Yi, C., Li, Y., Bi, W., Zhang, Q., & Hu, G. (2017). Glacial fluctuations around the Karola Pass, eastern Lhagoi Kangri Range, since the Last Glacial Maximum. Journal of Quaternary Science, 32(4), 516–527.

Lowell, T. V., Hall, B. L., Kelly, M. A., Bennike, O., Lusas, A. R., Honsaker, W., Smith, C. A., Levy, L. B., Travis, S., & Denton, G. H. (2013). Late Holocene expansion of Istorvet ice cap, Liverpool Land, east Greenland. Quaternary Science Reviews, 63, 128–140.

Lukas, S., 2011. Ice-cored moraines. In: Singh, V., Singh, P., Haritashya, U.K. (Eds.), Encyclopedia of Snow, Ice and Glaciers. Springer, Heidelberg, 616-619.

Luna, L. V., Bookhagen, B., Niedermann, S., Rugel, G., Scharf, A., & Merchel, S. (2018). Glacial chronology and production rate cross-calibration of five cosmogenic nuclide and mineral systems from the southern Central Andean Plateau. Earth and Planetary Science Letters, 500, 242–253.

Mackintosh, A. N., Anderson, B. M. and Pierrehumbert, R. T. (2017). Reconstructing climate from glaciers. Annual Review of Earth and Planetary Sciences, 45(1), 649-680.

Makos, M., Rinterknecht, V., Braucher, R., Tołoczko-Pasek, A., Arnold, M., Aumaître, G., Bourlès, D., & Keddadouche, K. (2018). Last Glacial Maximum and Lateglacial in the Polish High Tatra Mountains - Revised deglaciation chronology based on the 10Be exposure age dating. Quaternary Science Reviews, 187, 130–156.

Makos, M., Rinterknecht, V., Braucher, R., Zarnowski, M., & Aster Team. (2016). Glacial chronology and palaeoclimate in the Bystra catchment, Western Tatra Mountains (Poland) during the Late Pleistocene. Quaternary Science Reviews, 134, 74–91.

Mangerud, J., Goehring, B. M., Lohne, Ø. S., Svendsen, J. I., & Gyllencreutz, R. (2013). Collapse of marine-based outlet glaciers from the Scandinavian Ice Sheet. Quaternary Science Reviews, 67, 8–16.

Mangerud, J., Gosse, J., Matiouchkov, A., & Dolvik, T. (2008). Glaciers in the Polar Urals, Russia, were not much larger during the Last Global Glacial Maximum than today. Quaternary Science Reviews, 27(9–10), 1047–1057.

Marcott, S. A., Clark, P. U., Shakun, J. D., Brook, E. J., Davis, P. T., & Caffee, M. W. (2019). 10Be age constraints on latest Pleistocene and Holocene cirque glaciation across the western United States. Npj Climate and Atmospheric Science, 2(1).

Margold, M., Jansen, J. D., Gurinov, A. L., Codilean, A. T., Fink, D., Preusser, F., Reznichenko, N. V., & Mifsud, C. (2016). Extensive glaciation in Transbaikalia, Siberia, at the Last Glacial Maximum. Quaternary Science Reviews, 132, 161–174.

Margreth, A., Gosse, J. C., & Dyke, A. S. (2017). Wisconsinan and early Holocene glacial dynamics of Cumberland Peninsula, Baffin Island, Arctic Canada. Quaternary Science Reviews, 168, 79–100.

Marsella, K. A., Bierman, P. R., Davis, P. T., & Caffe, M. W. (2000). Cosmogenic 10Be and 26Al ages for the last glacial maximum, eastern Baffin Island, arctic Canada. Geological Society of America Bulletin, 112, 1296–1312.

Martin, L. C. P., Blard, P. H., Lavé, J., Condom, T., Prémaillon, M., Jomelli, V., Brunstein, D., Lupker, M., Charreau, J., Mariotti, V., Tibari, B., Team, A., & Davy, E. (2018). Lake tauca highstand (heinrich stadial 1a) driven by a southward shift of the bolivian high. Science Advances, 4(8).

Martin, L. C. P., Blard, P. H., Lavé, J., Jomelli, V., Charreau, J., Condom, T., Lupker, M., Arnold, M., Aumaître, G., Bourlès, D. L., & Keddadouche, K. (2020). Antarctic-like temperature variations in the Tropical Andes recorded by glaciers and lakes during the last deglaciation. Quaternary Science Reviews, 247.

Martini, M. A., Kaplan, M. R., Strelin, J. A., Astini, R. A., Schaefer, J. M., Caffee, M. W., & Schwartz, R. (2017). Late Pleistocene glacial fluctuations in Cordillera Oriental, subtropical Andes. Quaternary Science Reviews, 171, 245–259.

Masarik, J., & Beer, J. (1999). Simulation of particle fluxes and cosmogenic nuclide production in the Earth's atmosphere. Journal of Geophysical Research Atmospheres, 104(D10), 12099–12111.

Mathers, H. (2014). The impact of the Minch palaeo-ice stream in NW Scotland: Constraining glacial erosion and landscape evolution through geomorphology and cosmogenic nuclide analysis. Dissertation thesis, University of Glasgow.

Matmon, A., Briner, J. P., Carver, G., Bierman, P., & Finkel, R. C. (2010). Moraine chronosequence of the Donnelly Dome region, Alaska. Quaternary Research, 74(1), 63–72.

Matmon, A., Schwartz, D. P., Haeussler, P. J., Finkel, R., Lienkaemper, J. J., Stenner, H. D., & Dawson, T. E. (2006). Denali fault slip rates and Holocene-late Pleistocene kinematics of central Alaska. Geology, 34(8), 645–648.

Matsuoka, N. (1990). The rate of bedrock weathering by frost action: Field measurements and a predictive model. Earth Surface Processes and Landforms, 15(1), 73–90.

Matsuoka, N. (1995). Rock weathering processes and landform development in the Sør Rondane Mountains, Antarctica. Geomorphology, 12.

Mattas, L. A. (2021). 10Be Chronology of Moraines Deposited During the Last Glaciation by the Khumbu Glacier, Nepalese Himalaya. Ms Thesis, University of Maine.

Matthews, J. A., Shakesby, R. A., Schnabel, C., & Freeman, S. (2008). Cosmogenic 10Be and 26Al ages of Holocene moraines in southern Norway I: Testing the method and confirmation of the date of the Erdalen Event (c. 10 ka) at its type-site. Holocene, 18(8), 1155–1164.

May, J. H., Zech, J., Zech, R., Preusser, F., Argollo, J., Kubik, P. W., & Veit, H. (2011). Reconstruction of a complex late Quaternary glacial landscape in the Cordillera de Cochabamba (Bolivia) based on a morphostratigraphic and multiple dating approach. Quaternary Research, 76(1), 106–118.

McCarthy, A., Mackintosh, A., Rieser, U., & Fink, D. (2008). Mountain glacier chronology from Boulder Lake, New Zealand, indicates MIS 4 and MIS 2 ice advances of similar extent. Arctic, Antarctic, and Alpine Research, 40(4), 695–708.

McGreevy, J. P., & Whalley, W. B. (1982). The Geomorphic Significance of Rock Temperature Variations in Cold Environments: A Discussion. Arctic and Alpine Research, 14(2), 157–162.

Mendelová, M., Hein, A. S., Rodés, Á., & Xu, S. (2020). Extensive mountain glaciation in central Patagonia during Marine Isotope Stage 5. Quaternary Science Reviews, 227.

Menounos, B., Clague, J. J., Clarke, G. K. C., Marcott, S. A., Osborn, G., Clark, P. U., Tennant, C., & Novak, A. M. (2013a). Did rock avalanche deposits modulate the late Holocene advance of Tiedemann Glacier, southern Coast Mountains, British Columbia, Canada? Earth and Planetary Science Letters, 384, 154–164.

Menounos, B., Clague, J. J., Osborn, G., Davis, P. T., Ponce, F., Goehring, B., Maurer, M., Rabassa, J., Coronato, A., & Marr, R. (2013b). Latest Pleistocene and Holocene glacier fluctuations in southernmost Tierra del Fuego, Argentina. Quaternary Science Reviews, 77, 70–79.

Menounos, B., Goehring, B. M., Osborn, G., Margold, M., Ward, B., Bond, J., Clarke, G. K. C., Clague, J. J., Lakeman, T., Koch, J., Caffee, M. W., Gosse, J., Stroeven, A. P., Seguinot, J., & Heyman, J. (2017). Cordilleran Ice Sheet mass loss preceded climate reversals near the Pleistocene Termination. Science, 358, 781–784.

Mentlík, P., Engel, Z., Braucher, R., Léanni, L., Arnold, M., Aumaître, G., Bourlés, D., & Keddadouche, K. (2013). Chronology of the Late Weichselian glaciation in the Bohemian Forest in Central Europe. Quaternary Science Reviews, 65, 120–128.

Mériaux, A. S., Ryerson, F. J., Tapponnier, P., Van der Woerd, J., Finkel, R. C., Xu, X., Xu, Z., & Caffee, M. W. (2004). Rapid slip along the central Altyn Tagh Fault: Morphochronologic evidence from Cherchen He and Sulamu Tagh. Journal of Geophysical Research: Solid Earth, 109(6).

Mey, J., D'Arcy, M. K., Schildgen, T. F., Egholm, D. L., Wittmann, H., & Strecker, M. R. (2020). Temperature and precipitation in the southern Central Andes during the last glacial maximum, Heinrich Stadial 1, and the Younger Dryas. Quaternary Science Reviews, 248.

Meyer, M. C., Gliganic, L. A., May, J. H., Merchel, S., Rugel, G., Schlütz, F., Aldenderfer, M. S., & Krainer, K. (2020). Landscape dynamics and human-environment interactions in the northern foothills of Cho Oyu and Mount Everest (southern Tibet) during the Late Pleistocene and Holocene. Quaternary Science Reviews, 229.

Mifsud, Ch., Fujioka, T., Fink, D. (2013). Extraction and purification of quartz in rock using hot phosphoric acid for in situ cosmogenic exposure dating. Nuclear Instruments and Methods in Physics Research B, 294, 203-207.

Möller, P., Larsen, N. K., Kjær, K. H., Funder, S., Schomacker, A., Linge, H., & Fabel, D. (2010). Early to middle Holocene valley glaciations on northernmost Greenland. Quaternary Science Reviews, 29(25–26), 3379–3398.

Moore, E. M. M., Eaves, S. R., Norton, K. P., Mackintosh, A. N., Anderson, B. M., Dowling, L. H., & Hidy, A. J. (2022). Climate reconstructions for the Last Glacial Maximum from a simple cirque glacier in Fiordland, New Zealand. Quaternary Science Reviews, 275.

Moran, A. P., Ivy-Ochs, S., Schuh, M., Christl, M., & Kerschner, H. (2016a). Evidence of central Alpine glacier advances during the Younger Dryas–early Holocene transition period. Boreas, 45(3), 398–410.

Moran, A. P., Kerschner, H., & Ochs, S. I. (2016b). Redating the moraines in the Kromer Valley (Silvretta Mountains) – New evidence for an early Holocene glacier advance. Holocene, 26(4), 655–664.

Moran, A. P., Ivy Ochs, S., Christl, M., & Kerschner, H. (2017). Exposure dating of a pronounced glacier advance at the onset of the late-Holocene in the central Tyrolean Alps. Holocene, 27(9), 1350–1358.

Moreiras, S. M., Páez, M. S., Lauro, C., & Jeanneret, P. (2017). First cosmogenic ages for glacial deposits from the Plata range (33° S): New inferences for Quaternary landscape evolution in the Central Andes. Quaternary International, 438, 50–64.

Moreno, P. I., Kaplan, M. R., François, J. P., Vila-Martínez, R., Moy, C. M., Stern, C. R., & Kubik, P. W. (2009). Renewed glacial activity during the Antarctic cold reversal and persistence of cold conditions until 11.5 ka in southwestern Patagonia. Geology, 37(4), 375–378.

Muñoz Sabater, J. (2019). ERA5-Land monthly averaged data from 1981 to present. Copernicus Climate Change Service (C3S) Climate Data Store (CDS), (20. 6. 2024).

Munroe, J. S., Laabs, B. J. C., Shakun, J. D., Singer, B. S., Mickelson, D. M., Refsnider, K. A., & Caffee, M. W. (2006). Latest pleistocene advance of alpine glaciers in the southwestern Uinta

Mountains, Utah, USA: Evidence for the influence of local moisture sources. Geology, 34(10), 841–844.

Murari, M. K., Owen, L. A., Dortch, J. M., Caffee, M. W., Dietsch, C., Fuchs, M., Haneberg, W. C., Sharma, M. C., & Townsend-Small, A. (2014). Timing and climatic drivers for glaciation across monsoon-influenced regions of the Himalayan-Tibetan orogen. Quaternary Science Reviews, 88, 159–182.

Murray, D. S., Carlson, A. E., Singer, B. S., Anslow, F. S., He, F., Caffee, M., Marcott, S. A., Liu, Z., & Otto-Bliesner, B. L. (2012). Northern hemisphere forcing of the last deglaciation in southern Patagonia. Geology, 40(7), 631–634.

NASA/METI/AIST/Japan Space systems and U.S./Japan ASTER Science Team. (2019). ASTER Global Digital Elevation Model V003 [Data set]. NASA EOSDIS Land Processes Distributed Active Archive Center. (2024-03-10).

Nimick, D. A., McGrath, D., Mahan, S. A., Friesen, B. A., & Leidich, J. (2016). Latest Pleistocene and Holocene glacial events in the Colonia valley, Northern Patagonia Icefield, southern Chile. Journal of Quaternary Science, 31(6), 551–564.

Nishiizumi, K., Kohl, C. P., Arnold, J. R., Dorn, R., Klein, J., Fink, D., Middleton, R., & Lal, D. (1993). Role of in situ cosmogenic nuclides 10Be and 26Al in the study of diverse geomorphic processes. Earth Surface Processes and Landforms, 18, 407–425.

Norris, S. L., Tarasov, L., Monteath, A. J., Gosse, J. C., Hidy, A. J., Margold, M., & Froese, D. G. (2022). Rapid retreat of the southwestern Laurentide Ice Sheet during the Bølling-Allerød interval. Geology, 50(4), 417–421.

Oberholzer, P., Baroni, C., Schaefer, J. M., Orombelli, G., Ochs, S. I., Kubik, P. W., Baur, H., & Wieler, R. (2003). Limited Pliocene/Pleistocene glaciation in Deep Freeze Range, northern Victoria Land, Antarctica, derived from in situ cosmogenic nuclides. Antarctic Science, 15(4), 493–502.

O'Hara, S. L., Briner, J. P., & Kelley, S. E. (2017). A 10Be chronology of early Holocene local glacier moraines in central West Greenland. Boreas, 46(4), 655–666.

Oliva, M., Fernandes, M., Palacios, D., Fernández-Fernández, J. M., Schimmelpfennig, I., Antoniades, D., Aumaître, G., Bourlès, D., & Keddadouche, K. (2021). Rapid deglaciation during the Bølling-Allerød Interstadial in the Central Pyrenees and associated glacial and periglacial landforms. Geomorphology, 385.

Olvmo, M. (2010). Review of denudation processes and quantification of weathering and erosion rates at a 0.1 to 1 Ma time scale. Svensk Kärnbränslehantering AB, University of Gothenburg.

Orr, E. N., Owen, L. A., Murari, M. K., Saha, S., & Caffee, M. W. (2017). The timing and extent of Quaternary glaciation of Stok, northern Zanskar Range, Transhimalaya, of northern India. Geomorphology, 284, 142–155.

Orr, E. N., Owen, L. A., Saha, S., Caffee, M. W., & Murari, M. K. (2018). Quaternary glaciation of the Lato Massif, Zanskar Range of the NW Himalaya. Quaternary Science Reviews, 183, 140–156.

Owen, L. A., Finkel, R. C., Caffee, M. W., & Gualtieri, L. (2002). Timing of multiple late Quaternary glaciations in the Hunza Valley, Karakoram Mountains, northern Pakistan: Defined by cosmogenic radionuclide dating of moraines. Geological Society of America Bulletin 114, 593-604.

Owen, L. A., Finkel, R. C., Haizhou, M., Spencer, J. Q., Derbyshire, E., Barnard, P. L., & Caffee, M. W. (2003a). Timing and style of Late Quaternary glaciation in northeastern Tibet. Geological Society of America Bulletin 115, 1356-1364.

Owen, L. A., Finkel, R. C., Minnich, R. A., & Perez, A. E. (2003b). Extreme southwestern margin of late Quaternary glaciation in North America: Timing and controls. Geology 31, 729-732.

Owen, L. A., Spencer, J. Q., Haizhou, M., Barnard, P. L., Derbyshire, E., Finkel, R. C., Caffee, M. W., & Nian, Z. Y. (2003c). Timing of Late Quaternary glaciation along the southwestern slopes of the Qilian Shan, Tibet. Boreas, 32(2), 281–291.

Owen, L. A., Finkel, R. C., Barnard, P. L., Haizhou, M., Asahi, K., Caffee, M. W., & Derbyshire, E. (2005). Climatic and topographic controls on the style and timing of Late Quaternary glaciation throughout Tibet and the Himalaya defined by 10Be cosmogenic radionuclide surface exposure dating. Quaternary Science Reviews, 24(12–13), 1391–1411.

Owen, L. A., Caffee, M. W., Bovard, K. R., Finkel, R. C., & Sharma, M. C. (2006a). Terrestrial cosmogenic nuclide surface exposure dating of the oldest glacial successions in the Himalayan orogen: Ladakh Range, northern India. Bulletin of the Geological Society of America, 118(3–4), 383–392.

Owen, L. A., Finkel, R. C., Haizhou, M., & Barnard, P. L. (2006b). Late Quaternary landscape evolution in the Kunlun Mountains and Qaidam Basin, Northern Tibet: A framework for examining the links between glaciation, lake level changes and alluvial fan formation. Quaternary International, 154–155, 73–86.

Owen, L. A., Robinson, R., Benn, D. I., Finkel, R. C., Davis, N. K., Yi, C., Putkonen, J., Li, D., & Murray, A. S. (2009). Quaternary glaciation of Mount Everest. Quaternary Science Reviews, 28(15–16), 1412–1433.

Owen, L. A., Yi, C., Finkel, R. C., & Davis, N. K. (2010). Quaternary glaciation of Gurla Mandhata (Naimon'anyi). Quaternary Science Reviews, 29(15–16), 1817–1830.

Owen, L. A., Chen, J., Hedrick, K. A., Caffee, M. W., Robinson, A. C., Schoenbohm, L. M., Yuan, Z., Li, W., Imrecke, D. B., & Liu, J. (2012). Quaternary glaciation of the Tashkurgan Valley, Southeast Pamir. Quaternary Science Reviews, 47, 56–72.

Palacios, D., Gómez-Ortiz, A., Alcalá-Reygosa, J., Andrés, N., Oliva, M., Tanarro, L. M., Salvador-Franch, F., Schimmelpfennig, I., Fernández-Fernández, J. M., & Léanni, L. (2019). The challenging application of cosmogenic dating methods in residual glacial landforms: The case of Sierra Nevada (Spain). Geomorphology, 325, 103–118.

Palacios, D., Oliva, M., Gómez-Ortiz, A., Andrés, N., Fernández-Fernández, J. M., Schimmelpfennig, I., Léanni, L., & Team, A. S. T. E. R. (2020). Climate sensitivity and geomorphological response of cirque glaciers from the late glacial to the Holocene, Sierra Nevada, Spain. Quaternary Science Reviews, 248.

Pallàs, R., Rodés, Á., Braucher, R., Bourlès, D., Delmas, M., Calvet, M., & Gunnell, Y. (2010). Small, isolated glacial catchments as priority targets for cosmogenic surface exposure dating of pleistocene climate fluctuations, southeastern Pyrenees. Geology, 38(10), 891–894.

Pallàs, R., Rodés, Á., Braucher, R., Carcaillet, J., Ortuño, M., Bordonau, J., Bourlès, D., Vilaplana, J. M., Masana, E., & Santanach, P. (2006). Late Pleistocene and Holocene glaciation in the Pyrenees: a critical review and new evidence from 10Be exposure ages, south-central Pyrenees. Quaternary Science Reviews, 25(21–22), 2937–2963.

Pendleton, S. L., Briner, J. P., Kaufman, D. S., & Zimmerman, S. R. (2017). Using Cosmogenic 10Be Exposure Dating and Lichenometry to Constrain Holocene Glaciation in the Central Brooks Range, Alaska. Arctic, Antarctic, and Alpine Research, 49(1), 115–132.

Pendleton, S. L., Ceperley, E. G., Briner, J. P., Kaufman, D. S., & Zimmerman, S. (2015). Rapid and early deglaciation in the central Brooks Range, Arctic Alaska. Geology, 43(5), 419–422.

Peng, X., Chen, Y., Li, Y., Liu, B., Liu, Q., Yang, W., Cui, Z., & Liu, G. (2020). Late Holocene glacier fluctuations in the Bhutanese Himalaya. Global and Planetary Change, 187.

Peng, X., Chen, Y., Liu, G., Liu, B., Li, Y., Liu, Q., Han, Y., Yang, W., & Cui, Z. (2019). Late Quaternary glaciations in the Cogarbu valley, Bhutanese Himalaya. Journal of Quaternary Science, 34(1), 40–50.

Philipps, W., Briner, J. P., Gislefoss, L., Linge, H., Koffman, T., Fabel, D., Xu, S., & Hormes, A. (2017). Late Holocene glacier activity at inner Hornsund and Scottbreen, southern Svalbard. Journal of Quaternary Science, 32(4), 501–515.

Phillips, F. M., Kelly, M. A., Hudson, A. M., Stone, J. O. H., Schaefer, J., Marrero, S. M., Fifield, L. K., Finkel, R., & Lowell, T. (2016). CRONUS-Earth calibration samples from the Huancané II moraines, Quelccaya Ice Cap, Peru. Quaternary Geochronology, 31, 220–236.

Phillips, W. M., Sloan, V. F., Shroder Jr., J. F., Sharma, P., Clarke, M. L., & Rendell, H. M. (2000). Asynchronous glaciation at Nanga Parbat, northwestern Himalaya mountains, Pakistan. Geology, 28(5), 431–434.

Pierce, I. K. D., Wesnousky, S. G., & Owen, L. A. (2017). Terrestrial cosmogenic surface exposure dating of moraines at Lake Tahoe in the Sierra Nevada of California and slip rate estimate for the West Tahoe Fault. Geomorphology, 298, 63–71.

Porter, C., Morin, P., Howat, I., Noh, M.-J., Bates, B., Peterman, K., Keesey, S., Schlenk, M., Gardiner, J., Tomko, K., Willis, M., Kelleher, C., Cloutier, M., Husby, E., Foga, S., Nakamura, H., Platson, M., Wethington, M. Jr., Williamson, C., Bauer, G., Enos, J., Arnold, G., Kramer, W., Becker, P., Doshi, A., D'Souza, C., Cummens, P., Laurier, F., Bojesen, M., et al. (2018). ArcticDEM, Version 4.1. Harvard Dataverse, V1. (2024-04-20).

Pötsch, S. (2017). Dynamics and paleo-climatic forcing of late Pleistocene glaciers in the Turgen and Khangai mountains (Mongolia) reconstructed from geomorphology, 10Be surface exposure dating, and ice flow modelling. Dissertation thesis, Ernst-Moritz-Arndt-Universität.

Pratt-Sitaula, B., Burbank, D. W., Heimsath, A. M., Humphrey, N. F., Oskin, M., & Putkonen, J. (2011). Topographic control of asynchronous glacial advances: A case study from Annapurna, Nepal. Geophysical Research Letters, 38(24).

Protin, M. (2019). Preliminary work on reduced glacier extents and subglacial erosion rates in the Mont-Blanc massif. In: Protin M, Études des fluctuations glaciaires dans le massif du Mont-Blanc depuis la fin du Dryas Récent à partir des nucléides cosmogéniques in situ. Dissertation thesis, Aix-Marseille University.

Protin, M., Schimmelpfennig, I., Mugnier, J. L., Buoncristiani, J. F., Le Roy, M., Pohl, B., Moreau, L., Aumaître, G., Bourlès, D., & Keddadouche, K. (2021). Millennial-scale deglaciation across the European Alps at the transition between the Younger Dryas and the Early Holocene – evidence from a new cosmogenic nuclide chronology. Boreas, 50(3), 671–685.

Protin, M., Schimmelpfennig, I., Mugnier, J. L., Ravanel, L., Le Roy, M., Deline, P., Favier, V., Buoncristiani, J. F., Aumaître, G., Bourlès, D. L., & Keddadouche, K. (2019). Climatic reconstruction for the Younger Dryas/Early Holocene transition and the Little Ice Age based on paleo-extents of Argentière glacier (French Alps). Quaternary Science Reviews, 221.

Putnam, A. E., Bromley, G. R. M., Rademaker, K., & Schaefer, J. M. (2019). In situ 10Be production-rate calibration from a 14C-dated late-glacial moraine belt in Rannoch Moor, central Scottish Highlands. Quaternary Geochronology, 50, 109–125.

Putkonen, J., Connolly, J., & Orloff, T. (2008). Landscape evolution degrades the geologic signature of past glaciations. Geomorphology, 97(1–2), 208–217.

Putkonen, J., & O'Neal, M. (2006). Degradation of unconsolidated Quaternary landforms in the western North America. Geomorphology, 75(3–4), 408–419.

Putkonen, J., & Swanson, T. (2003). Accuracy of cosmogenic ages for moraines. Quaternary Research, 59(2), 255–261.

Putnam, A. E., Schaefer, J. M., Barrell, D. J. A., Vandergoes, M., Denton, G. H., Kaplan, M. R., Finkel, R. C., Schwartz, R., Goehring, B. M., & Kelley, S. E. (2010). In situ cosmogenic 10Be production-rate calibration from the Southern Alps, New Zealand. Quaternary Geochronology, 5(4), 392–409.

Putnam, A. E., Schaefer, J. M., Denton, G. H., Barrell, D. J. A., Andersen, B. G., Koffman, T. N. B., Rowan, A. V., Finkel, R. C., Rood, D. H., Schwartz, R., Vandergoes, M. J., Plummer, M. A., Brocklehurst, S. H., Kelley, S. E., & Ladig, K. L. (2013). Warming and glacier recession in the Rakaia valley, Southern Alps of New Zealand, during Heinrich Stadial 1. Earth and Planetary Science Letters, 382, 98–110.

Putnam, A. E., Schaefer, J. M., Denton, G. H., Barrell, D. J. A., Birkel, S. D., Andersen, B. G., Kaplan, M. R., Finkel, R. C., Schwartz, R., & Doughty, A. M. (2013). The Last Glacial Maximum at 44°S documented by a 10Be moraine chronology at Lake Ohau, Southern Alps of New Zealand. Quaternary Science Reviews, 62, 114–141.

Putnam, A. E., Schaefer, J. M., Denton, G. H., Barrell, D. J. A., Finkel, R. C., Andersen, B. G., Schwartz, R., Chinn, T. J. H., & Doughty, A. M. (2012). Regional climate control of glaciers in NewÂ Zealand and Europe during the pre-industrial Holocene. Nature Geoscience, 5(9), 627–630.

Quirk, B. J., Huss, E., Laabs, B. J. C., Leonard, E., Licciardi, J., Plummer, M. A., & Caffee, M. W. (2022). Late Pleistocene glacial chronologies and paleoclimate in the northern Rocky Mountains. Climate of the Past, 18(2), 293–312.

Quirk, B. J., Moore, J. R., Laabs, B. J. C., Caffee, M. W., & Plummer, M. A. (2018). Termination II, Last Glacial Maximum, and Lateglacial chronologies and paleoclimate from Big Cottonwood Canyon, Wasatch Mountains, Utah. Bulletin of the Geological Society of America, 130(11–12), 1889–1902.

Quirk, B. J., Moore, J. R., Laabs, B. J. C., Plummer, M. A., & Caffee, M. W. (2020). Latest Pleistocene glacial and climate history of the Wasatch Range, Utah. Quaternary Science Reviews, 238.

Reber, R., Akçar, N., Ivy-Ochs, S., Tikhomirov, D., Burkhalter, R., Zahno, C., Lüthold, A., Kubik, P. W., Vockenhuber, C., & Schlüchter, C. (2014a). Timing of retreat of the Reuss Glacier (Switzerland) at the end of the Last Glacial Maximum. Swiss Journal of Geosciences, 107(2–3), 293–307.

Reber, R., Akçar, N., Yesilyurt, S., Yavuz, V., Tikhomirov, D., Kubik, P. W., & Schlüchter, C. (2014b). Glacier advances in northeastern turkey before and during the global last glacial maximum. Quaternary Science Reviews, 101.

Refsnider, K. A., Laabs, B. J. C., Plummer, M. A., Mickelson, D. M., Singer, B. S., & Caffee, M. W. (2008). Last glacial maximum climate inferences from cosmogenic dating and glacier modeling of the western Uinta ice field, Uinta Mountains, Utah. Quaternary Research, 69(1), 130–144.

Regnéll, C., Briner, J. P., Haflidason, H., Mangerud, J., & Svendsen, J. I. (2022). Deglaciation of the Scandinavian Ice Sheet and a Younger Dryas ice cap in the outer Hardangerfjorden area, southwestern Norway. Boreas, 51(2), 255–273.

Reitner, J. M., Ivy-Ochs, S., Drescher-Schneider, R., Hajdas, I., & Linner, M. (2016). Reconsidering the current stratigraphy of the Alpine Lateglacial: Implications of the sedimentary and morphological record of the Lienz area (Tyrol/Austria). E and G Quaternary Science Journal, 65(2), 113–144.

Reusche, M. M., Marcott, S. A., Ceperley, E. G., Barth, A. M., Brook, E. J., Mix, A. C., & Caffee, M. W. (2018). Early to Late Holocene Surface Exposure Ages From Two Marine-Terminating Outlet Glaciers in Northwest Greenland. Geophysical Research Letters, 45(14), 7028–7039.

Reusche, M., Winsor, K., Carlson, A. E., Marcott, S. A., Rood, D. H., Novak, A., Roof, S., Retelle, M., Werner, A., Caffee, M., & Clark, P. U. (2014). 10Be surface exposure ages on the late-Pleistocene and Holocene history of Linnébreen on Svalbard. Quaternary Science Reviews, 89, 5–12.

Reuther, A. U., Fiebig, M., Ivy-Ochs, S., Kubik, P. W., Reitner, J. M., Jerz, H., & Heine, K. (2011). Deglaciation of a large piedmont lobe glacier in comparison with a small mountain glacier - new insight from surface exposure dating. Two studies from SE Germany. E and G Quaternary Science Journal, 60(2–3), 248–269.

Reuther, A. U., Urdea, P., Geiger, C., Ivy-Ochs, S., Niller, H. P., Kubik, P. W., & Heine, K. (2007). Late Pleistocene glacial chronology of the Pietrele Valley, Retezat Mountains, Southern Carpathians constrained by 10Be exposure ages and pedological investigations. Quaternary International, 164–165, 151–169.

Reynhout, S. A., Kaplan, M. R., Sagredo, E. A., Aravena, J. C., Soteres, R. L., Schwartz, R., & Schaefer, J. M. (2022). Holocene glacier history of northeastern Cordillera Darwin, southernmost South America (55°S). Quaternary Research (United States), 105, 166–181.

Reynhout, S. A., Sagredo, E. A., Kaplan, M. R., Aravena, J. C., Martini, M. A., Moreno, P. I., Rojas, M., Schwartz, R., & Schaefer, J. M. (2019). Holocene glacier fluctuations in Patagonia are modulated by summer insolation intensity and paced by Southern Annular Mode-like variability. Quaternary Science Reviews, 220, 178–187.

Ribolini, A., Bini, M., Isola, I., Spagnolo, M., Zanchetta, G., Pellitero, R., Mechernich, S., Gromig, R., Dunai, T., Wagner, B., & Milevski, I. (2018). An Oldest Dryas glacier expansion on Mount Pelister (Former Yugoslavian Republic of Macedonia) according to 10 Be cosmogenic dating.

Rinterknecht, V. R., Clark, P. U., Raisbeck, G. M., Yiou, F., Brook, E. J., Tschudi, S., & Lunkka, J. P. (2004). Cosmogenic 10Be dating of the Salpausselkä I Moraine in southwestern Finland. Quaternary Science Reviews, 23(23–24), 2283–2289.

Rinterknecht, V. R., Clark, P. U., Raisbeck, G. M., Yiou, F., Bitinas, A., Brook, E. J., Marks, L., Zelčs, V., Lunkka, J. P., Pavlovskaya, I. E., Piotrowski, J. A., & Raukas, A. (2006). The last deglaciation of the southeastern sector of the scandinavian ice sheet. Science, 311(5766), 1449–1452.

Rinterknecht, V., Gorokhovich, Y., Schaefer, J., & Caffee, M. (2009). Preliminary 10Be chronology for the last deglaciation of the western margin of the Greenland Ice Sheet. Journal of Quaternary Science, 24(3), 270–278.

Rinterknecht, V., Braucher, R., Böse, M., Bourlès, D., & Mercier, J. L. (2012a). Late Quaternary ice sheet extents in northeastern Germany inferred from surface exposure dating. Quaternary Science Reviews, 44, 89–95.

Rinterknecht, V., Matoshko, A., Gorokhovich, Y., Fabel, D., & Xu, S. (2012b). Expression of the Younger Dryas cold event in the Carpathian Mountains, Ukraine? Quaternary Science Reviews, 39, 106–114.

Rinterknecht, V., Börner, A., Bourlès, D., & Braucher, R. (2014). Cosmogenic 10Be dating of ice sheet marginal belts in Mecklenburg-Vorpommern, Western Pomerania (northeast Germany). Quaternary Geochronology, 19, 42–51.

Roberts, D. H., Rea, B. R., Lane, T. P., Schnabel, C., & Rodés, A. (2013). New constraints on Greenland ice sheet dynamics during the last glacial cycle: Evidence from the Uummannaq ice stream system. Journal of Geophysical Research: Earth Surface, 118(2), 519–541.

Rodríguez-Rodríguez, L., Domínguez-Cuesta, M. J., Rinterknecht, V., Jiménez-Sánchez, M., González-Lemos, S., Léanni, L., Sanjurjo, J., Ballesteros, D., Valenzuela, P., & Llana-Fúnez, S. (2018). Constraining the age of superimposed glacial records in mountain environments with multiple dating methods (Cantabrian Mountains, Iberian Peninsula). Quaternary Science Reviews, 195, 215–231.

Rodríguez-Rodríguez, L., Jiménez-Sánchez, M., Domínguez-Cuesta, M. J., Rinterknecht, V., & Pallàs, R. (2017). Timing of last deglaciation in the Cantabrian Mountains (Iberian Peninsula; North Atlantic Region) based on in situ-produced 10Be exposure dating. Quaternary Science Reviews, 171, 166–181.

Rodríguez-Rodríguez, L., Jiménez-Sánchez, M., Domínguez-Cuesta, M. J., Rinterknecht, V., Pallàs, R., & Bourlès, D. (2016). Chronology of glaciations in the Cantabrian Mountains (NW Iberia) during the Last Glacial Cycle based on in situ-produced 10Be. Quaternary Science Reviews, 138, 31–48.

Rodríguez-Rodríguez, L., Jiménez-Sánchez, M., Domínguez-Cuesta, M. J., Rinterknecht, V., Pallàs, R., Bourlès, D., & Valero-Garcés, B. (2014). A multiple dating-method approach applied to the Sanabria Lake moraine complex (NW Iberian Peninsula, SW Europe). Quaternary Science Reviews, 83, 1–10.

Röhringer, I., Zech, R., Abramowski, U., Sosin, P., Aldahan, A., Kubik, P. W., Zöller, L., & Zech, W. (2012). The late Pleistocene glaciation in the Bogchigir Valleys (Pamir, Tajikistan) based on 10Be surface exposure dating. Quaternary Research (United States), 78(3), 590–597.

Romundset, A., Akçar, N., Fredin, O., Tikhomirov, D., Reber, R., Vockenhuber, C., Christl, M., & Schlüchter, C. (2017). Lateglacial retreat chronology of the Scandinavian Ice Sheet in Finnmark, northern Norway, reconstructed from surface exposure dating of major end moraines. Quaternary Science Reviews, 177, 130–144.

Rood, D. H., Burbank, D. W., & Finkel, R. C. (2011). Chronology of glaciations in the Sierra Nevada, California, from 10Be surface exposure dating. Quaternary Science Reviews, 30(5–6), 646–661.

Rother, H. (2006). Late Pleistocene Glacial Geology of the Hope-Waiau Valley System in North Canterbury, New Zealand. PhD thesis, University of Canterbury.

Rother, H., Fink, D., Shulmeister, J., Mifsud, C., Evans, M., & Pugh, J. (2014a). The early rise and late demise of New Zealand's last glacial maximum. Proceedings of the National Academy of Sciences of the United States of America, 111(32), 11630–11635.

Rother, H., Lehmkuhl, F., Fink, D., & Nottebaum, V. (2014b). Surface exposure dating reveals MIS-3 glacial maximum in the Khangai Mountains of Mongolia. Quaternary Research (United States), 82(2), 297–308.

Rother, H., Stauch, G., Loibl, D., Lehmkuhl, F., & Freeman, S. P. H. T. (2017). Late Pleistocene glaciations at Lake Donggi Cona, eastern Kunlun Shan (NE Tibet): early maxima and a diminishing trend of glaciation during the last glacial cycle. Boreas, 46(3), 503–524.

Ruleman, C. A., Brandt, T. R., Caffee, M. W., & Goehring, B. M. (2018). Geologic map of the Leadville North 7.5 Quadrangle, Eagle and Lake Counties, Colorado. U.S. Geological Survey Scientific Investigations Map 3400.

Ruszkiczay-Rüdiger, Z., Kern, Z., Urdea, P., Braucher, R., Madarász, B., & Schimmelpfennig, I. (2016). Revised deglaciation history of the Pietrele–Stânişoara glacial complex, Retezat Mts, Southern Carpathians, Romania. Quaternary International, 415, 216–229.

Ruszkiczay-Rüdiger, Z., Kern, Z., Urdea, P., Madarász, B., & Braucher, R. (2021). Limited glacial erosion during the last glaciation in mid-latitude cirques (Retezat Mts, Southern Carpathians, Romania). Geomorphology, 384.

Sagredo, E. A., Kaplan, M. R., Araya, P. S., Lowell, T. V., Aravena, J. C., Moreno, P. I., Kelly, M. A., & Schaefer, J. M. (2018). Trans-pacific glacial response to the Antarctic Cold Reversal in the southern mid-latitudes. Quaternary Science Reviews, 188, 160–166.

Sagredo, E. A., Lowell, T. V., Kelly, M. A., Rupper, S., Aravena, J. C., Ward, D. J., & Malone, A. G. O. (2017). Equilibrium line altitudes along the Andes during the Last millennium: Paleoclimatic implications. Holocene, 27(7), 1019–1033.

Sagredo, E. A., Moreno, P. I., Villa-Martínez, R., Kaplan, M. R., Kubik, P. W., & Stern, C. R. (2011). Fluctuations of the Última Esperanza ice lobe (52°S), Chilean Patagonia, during the last glacial maximum and termination 1. Geomorphology, 125(1), 92–108.

Saha, S., Owen, L. A., Orr, E. N., & Caffee, M. W. (2018). Timing and nature of Holocene glacier advances at the northwestern end of the Himalayan-Tibetan orogen. Quaternary Science Reviews, 187, 177–202.

Saha, S., Owen, L. A., Orr, E. N., & Caffee, M. W. (2019). High-frequency Holocene glacier fluctuations in the Himalayan-Tibetan orogen. Quaternary Science Reviews, 220, 372–400.

Saha, S., Sharma, M. C., Murari, M. K., Owen, L. A., & Caffee, M. W. (2016). Geomorphology, sedimentology and minimum exposure ages of streamlined subglacial landforms in the NW Himalaya, India. Boreas, 45(2), 284–303.

Schaefer, J. M., Denton, G. H., Barrell, D. J. A., Ivy-Ochs, S., Kubik, P. W., Andersen, B. G., Phillips, F. M., Lowell, T. V., & Schlüchter, Ch. (2006). Near-Synchronous Interhemispheric Termination of the Last Glacial Maximum in Mid-Latitudes. Science, 312(5779), 1510–1513.

Schaefer, J. M., Denton, G. H., Kaplan, M., Putnam, A., Finkel, R. C., Barrell, D. J. A., Andersen, B. G., Schwartz, R., Mackintosh, A., Chinn, T., & Schlüchter, C. (2009). High-Frequency Holocene Glacier Fluctuations in New Zealand Differ from the Northern Signature. Science, 324, 622–625.

Schaefer, J. M., Oberholzer, P., Zhao, Z., Ivy-Ochs, S., Wieler, R., Baur, H., Kubik, P. W., & Schlüchter, C. (2008). Cosmogenic beryllium-10 and neon-21 dating of late Pleistocene glaciations in Nyalam, monsoonal Himalayas. Quaternary Science Reviews, 27(3–4), 295–311.

Schaefer, J. M., Putnam, A. E., Denton, G. H., Kaplan, M. R., Birkel, S., Doughty, A. M., Kelley, S., Barrell, D. J. A., Finkel, R. C., Winckler, G., Anderson, R. F., Ninneman, U. S., Barker, S., Schwartz, R., Andersen, B. G., & Schluechter, C. (2015). The Southern Glacial Maximum 65,000 years ago and its Unfinished Termination. Quaternary Science Reviews, 114, 52–60.

Schäfer, J. M., Tschudi, S., Zhao, Z., Wu, X., Ivy-Ochs, S., Wieler, R., Baur, H., Kubik, P. W., & Schlüchter, C. (2002). The limited in£uence of glaciations in Tibet on global climate over the past 170 000 yr. Earth and Planetary Science Letters, 194, 287–297.

Scherler, D., Bookhagen, B., Strecker, M. R., von Blanckenburg, F., & Rood, D. (2010). Timing and extent of late Quaternary glaciation in the western Himalaya constrained by 10Be moraine dating in Garhwal, India. Quaternary Science Reviews, 29(7–8), 815–831.

Scherler, D., Munack, H., Mey, J., Eugster, P., Wittmann, H., Codilean, A. T., Kubik, P., & Strecker, M. R. (2014). Ice dams, outburst floods, and glacial incision at the western margin of the Tibetan Plateau: A >100 k.y. chronology from the Shyok Valley, Karakoram. Bulletin of the Geological Society of America, 126(5–6), 738–758.

Schildgen, T. F., Phillips, W. M., Purves, R. S. (2005). Simulation of snow shielding corrections for cosmogenic nuclide surface exposure studies. Geomorphology, 64, 67-85.

Schimmelpfennig, I., Schaefer, J. M., Akçar, N., Ivy-Ochs, S., Finkel, R. C., & Schlüchter, C. (2012). Holocene glacier culminations in the Western Alps and their hemispheric relevance. Geology, 40(10), 891–894.

Schimmelpfennig, I., Schaefer, J. M., Akçar, N., Koffman, T., Ivy-Ochs, S., Schwartz, R., Finkel, R. C., Zimmerman, S., & Schlüchter, C. (2014). A chronology of Holocene and Little Ice Age glacier culminations of the Steingletscher, Central Alps, Switzerland, based on high-sensitivity beryllium-10 moraine dating. Earth and Planetary Science Letters, 393, 220–230.

Schindelwig, I., Akçar, N., Kubik, P. W., & Schlüchter, C. (2012). Lateglacial and early Holocene dynamics of adjacent valley glaciers in the Western Swiss Alps. Journal of Quaternary Science, 27(1), 114–124.

Schweinsberg, A. D., Briner, J. P., Licciardi, J. M., Bennike, O., Lifton, N. A., Graham, B. L., Young, N. E., Schaefer, J. M., & Zimmerman, S. H. (2019). Multiple independent records of local glacier variability on Nuussuaq, West Greenland, during the Holocene. Quaternary Science Reviews, 215, 253–271.

Schweinsberg, A. D., Briner, J. P., Licciardi, J. M., Shroba, R. R., & Leonard, E. M. (2020). Cosmogenic 10Be exposure dating of Bull Lake and Pinedale moraine sequences in the upper Arkansas river valley, Colorado Rocky Mountains, USA. Quaternary Research (United States), 97, 125–139.

Seong, Y. B., Owen, L. A., Bishop, M. P., Bush, A., Clendon, P., Copland, L., Finkel, R., Kamp, U., & Shroder, J. F. (2007). Quaternary glacial history of the Central Karakoram. Quaternary Science Reviews, 26(25–28), 3384–3405.

Seong, Y. B., Owen, L. A., Yi, Ch., & Finkel, R. C. (2009). Quaternary glaciation of Muztag Ata and Kongur Shan: Evidence for glacier response to rapid climate changes throughout the Late Glacial and Holocene in westernmost Tibet. GSA Bulletin, 121(3–4), 348–365.

Shakesby, R. A., Matthews, J. A., & Schnabel, C. (2008). Cosmogenic 10Be and 26Al ages of Holocene moraines in southern Norway II: Evidence for individualistic responses of high-altitude glaciers to millennial-scale climatic fluctuations. Holocene, 18(8), 1165–1177.

Shakun, J. D., Clark, P. U., Marcott, S. A., Brook, E. J., Lifton, N. A., Caffee, M., & Shakun, W. R. (2015). Cosmogenic dating of Late Pleistocene glaciation, southern tropical Andes, Peru. Journal of Quaternary Science, 30(8), 841–847.

Shulmeister, J., Fink, D., & Augustinus, P. C. (2005). A cosmogenic nuclide chronology of the last glacial transition in North-West Nelson, New Zealand - New insights in Southern Hemisphere climate forcing during the last deglaciation. Earth and Planetary Science Letters, 233(3–4), 455–466.

Shulmeister, J., Fink, D., Hyatt, O. M., Thackray, G. D., & Rother, H. (2010). Cosmogenic 10Be and 26Al exposure ages of moraines in the Rakaia Valley, New Zealand and the nature of the last termination in New Zealand glacial systems. Earth and Planetary Science Letters, 297(3–4), 558–566.

Shulmeister, J., Fink, D., Winkler, S., Thackray, G. D., Borsellino, R., Hemmingsen, M., & Rittenour, T. M. (2018). Evidence for slow late-glacial ice retreat in the upper Rangitata Valley, South Island, New Zealand. Quaternary Science Reviews, 185, 102–112.

Siame, L., Chu, H. T., Carcaillet, J., Bourlès, D., Braucher, R., Lu, W. C., Angelier, J., & Dussouliez, P. (2007). Glacial retreat history of Nanhuta Shan (north-east Taiwan) from preserved glacial features: the cosmic ray exposure perspective. Quaternary Science Reviews, 26(17–18), 2185–2200.

Sinclair, G. (2019). North Atlantic Climate and Cryosphere Variability Over the Past 20,000 Years. Dissertation thesis, Oregon State University.

Slater, T., Shepherd, A., McMillan, M., Muir, A., Gilbert, L., Hogg, A. E., Konrad, H. and Parrinello, T. (2018): A new Digital Elevation Model of Antarctica derived from CryoSat-2 altimetry, The Cryosphere.

Small, D., Benetti, S., Dove, D., Ballantyne, C. K., Fabel, D., Clark, C. D., Gheorghiu, D. M., Newall, J., & Xu, S. (2017). Cosmogenic exposure age constraints on deglaciation and flow behaviour of a marine-based ice stream in western Scotland, 21–16 ka. Quaternary Science Reviews, 167, 30–46.

Small, D., Bentley, M. J., Evans, D. J. A., Hein, A. S., & Freeman, S. P. H. T. (2021). Ice-free valleys in the Neptune Range of the Pensacola Mountains, Antarctica: Glacial geomorphology, geochronology and potential as palaeoenvironmental archives. Antarctic Science, 33(4), 428–455.

Small, D., & Fabel, D. (2016). Was Scotland deglaciated during the Younger Dryas? Quaternary Science Reviews, 145, 259–263.

Small, D., Rinterknecht, V., Austin, W., Fabel, D., Miguens-Rodriguez, M., & xu, S. (2012). In situ cosmogenic exposure ages from the Isle of Skye, northwest Scotland: Implications for the timing of deglaciation and readvance from 15 to 11ka. Journal of Quaternary Science, 27(2), 150–158.

Smith, C. A., Lowell, T. V., Owen, L. A., & Caffee, M. W. (2011). Late Quaternary glacial chronology on Nevado Illimani, Bolivia, and the implications for paleoclimatic reconstructions across the Andes. Quaternary Research, 75(1), 1–10.

Smith, J. A., Finkel, R. C., Farber, D. L., Rodbell, D. T., & Seltzer, G. O. (2005a). Moraine preservation and boulder erosion in the tropical Andes: Interpreting old surface exposure ages in glaciated valleys. Journal of Quaternary Science, 20(7–8), 735–758.

Smith, J. A., Seltzer, G. O., Farber, D. L., Rodbell, D. T., & Finkel, R. C. (2005b). Early Local Last Glacial Maximum in the Tropical Andes. Science, 308, 678–681. https://www.science.org

Smith, J. A., & Rodbell, D. T. (2010). Cross-cutting moraines reveal evidence for north Atlantic influence on glaciers in the tropical Andes. Journal of Quaternary Science, 25(3), 243–248.

Smith, S. G., Wegmann, K. W., Ancuta, L. D., Gosse, J. C., & Hopkins, C. E. (2016). Paleotopography and erosion rates in the central Hangay Dome, Mongolia: Landscape evolution since the mid-Miocene. Journal of Asian Earth Sciences, 125, 37–57.

Søndergaard, A. S., Larsen, N. K., Olsen, J., Strunk, A., & Woodroffe, S. (2019). Glacial history of the Greenland Ice Sheet and a local ice cap in Qaanaaq, northwest Greenland. Journal of Quaternary Science, 34(7), 536–547.

Standell, M. R. (2014). Lateglacial (Younger Dryas) Glaciers and Ice-Sheet Deglaciation in the Cairngorm Mountains, Scotland: Glacier Reconstructions and their Palaeoclimatic Implications. PhD thesis, Loughborough University.

Stansell, N. D., Licciardi, J. M., Rodbell, D. T., & Mark, B. G. (2017). Tropical ocean-atmospheric forcing of Late Glacial and Holocene glacier fluctuations in the Cordillera Blanca, Peru. Geophysical Research Letters, 44(9), 4176–4185.

Stansell, N. D., Rodbell, D. T., Licciardi, J. M., Sedlak, C. M., Schweinsberg, A. D., Huss, E. G., Delgado, G. M., Zimmerman, S. H., & Finkel, R. C. (2015). Late glacial and Holocene glacier fluctuations at Nevado Huaguruncho in the eastern cordillera of the Peruvian Andes. Geology, 43(8), 747–750.

Steig, E. J., Wolfe, A. P., & Miller, G. H. (1998). Wisconsinan refugia and the glacial history of eastern Baffin Island, arctic Canada: coupled evidence from cosmogenic isotopes and lake sediments. Geology, 26(9), 835–838.

Steinemann, O., Reitner, J. M., Ivy-Ochs, S., Christl, M., & Synal, H. A. (2020). Tracking rockglacier evolution in the Eastern Alps from the Lateglacial to the early Holocene. Quaternary Science Reviews, 241.

Stone, J. O. (2000). Air pressure and cosmogenic isotope production. Journal of Geophysical Research: Solid Earth, 105(B10), 23753–23759.

Storey, B. C., Fink, D., Hood, D., Joy, K., Shulmeister, J., Riger-Kusk, M., & Stevens, M. I. (2010). Cosmogenic nuclide exposure age constraints on the glacial history of the Lake Wellman area, Darwin Mountains, Antarctica. Antarctic Science, 22(6), 603–618.

Strand, P. D., Putnam, A. E., Sambuu, O., Putnam, D. E., Denton, G. H., Schaefer, J. M., Radue, M. J., Dorj, A., Amarsaikhan, P., Stevens, J., & Cole, D. G. (2022). A 10Be Moraine Chronology of the Last Glaciation and Termination at 49°N in the Mongolian Altai of Central Asia. Paleoceanography and Paleoclimatology, 37(5).

Strand, P. D., Schaefer, J. M., Putnam, A. E., Denton, G. H., Barrell, D. J. A., Koffman, T. N. B., & Schwartz, R. (2019). Millennial-scale pulsebeat of glaciation in the Southern Alps of New Zealand. Quaternary Science Reviews, 220, 165–177.

Strasky, S., Di Nicola, L., Baroni, C., Salvatore, M. C., Baur, H., Kubik, P. W., Schlüchter, C., & Wieler, R. (2009a). Surface exposure ages imply multiple low-amplitude Pleistocene variations in East Antarctic Ice Sheet, Ricker Hills, Victoria Land. Antarctic Science, 21(1), 59–69.

Strasky, S., Graf, A. A., Zhao, Z., Kubik, P. W., Baur, H., Schlüchter, C., & Wieler, R. (2009b). Late Glacial ice advances in southeast Tibet. Journal of Asian Earth Sciences, 34(3), 458–465.

Strelin, J. A., Kaplan, M. R., Vandergoes, M. J., Denton, G. H., & Schaefer, J. M. (2014). Holocene glacier history of the Lago Argentino basin, Southern Patagonian Icefield. Quaternary Science Reviews, 101, 124–145.

Stroeven, A. P., Fabel, D., Codilean, A. T., Kleman, J., Clague, J. J., Miguens-Rodriguez, M., & Xu, S. (2010). Investigating the glacial history of the northern sector of the Cordilleran Ice Sheet with cosmogenic 10Be concentrations in quartz. Quaternary Science Reviews, 29(25–26), 3630–3643.

Stroeven, A. P., Fabel, D., Margold, M., Clague, J. J., & Xu, S. (2014). Investigating absolute chronologies of glacial advances in the NW sector of the Cordilleran Ice Sheet with terrestrial in situ cosmogenic nuclides. Quaternary Science Reviews, 92, 429–443.

Stroup, J. S., Kelly, M. A., Lowell, T. V., Applegate, P. J., & Howley, J. A. (2014). Late Holocene fluctuations of Qori Kalis outlet glacier, Quelccaya Ice Cap, Peruvian Andes. Geology, 42(4), 347–350.

Stroup, J. S., Kelly, M. A., Lowell, T. V., Smith, C. A., Beal, S. A., Landis, J. D., & Tapia, P. M. (2015). Late Holocene fluctuations of Quelccaya Ice Cap, Peru, registered by nearby lake sediments. Journal of Quaternary Science, 30(8), 830–840.

Stübner, K., Grin, E., Hidy, A. J., Schaller, M., Gold, R. D., Ratschbacher, L., & Ehlers, T. (2017). Middle and Late Pleistocene glaciations in the southwestern Pamir and their effects on topography. Earth and Planetary Science Letters, 466, 181–194.

Suganuma, Y., Miura, H., Zondervan, A., & Okuno, J. (2014). East Antarctic deglaciation and the link to global cooling during the Quaternary: Evidence from glacial geomorphology and 10Be surface exposure dating of the Sør Rondane Mountains, Dronning Maud Land. Quaternary Science Reviews, 97, 102–120.

Summerfield, M. A., Stuart, F. M., Cockburn, H. A. P., Sugden, D. E., Denton, G. H., Dunai, T., & Marchant, D. R. (1999). Long-term rates of denudation in the Dry Valleys, Transantarctic Mountains, southern Victoria Land, Antarctica based on in-situ-produced cosmogenic 21 Ne. Geomorphology, 27.

Sutherland, R., Kim, K., Zondervan, A., & McSaveney, M. (2007). Orbital forcing of mid-latitude Southern Hemisphere glaciation since 100 ka inferred from cosmogenic nuclide ages of moraine boulders from the Cascade Plateau, southwest New Zealand. Bulletin of the Geological Society of America, 119(3–4), 443–451.

Svendsen, J. I., Færseth, L. M. B., Gyllencreutz, R., Haflidason, H., Henriksen, M., Hovland, M. N., Lohne, Ø. S., Mangerud, J., Nazarov, D., Regnéll, C., & Schaefer, J. M. (2019). Glacial and environmental changes over the last 60 000 years in the Polar Ural Mountains, Arctic Russia, inferred from a high-resolution lake record and other observations from adjacent areas. Boreas, 48(2), 407–431.

Terrizzano, C. M., García Morabito, E., Christl, M., Likerman, J., Tobal, J., Yamin, M., & Zech, R. (2017). Climatic and Tectonic forcing on alluvial fans in the Southern Central Andes. Quaternary Science Reviews, 172, 131–141.

Thorndycraft, V. R., Bendle, J. M., Benito, G., Davies, B. J., Sancho, C., Palmer, A. P., Fabel, D., Medialdea, A., & Martin, J. R. V. (2019). Glacial lake evolution and Atlantic-Pacific drainage reversals during deglaciation of the Patagonian Ice Sheet. Quaternary Science Reviews, 203, 102–127.

Tielidze, L. G., Solomina, O. N., Jomelli, V., Dolgova, E. A., Bushueva, I. S., Mikhalenko, V. N., & Brauche, R. (2020). Change of Chalaati Glacier (Georgian Caucasus) since the Little Ice Age based on dendrochronological and Beryllium-10 data. Ice and Snow, 60(3), 453–470.

Todd, C., Stone, J., Conway, H., Hall, B., & Bromley, G. (2010). Late Quaternary evolution of Reedy Glacier, Antarctica. Quaternary Science Reviews, 29(11–12), 1328–1341.

Tschudi, S., Schäfer, J. M., Zhao, Z., Wu, X., Ivy-Ochs, S., Kubik, P. W., & Schlüchter, C. (2003). Glacial advances in Tibet during the Younger Dryas? Evidence from cosmogenic 10Be, 26Al, and 21Ne. Journal of Asian Earth Sciences, 22(4), 301–306.

Tulenko, J. P., Briner, J. P., Young, N. E., & Schaefer, J. M. (2018). Beryllium-10 chronology of early and late Wisconsinan moraines in the Revelation Mountains, Alaska: Insights into the forcing of Wisconsinan glaciation in Beringia. Quaternary Science Reviews, 197, 129–141.

Ullman, D. J., Carlson, A. E., Hostetler, S. W., Clark, P. U., Cuzzone, J., Milne, G. A., Winsor, K., & Caffee, M. (2016). Final Laurentide ice-sheet deglaciation and Holocene climate-sea level change. Quaternary Science Reviews, 152, 49–59.

Ullman, D. J., Carlson, A. E., LeGrande, A. N., Anslow, F. S., Moore, A. K., Caffee, M., Syverson, K. M., & Licciardi, J. M. (2015). Southern Laurentide ice-sheet retreat synchronous with rising boreal summer insolation. Geology, 43(1), 23–26.

Valentino, J. D., Owen, L. A., Spotila, J. A., Cesta, J. M., & Caffee, M. W. (2021). Timing and extent of Late Pleistocene glaciation in the Chugach Mountains, Alaska. Quaternary Research (United States), 101, 205–224.

Valletta, R. D., Willenbring, J. K., & Lewis, A. R. (2017). "Difference Dating": A novel approach towards dating alpine glacial moraines. Quaternary Geochronology, 41, 1–10.

Voisine, E., Rolland, Y., Bernet, M., Carcaillet, J., Duclaux, G., Bascou, J., Sue, C., Balvay, M., & Ménot, R. P. (2020). Antarctic erosion history reconstructed by Terre Adélie moraine geochronology. Antarctic Science, 32(5), 382–395.

Von Blanckenburg, F., & Willenbring, J. K. (2014). Cosmogenic nuclides: Dates and rates of earth-surface change. Elements, 10(5), 341–346.

Wang, J., Kassab, C., Harbor, J. M., Caffee, M. W., Cui, H., & Zhang, G. (2013). Cosmogenic nuclide constraints on late Quaternary glacial chronology on the Dalijia Shan, northeastern Tibetan Plateau. Quaternary Research (United States), 79(3), 439–451.

Wang, J., Raisbeck, G., Xu, X., Yiou, F., & Bai, S. (2006). In situ cosmogenic 10Be dating of the Quaternary glaciations in the southern Shaluli Mountain on the Southeastern Tibetan Plateau. Science in China, Series D: Earth Sciences, 49(12), 1291–1298.

Wang, S., Chevalier, M. L., Pan, J., Bai, M., Li, K., Li, H., & Wang, G. (2020). Quantification of the late Quaternary throw rates along the Yadong rift, southern Tibet. Tectonophysics, 790.

Ward, D. J., & Anderson, R. S. (2011). The use of ablation-dominated medial moraines as samplers for 10Be-derived erosion rates of glacier valley walls, Kichatna Mountains, AK. Earth Surface Processes and Landforms, 36(4), 495–512.

Ward, D. J., Cesta, J. M., Galewsky, J., & Sagredo, E. (2015). Late pleistocene glaciations of the arid subtropical Andes and new results from the Chajnantor Plateau, northern Chile. Quaternary Science Reviews, 128, 98–116.

Wesnousky, S. G., Aranguren, R., Rengifo, M., Owen, L. A., Caffee, M. W., Murari, M. K., & Pérez, O. J. (2012). Toward quantifying geomorphic rates of crustal displacement, landscape development, and the age of glaciation in the Venezuelan Andes. Geomorphology, 141–142, 99–113.

Wesnousky, S. G., Briggs, R. W., Caffee, M. W., Ryerson, F. J., Finkel, R. C., & Owen, L. A. (2016). Terrestrial cosmogenic surface exposure dating of glacial and associated landforms in the Ruby Mountains-East Humboldt Range of central Nevada and along the northeastern flank of the Sierra Nevada. Geomorphology, 268, 72–81.

Wilson, P., Linge, H., Matthews, J. A., Mourne, R. W., & Olsen, J. (2019). Comparative numerical surface exposure-age dating (10Be and Schmidt hammer) of an early-Holocene rock avalanche at Alstadfjellet, Valldalen, southern Norway. Geografiska Annaler, Series A: Physical Geography, 101(4), 293–309.

Wilson, P., Matthews, J. A., Mourne, R. W., Linge, H., & Olsen, J. (2020). Interpretation, age and significance of a relict paraglacial and periglacial boulder-dominated landform assemblage in Alnesdalen, Romsdalsalpane, southern Norway. Geomorphology, 369.

Wilson, P., Rodés, Á., & Smith, A. (2018). Valley glaciers persisted in the Lake District, north-west England, until ~16–15 ka as revealed by terrestrial cosmogenic nuclide (10Be) dating: a response to Heinrich event 1? Journal of Quaternary Science, 33(5), 518–526.

Wilson, P., Schnabel, C., Wilcken, K. M., & Vincent, P. J. (2013). Surface exposure dating (36Cl and 10Be) of post-Last Glacial Maximum valley moraines, Lake District, northwest England: Some issues and implications. Journal of Quaternary Science, 28(4), 379–390.

Winkler, S. (2014). Investigation of late-Holocene moraines in the western Southern Alps, New Zealand, applying Schmidt-hammer exposure-age dating. Holocene, 24(1), 48–66.

Winsor, K., Carlson, A. E., Caffee, M. W., & Rood, D. H. (2015). Rapid last-deglacial thinning and retreat of the marine-terminating southwestern Greenland ice sheet. Earth and Planetary Science Letters, 426, 1–12.

Winsor, K., Carlson, A. E., & Rood, D. H. (2014). 10Be dating of the Narsarsuaq moraine in southernmost Greenland: Evidence for a late-Holocene ice advance exceeding the Little Ice Age maximum. Quaternary Science Reviews, 98, 135–143.

Wittmeier, H. E., Schaefer, J. M., Bakke, J., Rupper, S., Paasche, Ø., Schwartz, R., & Finkel, R. C. (2020). Late Glacial Mountain glacier culmination in Arctic Norway prior to the Younger Dryas. Quaternary Science Reviews, 245.

Wüthrich, L., Morabito, E. G., Zech, J., Trauerstein, M., Veit, H., Gnägi, C., Merchel, S., Scharf, A., Rugel, G., Christl, M., & Zech, R. (2018). 10Be surface exposure dating of the last deglaciation in the Aare Valley, Switzerland. Swiss Journal of Geosciences, 111(1–2), 295–303.

Xu, X., Hu, G., & Qiao, B. (2013). Last glacial maximum climate based on cosmogenic 10Be exposure ages and glacier modelling for the head of Tashkurgan Valley, northwest Tibetan Plateau. Quaternary Science Reviews, 80, 91–101.

Xu, X., Yao, T., Xu, B., Yi, C., Sun, Y., Zeng, X., Dong, G., & Pan, B. (2020). Glacial events during the last glacial termination in the Pagele valley, Qiongmu Gangri peak, southern Tibetan Plateau, and their links to oceanic and atmospheric circulation. Quaternary Research (United States), 95, 129–141.

Young, N. E., Briner, J. P., & Kaufman, D. S. (2009). Late Pleistocene and Holocene glaciation of the Fish Lake valley, northeastern Alaska Range, Alaska. Journal of Quaternary Science, 24(7), 677–689.

Young, N. E., Briner, J. P., Axford, Y., Csatho, B., Babonis, G. S., Rood, D. H., & Finkel, R. C. (2011a). Response of a marine-terminating Greenland outlet glacier to abrupt cooling 8200 and 9300 years ago. Geophysical Research Letters, 38(24).

Young, N. E., Briner, J. P., Leonard, E. M., Licciardi, J. M., & Lee, K. (2011b). Assessing climatic and nonclimatic forcing of Pinedale glaciation and deglaciation in the western United States. Geology, 39(2), 171–174.

Young, N. E., Briner, J. P., Rood, D. H., & Finkel, R. C. (2012). Glacier Extent During the Younger Dryas and 8.2-ka Event on Baffin Island, Arctic Canada. Science, 337, 1330–1333.

Young, N. E., Schaefer, J. M., Briner, J. P., & Goehring, B. M. (2013). A 10Be production-rate calibration for the Arctic. Journal of Quaternary Science, 28(5), 515–526.

Young, N. E., Schweinsberg, A. D., Briner, J. P., & Schaefer, J. M. (2015). Glacier maxima in Baffin Bay during the Medieval Warm Period coeval with Norse settlement. Science Advances, 1(11).

Young, N. E., Briner, J. P., Schaefer, J., Zimmerman, S., & Finkel, R. C. (2019). Early Younger Dryas glacier culmination in southern Alaska: Implications for North Atlantic climate change during the last deglaciation. Geology, 47(6), 550–554.

Young, N. E., Briner, J. P., Miller, G. H., Lesnek, A. J., Crump, S. E., Thomas, E. K., Pendleton, S. L., Cuzzone, J., Lamp, J., Zimmerman, S., Caffee, M., & Schaefer, J. M. (2020). Deglaciation of the Greenland and Laurentide ice sheets interrupted by glacier advance during abrupt coolings. Quaternary Science Reviews, 229.

Young, N. E., Briner, J. P., Miller, G. H., Lesnek, A. J., Crump, S. E., Pendleton, S. L., Schwartz, R., & Schaefer, J. M. (2021a). Pulsebeat of early Holocene glaciation in Baffin Bay from high-resolution beryllium-10 moraine chronologies. Quaternary Science Reviews, 270, Elsevier Ltd.

Young, N. E., Lesnek, A. J., Cuzzone, J. K., Briner, J. P., Badgeley, J. A., Balter-Kennedy, A., Graham, B. L., Cluett, A., Lamp, J. L., Schwartz, R., Tuna, T., Bard, E., Caffee, M. W., Zimmerman, S. R. H., & Schaefer, J. M. (2021b). In situ cosmogenic 10Be-14C-26Al measurements from recently deglaciated bedrock as a new tool to decipher changes in Greenland Ice Sheet size. Climate of the Past, 17(1), 419–450.

Zahno, C., Akçar, N., Yavuz, V., Kubik, P. W., & Schlüchter, C. (2009). Surface exposure dating of Late Pleistocene glaciations at the Dedegöl Mountains (Lake Beyşehir, SW Turkey). Journal of Quaternary Science, 24(8), 1016–1028.

Zahno, C., Akçar, N., Yavuz, V., Kubik, P. W., & Schlüchter, C. (2010). Chronology of Late Pleistocene glacier variations at the Uludağ Mountain, NW Turkey. Quaternary Science Reviews, 29(9–10), 1173–1187.

Zasadni, J., Kłapyta, P., Broś, E., Ivy-Ochs, S., Świąder, A., Christl, M., & Balážovičová, L. (2020). Latest Pleistocene glacier advances and post-Younger Dryas rock glacier stabilization in the Mt. Kriváň group, High Tatra Mountains, Slovakia. Geomorphology, 358.

Zech, J., Terrizzano, C., García-Morabito, E., Veit, H., & Zech, R. (2017). Timing and extent of late pleistocene glaciation in the arid central andes of Argentina and Chile (22°-41°s). Cuadernos de Investigacion Geografica, 43(2), 697–718.

Zech, J., Zech, R., Kubik, P. W., & Veit, H. (2009). Glacier and climate reconstruction at Tres Lagunas, NW Argentina, based on 10Be surface exposure dating and lake sediment analyses. Palaeogeography, Palaeoclimatology, Palaeoecology, 284(3–4), 180–190.

Zech, J., Zech, R., May, J. H., Kubik, P. W., & Veit, H. (2010). Lateglacial and early Holocene glaciation in the tropical Andes caused by La Niña-like conditions. Palaeogeography, Palaeoclimatology, Palaeoecology, 293(1–2), 248–254.

Zech, R. (2012). A late Pleistocene glacial chronology from the Kitschi-Kurumdu Valley, Tien Shan (Kyrgyzstan), based on 10Be surface exposure dating. Quaternary Research, 77(2), 281–288.

Zech, R., Abramowski, U., Glaser, B., Sosin, P., Kubik, P. W., & Zech, W. (2005). Late Quaternary glacial and climate history of the Pamir Mountains derived from cosmogenic 10Be exposure ages. Quaternary Research, 64(2), 212–220.

Zech, R., Kull, C., Kubik, P. W., & Veit, H. (2007a). Climate of the Past LGM and Late Glacial glacier advances in the Cordillera Real and Cochabamba (Bolivia) deduced from 10 Be surface exposure dating. Climate of the Past 3, 623-635.

Zech, R., Kull, C., Kubik, P. W., & Veit, H. (2007b). Exposure dating of Late Glacial and pre-LGM moraines in the Cordon de Doña Rosa, Northern/Central Chile (~31°S). Climate of the Past 3, 1-14.

Zech, R., Kull, C., & Veit, H. (2006). Late Quaternary glacial history in the Encierro Valley, northern Chile (29°S), deduced from 10Be surface exposure dating. Palaeogeography, Palaeoclimatology, Palaeoecology, 234(2–4), 277–286.

Zech, R., Röhringer, I., Sosin, P., Kabgov, H., Merchel, S., Akhmadaliev, S., & Zech, W. (2013). Late Pleistocene glaciations in the Gissar Range, Tajikistan, based on 10Be surface exposure dating. Palaeogeography, Palaeoclimatology, Palaeoecology, 369, 253–261.

Zech, R., Zech, J., Kull, C., Kubik, P. W., & Veit, H. (2011). Early last glacial maximum in the southern Central Andes reveals northward shift of the westerlies at ~39 ka. Climate of the Past, 7(1), 41–46.

Zech, R., Zech, M., Kubik, P. W., Kharki, K., & Zech, W. (2009). Deglaciation and landscape history around Annapurna, Nepal, based on 10Be surface exposure dating. Quaternary Science Reviews, 28(11–12), 1106–1118.

Zeng, X., Xu, X., Yi, C., Sun, Y., & Li, J. (2021). Extensive glaciations between MIS 8 and MIS 5 on the eastern side of the Guliya ice cap, West Kunlun Mountains. Quaternary International, 604, 28–37.

Zhang, M., Chen, Y., Li, Y., & Liu, G. (2016). Late Quaternary glacial history of the Nalati Range, central Tian Shan, China, investigated using 10Be surface exposure dating. Journal of Quaternary Science, 31(7), 659–670.

Zhang, Q., Yi, C., Dong, G., Fu, P., Wang, N., & Capolongo, D. (2018). Quaternary glaciations in the Lopu Kangri area, central Gangdise Mountains, southern Tibetan Plateau. Quaternary Science Reviews, 201, 470–482.

Zhou, S., Xu, L., Colgan, P. M., Mickelson, D. M., Wang, X., Wang, J., & Zhong, W. (2007). Cosmogenic 10Be dating of Guxiang and Baiyu Glaciations. Chinese Science Bulletin, 52(10), 1387–1393.

10. List of Figures and Tables

10.1. List of figures

10.2. List of tables